Selective NOx Recirculation for Stationary Lean-Burn Natural Gas Engines

Final Report

DOE Award Number: DE-FC26-02NT41608

Reporting Period

October 1, 2002 – December 31, 2006

Principal Investigator:

Nigel N. Clark

Center for Alternative Fuels, Engines and Emissions

Department of Mechanical and Aerospace Engineering

West Virginia University

Morgantown, WV 26506

Participating Researchers

Gregory Thompson, Richard Turton, Emre Tatli, Chamila Tissera, Richard Atkinson, Andrew Nix, Matthew Swartz, Ramprabhu Vellaisamy & Andrew Zimmerman

April 30, 2007

Disclaimer

Abstract

Nitric oxide (NO) and nitrogen dioxide (NO_2) generated by internal combustion (IC) engines are implicated in adverse environmental and health effects. Even though lean-burn natural gas engines have traditionally emitted lower oxides of nitrogen (NOx) emissions compared to their diesel counterparts, natural gas engines are being further challenged to reduce NOx emissions to 0.1 g/bhp-hr.

The Selective NOx Recirculation (SNR) approach for NOx reduction involves cooling the engine exhaust gas and then adsorbing the NOx from the exhaust stream, followed by the periodic desorption of NOx. By sending the desorbed NOx back into the intake and through the engine, a percentage of the NOx can be decomposed during the combustion process. SNR technology has the support of the Department of Energy (DOE), under the Advanced Reciprocating Engine Systems (ARES) program to reduce NOx emissions to under 0.1 g/bhp-hr from stationary natural gas engines by 2010.

The NO decomposition phenomenon was studied using two Cummins L10G natural gas fueled spark-ignited (SI) engines in three experimental campaigns. It was observed that the air/fuel ratio (λ), injected NO quantity, added exhaust gas recirculation (EGR) percentage, and engine operating points affected NOx decomposition rates within the engine.

Chemical kinetic model predictions using the software package CHEMKIN were performed to relate the experimental data with established rate and equilibrium models. The model was used to predict NO decomposition during lean-burn, stoichiometric burn, and slightly rich-burn cases with added EGR. NOx decomposition rates were estimated from the model to be from 35 to 42% for the lean-burn cases and from 50 to 70% for the rich-burn cases. The modeling results provided an insight as to how to maximize NOx decomposition rates for the experimental engine.

Results from this experiment along with chemical kinetic modeling solutions prompted the investigation of rich-burn operating conditions, with added EGR to prevent pre-ignition. It was observed that the relative air/fuel ratio, injected NO quantity, added

EGR fraction, and engine operating points affected the NO decomposition rates. While operating under these modified conditions, the highest NO decomposition rate of 92% was observed. In-cylinder pressure data gathered during the experiments showed minimum deviation from peak pressure as a result of NO injections into the engine.

A NOx adsorption system, from Sorbent Technologies, Inc., was integrated with the Cummins engine, comprised a NOx adsorbent chamber, heat exchanger, demister, and a hot air blower. Data were gathered to show the possibility of NOx adsorption from the engine exhaust, and desorption of NOx from the sorbent material. In order to quantify the NOx adsorption/desorption characteristics of the sorbent material, a benchtop adsorption system was constructed. The temperature of this apparatus was controlled while data were gathered on the characteristics of the sorbent material for development of a system model. A simplified linear driving force model was developed to predict NOx adsorption into the sorbent material as cooled exhaust passed over fresh sorbent material. A mass heat transfer analysis was conducted to analyze the possibility of using hot exhaust gas for the desorption process. It was found in the adsorption studies, and through literature review, that NO adsorption was poor when the carrier gas was nitrogen, but that NO in the presence of oxygen was adsorbed at levels exceeding 1% by mass of the sorbent.

From the three experimental campaigns, chemical kinetic modeling analysis, and the scaled benchtop NOx adsorption system, an overall SNR system model was developed. An economic analysis was completed, and showed that the system was impractical in cost for small engines, but that economies of scale favored the technology.

Acknowledgements

This research was funded by the U.S. Department of Energy (DOE) through the ARES program contract number: DE-FC26-02NT41608. The authors are grateful to Ronald Fiskum of the DOE, William Cary Smith of NETL, and Raj Sekar of Argonne National Laboratories for their support and guidance, and thank Thomas George of NETL for guiding the program in its first year.

The authors extend their gratitude to Sorbent Technologies, Inc. for their advice and for the loan of equipment used in the study. The authors also thank Cummins Engine Company (and Vinod Duggal of Cummins) and Bell Power System (and Scot Lengel of Bell) for their contribution in providing two Cummins L10 natural gas engines for the study.

The authors also thank Thomas Spencer and the staff at the Center for Alternative Fuels, Engines & Emissions at West Virginia University for invaluable support of the laboratory experiments.

Richard Turton is affiliated with the Department of Chemical Engineering at West Virginia University (WVU). All remaining authors are affiliated with the Department of Mechanical and Aerospace Engineering at WVU.

Project Reporting and Education

Publication arising from this Research

- Tissera, C. A., Tatli, E., Swartz, M. M., Vellaisamy, R., Clark, N. N., Thompson, G. J., Nine, R. D., and Atkinson, R. J. "Selective NOx Recirculation for Stationary Lean-Burn Natural Gas Engines," ASME Conference Paper, ICEF2004-839, 2004.

- Swartz, M. M., Tissera, C. A., Tatli, E., Vellaisamy, R., Clark, N. N., Thompson, G. J., and Atkinson, R. J. "Nitric Oxide Conversion in a Spark Ignited Natural Gas Engine," SAE Paper 2005-01-0234, 2005.

- Tissera, C. A., Swartz, M. M., Vellaisamy, R., Clark, N.N., Thompson, G.J., and Atkinson, R.J., "Selective NOx Recirculation for Stationary Lean-Burn Engines," SAE Paper 2005-01-2144, 2005.

- Zimmerman, A. J., Tissera, C. A., Tatli, E., Clark N. N., Turton, R., Atkinson R. J. and Thompson, G. J. "System Model for Selective NOx Recirculation to be used in Stationary Lean-Burn Natural Gas Engines," ASME Conference Paper, ICEF2006-1542, 2006.

Presentations associated with this Research

- Tissera, C. A., Tatli, E., Zimmerman, A. J., Clark, N. N., Thompson, G. J., and Atkinson, R. J. "Selective NOx Recirculation for Stationary Lean-Burn Natural Gas Engines," Distributed Energy Peer Review, Washington DC, December 02-05, 2003.

- Swartz, M. M., Tissera, C. A., Tatli, E., Vellaisamy, R., Clark, N. N., Thompson, G. J., and Atkinson, R. J. "Selective NOx Recirculation for Stationary Lean-Burn Natural Gas Engines," Poster presentation held at the West Virginia State Capitol building, Charleston WV, March, 2004.

- Tissera, C. A., Tatli, E., Zimmerman, A. J., Clark, N. N., Thompson, G. J., Atkinson, R. J., and Swartz, M. M. "Selective NOX Recirculation for Stationary Lean-Burn Natural Gas Engines," 2nd Annual Advanced Stationary Reciprocating Engines

Conference, Hosted by, South Coast Air Quality Management District, Diamond Bar, CA. March 15-16, 2005.

- Tissera, C. A., Tatli, E., Zimmerman, A. J., Clark, N. N., Thompson, G. J., and Atkinson, R. J. Presentation at ARES catalysis group workshop, ORNL, Knoxville TN, April 27- 28, 2005.

- Tissera, C. A., Tatli, E., Zimmerman, A. J., Clark, N. N., Thompson, G. J., and Atkinson, R. J. "Selective NOx Recirculation for Stationary Lean-Burn Natural Gas Engines," Poster presentation, 2005 Distributed Energy Peer Review held at Crystal City, Virginia, December 13-15, 2005.

- Clark, N. N., Tissera, C. A., Tatli, E., Zimmerman, A. J., Thompson, G. J., and Atkinson, R. J "Selective NOX Recirculation for Stationary Lean-Burn Natural Gas Engines," Presentation at the 2005 ARES University Program review held at Argonne National Laboratory, Argonne, Illinois, 2004, 2005, 2006

Graduate Students associated with this Research

Matthew Swartz, MS Mechanical Engineering. Nitric Oxide Conversion in a Spark Ignited Natural Gas Engine (May 2005)

Ramprabhu Vellaisamy, MS Mechanical Engineering. Assessment of NOx Destruction in Heavy-Duty Diesel Engines by Injecting Nitric Oxide into the Intake (May 2005)

Andy Zimmerman, MS Mechanical Engineering. Evaluation of the Selective NOx Recirculation Technique using Activated Carbon (May 2007)

Chamila Tissera, Ph.D. Mechanical Engineering. Selective NOx Recirculation for Stationary Lean-Burn Natural Gas Engines (Expected Graduation - Summer 2007)

Table of Contents

List of Figures

List of Tables

Nomenclature

AC	Alternating Current
acfm	actual cubic feet per minute
ADC	Analog to Digital Converter
ARES	Advanced Reciprocating Engine Systems
bhp	a measure of mechanical power generated by a reciprocating engine determined by a brake attached to the shaft coupling
bhp-hr	brake horsepower-hour, work done by a mechanism with a power output of one brake horsepower over a period of one hour
BMEP	Brake Mean Effective Pressure
BSFC	Brake Specific Fuel Consumption
BTE	Brake Thermal Efficiency
CFR	Code of Federal Regulations
CFV	Critical Flow Venturi
CHP	Combined Heat and Power
CI	Compression Ignition
CO	Carbon Monoxide
CO_2	Carbon Dioxide
CVS	Constant Volume Sampling
DC	Direct Current
DOE	Department of Energy
EGR	Exhaust Gas Recirculation
EPA	Environmental Protection Agency
FID	Flame Ionization Detector
fNOx	fast NOx
g/bhp-hr	grams per brake horsepower-hour
HCs	Hydrocarbons
HCCI	Homogeneous Charge Compression Ignition
HEAT	High Efficiency Advanced Turbocharger
hp	horsepower
IC	Internal Combustion
IMEP	Indicated Mean Effective Pressure
LFE	Laminar Flow Element
LNT	Lean NOx Trap

lpm	liters per minute
lps	liters per second
NO	Nitrogen Oxide
NO_2	Nitrogen Dioxide
NOx	Oxides of Nitrogen
O_3	Ozone
ORNL	Oak Ridge National Laboratory
PM	Particulate Matter
ppm	parts per million
rpm	revolutions per minute
scfm	standard cubic feet per minute
SC-3	Stoichiometric, Clean exhaust induction, 3 way catalyst
SCR	Selective Catalytic Reduction
SI	Spark Ignition
SNR	Selective NOx Recirculation
THC	Total Hydrocarbon
TWC	Three Way Catalyst
UEGO	Universal Exhaust Gas Oxygen
VOCs	Volatile Organic Compounds
λ	Lambda (relative air/fuel ratio)

1. Introduction

Spark ignited natural gas engines of all sizes are able to achieve acceptable efficiencies by operating in a lean-burn mode. Lean-burn operation is also desirable to extend engine life by reducing the thermal load. One method for oxides of nitrogen (NOx) reduction is to operate lean-burn natural gas engines with high air/fuel ratios. The air/fuel ratio is often expressed as a ratio to the stoichiometric mixture ratio; this resulting lambda ratio implies lean operation for values greater than unity. Practically, the region of lean operation is relatively narrow because the leaner end ($\lambda \approx 1.3$) produces elevated levels of NOx, while the leaner end ($\lambda \approx 1.7$) leads to incomplete combustion and high unburned hydrocarbon (HC) emissions due to misfire, with corresponding loss of power density. Some further NOx reductions can be effected by retarding the ignition timing and introducing EGR. However, applying these methods too aggressively may result in power reduction and durability problems. In the automotive world, heavy-duty high-speed natural gas lean-burn engines have used wide range oxygen sensor feedback to approach 1g/bhp-hr of NOx, but further reductions are desirable for both transportation and stationary engines in the future.

The Advanced Reciprocating Engines Systems (ARES) program was established by the US Department of Energy to promote and aid the development of clean, efficient power generation engines. The ARES goals include a brake specific NOx emissions target level of 0.1 g/bhp-hr and 50% thermal efficiency, using affordable technology. This NOx goal most likely cannot be met without aftertreatment. Modifying the combustion process itself cannot reduce NOx to these levels for lean-burn operation [1]-[5]. One aftertreatment option that has been considered for lean-burn engines is Selective Catalytic Reduction (SCR) which involves the injection of urea or ammonia ahead of an exhaust catalyst. An alternative approach, now being contemplated by both the stationary and transportation engine sectors, is to employ stoichiometric engine operation with three-way catalysis, but this approach requires careful management of in-cylinder temperatures.

Large-bore natural gas engines, even with careful control, are an order of magnitude off the 0.1 g/bhp-hr target. Conventional NOx reduction catalysts, used widely to tame stoichiometric-burn gasoline and natural gas automobile emissions, cannot be employed because the lean-burn exhaust contains excess oxygen, which leads to unfavorable reaction conditions. Natural gas fueled internal combustion engines currently achieve thermal efficiencies between 37 and 40 percent, and produce NOx levels of 1 g/bhp-hr [6]. These engines are commercially available, with demonstrated abilities to support electrical generation, to provide power for gas compression, or in combined heat and power applications.

Natural gas fuel used in IC engines has inherently low amounts of carbon as it contains typically 95% methane (CH_4). Also, natural gas has been approximately 40% less expensive than crude oil during the past fourteen years [1]. Natural gas is available worldwide and is taking an increasing share of the energy mix.

The primary objective of the Selective NOx Recirculation (SNR) research reported below was to demonstrate that one can reduce NOx emissions from reciprocating natural gas engines to acceptable levels while maintaining high fuel efficiency. SNR involves cooling the engine exhaust gas and then adsorbing the NOx from the exhaust stream, followed by the periodic desorption of NOx. By returning the desorbed, concentrated NOx into the engine intake and passing it through the combustion chamber, a fraction of the recirculated NOx is decomposed during the combustion process. The research objectives are to characterize the decomposition of NOx in a natural gas engine over a range of operating conditions, to characterize the adsorption and desorption processes, and to examine the overall system performance using modeling based on acceted design approaches and experimental results.

The benefits of this program are projected to be the reduction of NOx from engines normally operating in an efficient lean-burn mode, without the use of dedicated reductants (as in urea injection with selective catalytic reduction), and with carbon-based sorbent that is not readily poisoned. Carbon sorbent has been used previously to absorb NOx from diesel engine exhaust by Sorbent Technologies, Inc. (Twinsburg, Ohio).

The first SNR experimental campaign in this program was focused on quantifying NOx decomposition in a lean-burn 1993 Cummins L10G natural gas engine with the use of a full scale dilution tunnel and analyzers capable of measuring NOx, CO_2, CO, HC concentrations. Commercially available nitric oxide (NO, 98.8% purity) was used to mimic the desorption process to obtain NOx decomposition rates at various steady state engine operating points. A substantial set of NOx decomposition data was acquired under lean-burn conditions ($\lambda \approx 1.4$), but decomposition rates were modest (14 to 26%). The experimental setup, test procedure and preliminary NOx decomposition rates are presented in the body of the report.

Further NOx decomposition research was conducted usig a later technology Cummins 10 liter natural gas engine, which was procured with the assistance of Cummins Inc. to replace the early engine used in prior research. The engine, equipped with an in-cylinder pressure measurement system and electronic controls, was connected to a newly commissioned motoring dynamometer, and was adapted to operate over a range of air/fuel ratios. Effect of NO injection on exhaust composition was characterized. Chemical kinetic modeling, using the package CHEMKIN, was used to assess decomposition rates at steady-state temperatures and gas compositions chosen to mimic conditions in the engine cylinder near top dead center. This modeling confirmed that decomposition rates would be low under lean-burn conditions, and suggested that stoichiometric operation would be desirable during the NOx decomposition phase.

A second experimental campaign was completed to acquire both stoichiometric and slightly rich ($\lambda = 0.97$) burn NOx decomposition rates. Effects of engine load and speed (800, 1300 and 2100 rpm) were quantified, but EGR was not managed as an independent variable. Decomposition rates of up to 92% were demonstrated. In-cylinder pressure was measured to calculate engine indicated mean effective pressure (IMEP) changes due to NOx injections and EGR variations, and to confirm conditions in the cylinder. Using a full exhaust flow adsorber and heat exchanger system provided by industry (Sorbent Technologies, Inc., Twinsburg, OH), preliminary data were gathered to show both the successful adsorption of NOx from the Cummins engine, and the successful desorption of NOx from the carbon-based sorbent material using a heated air stream.

A third experimental campaign gathered NO decomposition data at 800, 1200 and 1800 rpm with EGR managed in an external loop from 0% to point of misfire, and with individual exhaust thermocouple data. These three campaigns provided the data needed for a comprehensive model of NOx decomposition. A benchtop adsorption system was constructed, and instrumented with thermocouples and a NOx analyzer to gather adsorption data. These data were required for the development of a system model. An important finding was that NO adsorption was strongly affected by the presence of oxygen in the gas stream sent to the adsorber. A SNR system could not be designed on a two-phase adsorption/desorption assumption, but had to account for the four phases of cooling, adsorbing, heating, and desorbing.

2. Literature Review

2.1 Oxides of Nitrogen (NOx)

Oxides of nitrogen (NOx) are a combination of nitric oxide (NO), nitrogen dioxide (NO_2) and minor amounts of nitrous oxide (N_2O). N_2O is stable and is a powerful greenhouse gas. NO and NO_2 can be considered as the source of a wide variety of environmental and health impacts, and there is concern that NOx has not been abated as much as other pollutant species [7].

NO_2 is found in urban atmospheres, and is attributed to both mobile and stationary sources. It is categorized as a pulmonary irritant. Asthmatic individuals, and those with respiratory ailments or lung disease are particularly sensitive to the effects of NO_2. Healthy individuals exposed to high concentrations of NO_2 can develop abnormalities in their pulmonary airways [8]. NO_2 is a strong oxidizing agent that reacts in the air to form nitric acid [7],[8]. NO_2 plays a major role in atmospheric reactions that produce ground level ozone (O_3) and acid rain [7][9]. NOx is also responsible for forming secondary particulate matter (PM) in the atmosphere. "The current primary National Atmospheric Air Quality Standards (NAAQS) for NO_2 is an annual arithmetic mean value not to exceed 0.053 ppm. In order for a violation to occur, NO_2 concentrations would have to be high enough that the average over the entire year would exceed 0.053 ppm."[8]

In this report only reciprocating engine exhaust sources of NOx are considered. Air is approximately 20% O_2 and 80% N_2, and these two gases do not react with each other appreciably under normal atmospheric conditions. However, if mixtures containing O_2 and N_2 are heated to high temperatures, reaction occurs to form NOx. For example, at any given temperature there exists a dynamic equilibrium with NO as expressed in Equation 1 [10].

$$N_2 + O_2 \longleftrightarrow 2NO - 43{,}200Cal \quad (1)$$

When the temperature increases the equilibrium shifts to the right, increasing the proportion of NO. When NO is produced in engines, in many cases the quantity of NO

produced may be rate-limited, rather than indicative of the equilibrium quantity. NO is a precursor to formation of NO_2 in the atmosphere. If the mixture of gases in Equation 1 is cooled rapidly, the rate of reverse reaction drops and the decomposition of NO slows, leaving a rate-limited "frozen" composition. NO does not remain long in the cooled gas mixture since it reacts with O_2 present when the temperature falls below 600°C [10] as shown in Equation 2. The reaction proceeds until nearly all the NO has been converted to NO_2.

$$2NO + O_2 \longleftrightarrow 2NO_2 \tag{2}$$

The NO_2 formation may slow down in its later stages, so that a short time of contact is necessary for complete oxidation and with dilute gases several minutes may be necessary for complete oxidation [10]. Ozone (O_3) can also oxidize NO into NO_2 and NO_3 as shown in the following equations.

$$NO + O_3 \longrightarrow NO_2 + O_2 \tag{3}$$

$$NO_2 + O_3 \longrightarrow NO_3 + O_2 \tag{4}$$

Equation 2 is known as the chemiluminescence reaction of NO to NO_2. This reaction is used as the working principle for NO detection in research-grade analyzers.

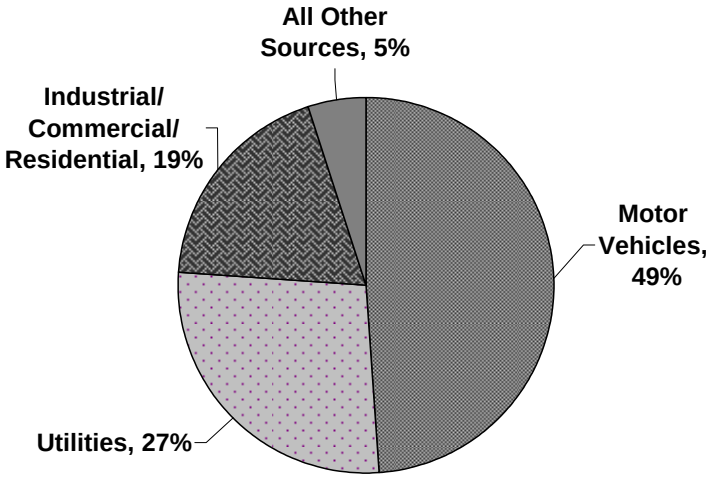

Figure 1. Primary sources of man-made NOx [6]

The major man-made source of NO_2 emissions is fossil fuel combustion at high temperatures, in internal combustion engines and in furnaces and boilers. Nitrogen oxides are formed through three different mechanisms. These are referred to as thermal NOx, fuel NOx and prompt NOx mechanisms. Thermal NOx is formed by dissociation of N_2 and O_2 into atomic states at high temperatures in the combustion mixture. The creation of thermal NOx is often described by the Zeldovich mechanism [11],[12].

$$N_2 + O \longleftrightarrow NO + N \tag{5}$$

$$N + O_2 \longleftrightarrow NO + O \tag{6}$$

The principal mechanism of NOx formation with gas engines is thermal NOx [11]. Most NOx is formed through the thermal NOx mechanism that occurs in high temperature regions in the cylinder where combustion air has mixed sufficiently with the fuel to produce the peak temperature in the fuel/air interface. The rates of these thermal NOx reactions are highly dependent on the air/fuel (λ) ratio of the combustion mixture, flame temperature (which is also influenced by the λ), and the residence time at that flame temperature. Figure 2 shows that the maximum thermal NOx production occurs at slightly lean mixture due to the excess amount of O_2 available within the hot flame zone [12]. A reduction in NOx formation can be observed as the mixture is made leaner or richer from the highest NOx production peak, indicating that controlling the local flame temperature and oxygen availability would result in lower thermal NOx production [12],[13].

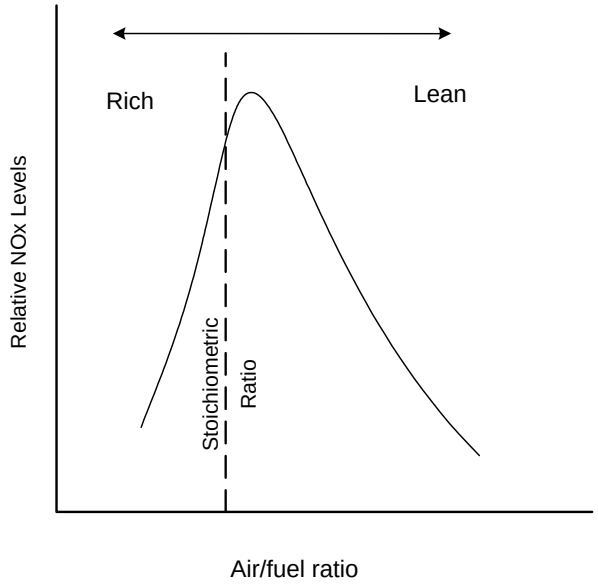

Figure 2. Effect of air/fuel ratio on thermal NOx production

Figure 3 shows, for a given air/fuel ratio, that thermal NOx generation decreases as the flame temperature drops below the adiabatic stoichiometric flame temperature [12]. Most of the NOx is generated in the flame core since heat is radiated rapidly out of the local flame. Almost all NOx formed in natural gas reciprocating engines occurs through the thermal NOx mechanism.

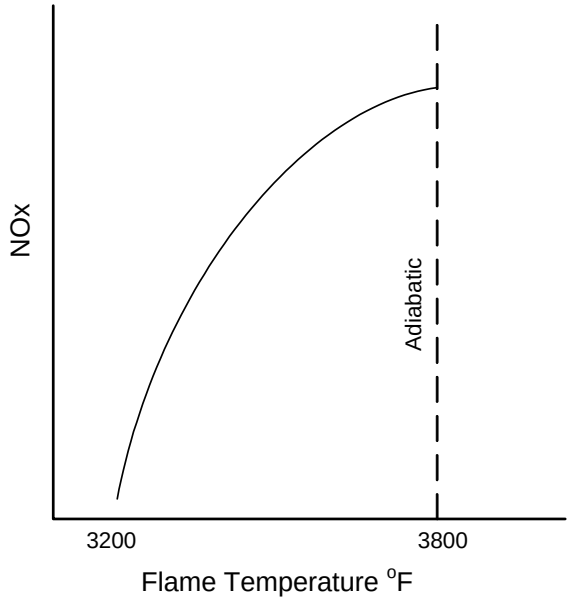

Figure 3. Thermal NOx formation dependence on flame temperature [12]

Fuel NOx is formed by two different mechanisms through reactions occurring within the nitrogen compounds found in fossil fuels. One mechanism is through nitrogen found in solid phase fuels that converts to NOx through complex reactions. Another is through gas phase fuel reactions that include intermediate species such as HCN, HOCN, and NH_2 which are produced in rapid reactions. However, the decay of these species into N_2 and NOx is slower by an order of magnitude and is strongly dependent on air/fuel ratio and gas phase fuel nitrogen concentration and weakly dependent on flame temperature and the nature of the organic compound [14]. In natural gas, although there is some molecular nitrogen, the amount of chemically bound fuel nitrogen is considered negligible [13].

Prompt NOx occurs through early reactions of nitrogen molecules in the combustion air and hydrocarbon radicals available from the fuel. Prompt NOx reactions have weak temperature dependence and a very short lifetime. Their levels are usually negligible compared to the level of NOx formed through the thermal NOx mechanism. Prompt NOx can become significant in extremely fuel rich flames [13],[15], which are not of interest in this report.

2.2 *Stationary Reciprocating Internal Combustion Engines*

There are two types of reciprocating stationary IC engines that primarily differ in the method used to ignite the fuel-air mixture in the combustion chamber. Spark ignition (SI) engines can be fueled by a variety of fuels, most typically gasoline, but for power generation and pumping stations natural gas is used as the preferred fuel. They also can be setup to operate on propane, or landfill gas. Compression ignition (CI) engines are usually fueled by diesel oil, or they can be configured to burn a combination of natural gas and diesel as a pilot fuel in what is termed a dual-fuel engine. This research report is focused on IC engines that are spark ignited and fueled by natural gas.

2.2.1 Natural gas as fuel

Pipeline natural gas is primarily composed of methane (CH_4) that typically makes up 85-99% of the total volume, depending on the field from which it is extracted [16]. In the United States there is an abundant supply of natural gas with over 1.2 million miles of pipeline delivery system in place [17]. The average US natural gas composition is shown in Table 1 [18].

Table 1. US average natural gas composition [18]

Component	**Formula**	**Volume %**	**Mass %**
Methane	CH_4	92.3	84.4
Ethane	C_2H_6	3.6	6.2
Propane	C_3H_8	0.8	2.1
Butane	C_4H_{10}	0.29	0.99
Pentane	C_5H_{12}	0.13	0.53
Hexane	C_6H_{14}	0.08	0.39
Carbon Dioxide	CO_2	1	2.52
Nitrogen	N_2	1.8	2.89
Water	H_2O	0.01	0.01
Total		**100**	**100**

Higher amounts of hydrocarbon increase the volumetric energy and may richen the mixture and reduce the octane number, leading to higher emissions and pre-ignition concerns. On the other hand, increased ratios of inert gases in the mixture reduce the

volumetric energy and may lean the mixture, reducing power output and increasing engine misfire [15]. In other words, ignition strength affects engine misfire.

The gas composition is defined in part by the Wobbe Number (W), where the higher heating value (British thermal unit per standard cubic foot) is divided by the square root of its specific gravity with respect to air [19].

$$W = \frac{H(Btu/scf)}{\sqrt{sg}} \tag{7}$$

The Wobbe number is an index of energy flow rate through an orifice in response to a given pressure drop. Pure methane has a Wobbe number of 1363, while pipeline quality natural gas in the United States typically exibits a Wobbe number between 1310 and 1390 [20].

Using natural gas to fuel Otto cycle or spark ignited engines has significant benefits. Natural gas mixes quite easily with air, unlike liquid fuels that need to be vaporized before combustion. A high autoignition temperature or high octane rating favors natural gas use. Pure methane has an octane number of 130, which is the highest in regularly used fuel [20]. The inert gases contained in the natural gas mixture lower the tendency to knock: therefore it can be used in engines with compression ratios of around 15:1 [20] (this is higher than compression ratios of 8-10:1 used in 91 octane gasoline engines) or with boost. With higher compression ratios higher engine efficiency can be achieved.

2.2.2 Natural gas engine categories

Natural gas fueled reciprocating engines can be categorized into three designs (all engines in these categories are spark-ignited).

- Two-stroke lean-burn engines
- Four-stroke lean-burn engines
- Four-stroke rich-burn engines (a term usually referring to stoichiometric operation)

A two-stroke engine completes the power cycle in a single crankshaft revolution as compared to the two crankshaft revolutions required in a four-stroke engine. Two-stroke engines can be turbocharged to increase intake flow velocity resulting in an increase in cylinder scavenging. Historically, two-stroke natural gas engines have been widely used in pipeline applications. Due to poor in-cylinder mixing, poor cylinder to cylinder fuel distribution and due to more stringent air emission regulations there has been a decline in the usage of new two-stroke natural gas engines for stationary applications [11].

Four-stroke engines use a separate engine revolution for the intake and compression cycles and for the power and exhaust cycles. These engines can be either naturally aspirated or turbocharged.

Rich-burn natural gas engines operate near the stoichiometric air/fuel ratio with exhaust excess oxygen levels less than 4%, but in reality most engines will operate where oxygen levels are closer to 1%. The emissions levels can be significantly different for a rich-burn engine producing 4% oxygen than when it is operated closer to stoichiometric conditions. Even in this narrow operating range emissions can vary by more than an order of magnitude [19].

Lean-burn engines can operate up to the lean flame extinction limit, with exhaust oxygen levels at 12% or greater. Natural gas is more suitable for lean-burn engines than gasoline engines due to its tolerance to leaner combustion. The relative air/fuel ratios of lean-burn natural gas engines range from λ=1.2 to 1.8. The excess oxygen levels of lean-burn engine exhaust range typically from 4% to 17%. Both the rich-burn and lean-burn combustion systems have their benefits and drawbacks. Table 2 contains a summary of the main characteristics of the two combustion systems for heavy-duty applications [21]-[24].

Table 2. Characteristics related to lean, stoichiometric and rich operation of natural gas engines

Rich/stoichiometric operation	
Benefits	**Drawbacks**
achieve low exhaust emissions with a TWC	closed-loop fuel system and a three-way catalyst needed for emissions control
stable engine operation	not suitable for fuels with low knock resistance
moderate requirements on the ignition system	high thermal loadings compared to diesel or lean-burn operation
high BMEP for a naturally aspirated engines	restricted possibilities for turbocharging
	fuel consumption penalty compared to lean-burn operation
Lean-burn operation	
moderate exhaust emissions	turbocharging necessary to obtain sufficient power output
NOx formation controlled during combustion	transient engine response
high power output if turbocharged	high requirements on the ignition system
thermal loading close to diesel operation	high cycle-to-cycle variations
	high methane emission with natural gas
	oxidation catalyst needed for CO and HC control

In general, lean-burn combustion is preferred by the engine manufacturers, for reasons of lower thermal loading and higher power output. Stoichiometric operation often requires changes in both materials and component design, which add to the price of the conversion from lean-burn [25]. However, at time of writing, natural gas engines used in transit bus applications in North America are moving from a lean-burn to a stoichiometric strategy.

2.2.3 Engine Applications

Natural gas reciprocating engines offer many advantages over other technologies for small-scale power generation, including the ability to provide highly reliable, inexpensive backup power, provide power for remote locations, and generate onsite power during peak periods when utility charges are at their highest. Reciprocating engines can be used

for peak-shaving, remote power, in combined heat and power (CHP) applications, and for standby power. Natural gas engines have also been the obvious choice for pipeline compression power demands.

Commercially available natural gas IC engines produce power from 0.5 kW to 10 MW, have efficiencies between 37 – 40%, and lean-burn engines can operate down to NOx levels of about 1 g/bhp-hr. When properly maintained, these engines can run on low grade fuel generated by waste treatment. By using recuperators that capture and return waste exhaust heat, reciprocating engines also can be used in CHP systems in buildings to achieve their energy needs in a cost effective manner [26].

2.3 Emissions control techniques

Various emission control technologies exist for IC engines and these technologies can substantially reduce pollutants of non-methane hydrocarbons (NMHC), CO, and NOx from engine exhaust. Particulate matter (PM) is usually emitted at low mass levels from natural gas engines and should not require aftertreatment. The choice of aftertreatment mainly depends on the whether the engine is run slightly rich, stoichiometric, or lean, because this influences the concentrations of regulated pollutants in the exhaust. Therefore, a single NOx reduction technique should not be applied to both rich-burn and lean-burn natural gas engines. For example, in a lean-burn engine application, an oxidation catalyst can be used to reduce HC, CO, and even PM emissions, but for NOx reduction an additional Selective Catalytic Reduction (SCR) system might be chosen. Table 3 represents typical emission levels that can be expected from a natural gas fueled engine.

Table 3. Typical emissions levels from natural gas engines [27]

Air/Fuel Ratio Lambda (λ)	**Mode**	**Emissions (g/bhp-hr)**			
		NOx	**NMHC**	**CO**	**PM**
0.98	slightly rich	8.3	0.3	13.9	Low
0.99	stoichiometric	11.0	0.2	8.0	Low
1.06	slightly lean	18.0	1.0	1.0	Low
1.74	lean	0.7	1.0	3.0	Low

Commonly applied aftertreatment emissions control techniques for rich stoichiometric and lean-burn engines are listed in Table 4.

Table 4. Commonly applied emissions control technologies [27]

Engine Operation	**Control Technology**	**Targeted Pollutants**	**NOx Reduction %**
Rich/ Stoichiometric	Three-way catalyst	NOx, CO, NMHC	>98
Lean	Oxidation catalyst (two-way)	CO, NMHC	NA
	Lean NOx trap	NOx, CO, NMHC	>80
	SCR	NOx	>95
	Engine coating + Oxidation catalyst	NOx, CO, NMHC	40

2.2.3 NOx control techniques for rich-burn engines

2.3.1.1 Air/fuel ratio adjustment

Adjusting the air/fuel ratio to favor operation reduces the available O_2 to combine with N_2 thereby limiting NOx formation (see Figure 2). The downside to this method is that lower O_2 contributes to incomplete combustion and increases CO and HC emissions. The brake specific fuel consumption (BSFC) suffers as this operation becomes increasingly rich. Also, unless substantial EGR is used, throttling losses at part load may reduce efficiency and thermal losses in the engine may be high.

2.3.1.2 Retarding ignition timing

In most engines the quantity of NOx produced is limited by reaction rate. Retarding the ignition timing delays the initial combustion to a later stage in the power stroke, which in turn reduces the time available at high tempoerature that is needed for NOx formation. However, this increases exhaust gas temperatures, resulting in thermal management issues. Further retarding the timing results in combustion instability, loss of power, and increase in BSFC.

2.3.1.3 Three-way catalyst (TWC)

A Three-way Catalyst, also known as Nonselective Catalytic Reduction (NSCR) has been used for decades to control NOx, CO, and HC emission in gasoline automotive applications. While 1% oxygen content typically gives most efficient engine performance, a net oxygen content of less than 0.5% is required for the successful application of a TWC [28]. A traditional TWC may not be used on a lean-burn engine.

TWC systems have demonstrated the capability of achieving greater than 98% NOx reduction. When running slightly rich, the high exhaust temperature enhances the catalyst performance. Conventional platinum (Pt) and rhodium (Rh) catalysts have been used for stoichiometric natural gas engines [29],[30]. In order for conversion efficiencies to remain high, the air/fuel ratio must be held close to the stoichiometric air/fuel ratio. NOx conversion efficiency drops when the engine is run lean, and the NMHC and CO conversions also decline.

In a TWC, NOx is reduced to N_2 and H_2O, with the simultaneous oxidation of CO and HC to CO_2 and H_2O. For a TWC to operate effectively [31], the

inlet NOx level should be between 2000 - 4000 ppm;

inlet CO level should be between 3000 - 6000 ppm ;

inlet HC level should be between 1000 - 2000 ppm; and

inlet exhaust gas temperature should be between 800 - 1200°F (425 - 650°C)

Figure 4 and Figure 5 show qualitatively the influence of air/fuel ratio on the performance of a TWC. For rich mixtures CO and HC emissions are high, while on lean mixtures NOx is high, with a trade-off between CO and NOx [32]. There is a narrow air/fuel ratio band in which the TWC operates and produces simultaneously low values of CO, HC and NOx. It has been reported that combustion of methane produces less CO than combustion of gasoline [32]. Since CO is needed for the reduction of NOx, the mixture with methane needs to be richer than with gasoline for proper catalyst operation [33].

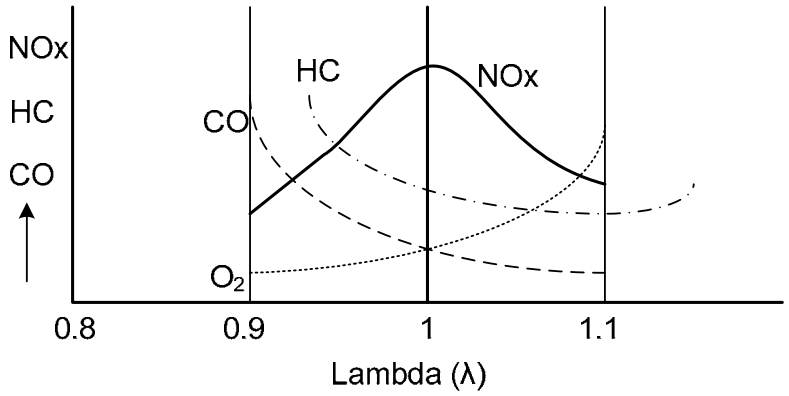

Figure 4. Emissions before TWC [32]

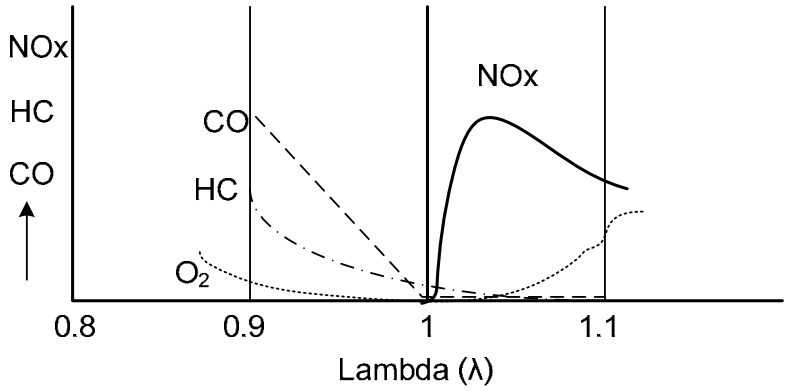

Figure 5. Emissions after TWC [32]

Even though a TWC may be economically applied to a stoichiometric natural gas engine, conventional wisdom argues that stoichiometric operation implies a loss of thermal efficiency and would therefore be employed only if emissions standards cannot be met by alternative systems. However, in-cylinder heat transfer and throttling losses may be reduced by using cooled EGR, and stoichiometric engines are emerging as an attractive option for low NOx operation.

2.3.1.4 Exhaust Gas Recirculation (EGR)

Exhaust gas recirculation replaces a portion of the intake air with recirculated exhaust gas. The exhaust gas acts as a heat sink and also reduces the available O_2 content, resulting in lower combustion temperature and NOx emissions. The presence of CO_2 and water vapor in the recirculated exhaust gas increases the specific heat capacity of the in-cylinder mixture and this reduces the combustion temperature [34].

2.3.2 NOx control techniques for lean-burn engines

2.3.2.1 Air/fuel ratio adjustment

In a lean-burn engine, adjusting the air/fuel ratio towards the lean operation side increases the volume of air available for the combustion process. This increases the heat capacity of the mixture and lowers the combustion temperature, resulting in lower NOx formation. Excessively lean mixtures may result in combustion instability and may lead to misfire and incomplete combustion. Leaning the mixture is an attractive way to reduce NOx, but there is a limit to the amount that NOx may be reduced in this way.

2.3.2.2 Ignition timing adjustment

Retarding the ignition timing in lean-burn natural gas engines has a similar effect on NOx emissions compared to rich-burn engines.

2.3.2.3 Exhaust Gas Recirculation (EGR)

EGR (whether internal or external) reduces oxygen concentration in the combustion chamber by diluting the incoming ambient air with exhaust. During combustion, the lower oxygen content has the effect of reducing flame temperatures, which in turn reduces NOx production since the NOx production rate is exponentially proportional to flame temperature [35]. However, since the exhaust gas is still quite hot when directly recirculated back into the combustion chamber, the benefits are limited. Cooled EGR, now commonplace on diesel engines, is therefore attractive.

2.3.2.4 Selective Catalytic Reduction (SCR)

SCR technology reduces NOx to N_2 from lean-burn exhaust gas when it passes through a catalyst in the presence of a reducing agent such as ammonia (NH_3) or urea ($(NH_2)_2 CO$). NOx reductions of 80 to 90% are possible with SCR, and higher reductions are possible with the use of more catalyst area, greater volume of reducing agent and more subtle controls, but there is risk of exhausting ammonia if too much reductant is used. Urea decomposes in the hot exhaust gas and SCR catalyst, releasing ammonia. Approximately one mole of ammonia is required per mole of NOx at the SCR reactor inlet in order to achieve an 80 to 90% NOx reduction [36].

Urea is commonly used as nitrogen fertilizer. Over 85% of urea consumption is for fertilizer use with the balance consumed in various industrial processes [37]. Properties and manufacture of urea are presented in references [38], [39] and [40].

Johnson Matthey is one of the largest suppliers of SCR catalysts. Their webpage [41] states that, in general, SCR catalysts are used in lean-burn applications where oxygen content is greater than 1% in the exhaust gas stream. The basic reaction steps in an SCR catalyst are shown below, where NO and NO_2 are converted to N_2 and H_2O using ammonia as a reducing agent

$$4NO + 4NH_3 + O_2 \longrightarrow 4N_2 + 6H_2O \quad (8)$$

$$2NO_2 + 4NH_3 + O_2 \longrightarrow 3N_2 + 6H_2O \quad (9)$$

$$NO + NO_2 + 2NH_3 \longrightarrow 2N_2 + 3H_2O \quad (10)$$

In Equation 8, the NOx conversion rate increases when there is a mixture of NO and NO_2 present in the exhaust gas as the reactions in Equation 6 and 7 occur in parallel. For each 1 g/bhp-hr reduction of NOx, an engine with SCR consumes urea at a rate of approximately 1.5% of the amount of fuel used [35].

SCR systems add a significant cost to the installation and maintenance when integrated to an existing engine system (Table 5). A SCR system can be retrofitted on a 2300hp IC

engine for approximately $158,000 [42]. The annual operating costs of the system can be as high as $67,000 per year. This includes the ammonia or urea supply cost, catalyst washing, the replacement of sensors, thermocouples, and labor. The annual operating costs of an SCR system are significantly affected by the size of the engine system on which it is implemented.

Table 5. SCR cost analysis [42]

Variables	**For 90% NOx reduction**	**For 50% NOx reduction**
Engine (hp)	2336	2336
Annual operation (hours)	8000	8000
Fuel consumptions (lb/bhp-hr)	0.34	0.34
Engine speed (rpm)	1800	1800
Engine load (%)	100	100
NOx (ppm)	687	687
Urea wt% with balance water	0.32	0.32
NOx emissions (tons/year)	101	101
NOx Reduction (%)	90	50
Tons of NOx reduced	91	50
Capital cost for system ($)	**157,590**	**142,290**
Annual operating cost ($)	**66,882**	**46,116**

Since the difference in capital cost for the 50% and 90% installations are relatively small, it is preferable to use a 90% reduction system.

The cost of the reducing agent (urea) greatly affects the implementation of an SCR system. A study was conducted by Fable et al. [43] to evaluate the cost of delivering aqueous urea to service stations for use in transportation. The study showed that the production cost of 32% aqueous urea solution could range from $0.12 to $0.30 per gallon. But the cost to the end customer would be dominated by the distribution cost which could range anywhere from $0.70 to $35 per gallon.

The Fable et al. study also mentions that the cost to purchase and manufacture urea for SCR systems is influenced by the price of natural gas. Figure 6 shows the manufacturing cost of urea vs natural gas prices. In 2002 the average price for natural gas was $3.00 per million Btu. The price of natural gas was $6.14 per million Btu as of July 21, 2006 according to the New York Mercantile Exchange Inc. (NYMEX) [44].

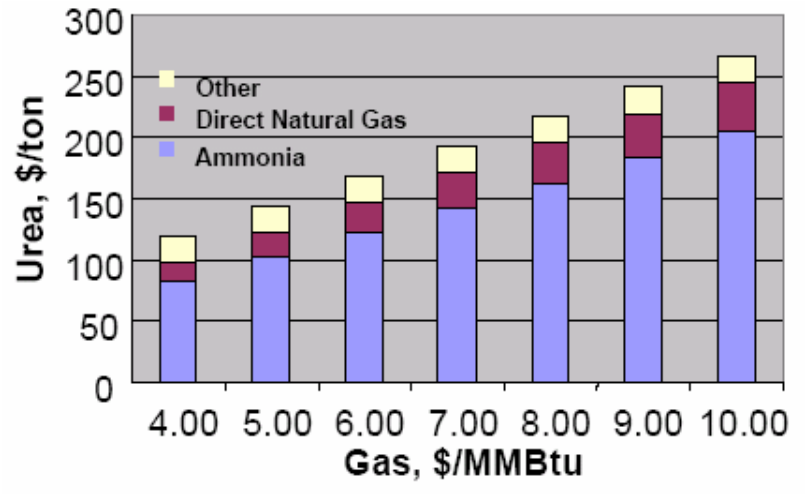

Figure 6. Urea manufacturing cost $/ton vs. natural gas price $/million Btu [42]

Another study conducted by NREL/DOE showed that about 1 gallon of urea would be consumed for each 18 gallons of diesel fuel on heavy-duty diesel vehicles equipped with SCR systems in order to reach the 2007 NOx targets [45]. Note that reduced engine-out NOx emissions reduce the urea requirement.

2.3.2.4 Lean NOx Trap (LNT) or NOx Adsorber Catalyst (NAC)

The concept of a LNT involves adsorption of NOx under lean exhaust conditions and conversion of the stored NOx into N_2 under rich exhaust conditions. The temperature window for NOx conversion is between 200-550˚C [46]. The catalysts are sensitive to sulfur poisoning and therefore require fuels with extremely low sulfur content, and perhaps even low sulfur lubricants.

A typical LNT consists of a ceramic substrate coated with a washcoat that combines three active components, an oxidation catalyst (platinum - Pt), an adsorbent (Barium Oxide - BaO) and a reduction catalyst (Rhodium - Rh).

NOx from the exhaust gas reacts with oxygen and is adsorbed in the form of nitrates produced by reversible reactions between the NOx and Ba [47]-[49].

$$NO + \tfrac{1}{2} O_2 \longleftrightarrow NO_2 \qquad (11)$$

$$BaO + 2NO_2 + \tfrac{1}{2}O_2 \longleftrightarrow Ba(NO_3)_2 \quad (12)$$

During regeneration periods, when the engine runs at fuel rich conditions the barium nitrate becomes unstable and decomposes producing NO and NO_2.

$$Ba(NO_3)_2 \longleftrightarrow BaO + 2NO + 1\tfrac{1}{2}O_2 \quad (83)$$

$$Ba(NO_3)_2 \longleftrightarrow BaO + 2NO_2 + \tfrac{1}{2}O_2 \quad (94)$$

The NOx is then reduced.

$$NO + CO \longleftrightarrow \tfrac{1}{2}N_2 + CO_2 \quad (105)$$

The NOx adsorption reactions are what make the LNT different from traditional TWC NOx decomposition. Reactions with sulfur in the LNT are problematic. The sulfate is more stable than the nitrate, and renders the barium site useless for NOx adsorption. Very high temperature regeneration can re-enable the sites.

$$SO_2 + \tfrac{1}{2}O_2 \longleftrightarrow SO_3 \quad (116)$$

$$BaO + SO_3 \longleftrightarrow BaSO_4 \quad (127)$$

Much has been written on the durability and poisoning issues of NOx- Trap catalysts [50]-[63].

2.3.2.5 Lean NOx Catalysts (LNC)

A LNC uses unburned hydrocarbons to reduce NOx over a catalyst. The catalyst can be made up of platinum or zeolite. The operation of a LNC requires continuous injection of fuel upstream of the catalyst. The NOx conversion efficiency is usually too low to provide an order of magnitude NOx reduction. LNC have temperature range limitations that cause conversion efficiencies to be lower than desired in typical operation [64]. A passive LNC uses the hydrocarbons present in the exhaust, where as an active LNC requires additional hydrocarbons to be injected upstream of the the catalyst [65]. A zeolite based catalyst is active at temperatures between 350 and 450°C, resulting in 60% NOx

conversion, while a platinum catalyst is active at lower temperatures of approximately 200 - 300˚C with 50% NOx conversion capability in laboratory conditions [66].

2.3.3 Other NOx control techniques for natural gas engines

2.3.3.1 Water injection

Addition of water into the combustion chamber acts in the same way that EGR does. It lowers peak combustion temperatures and decreases NOx formation. Water can be introduced to the engine cylinder through direct injection or fumigation into the intake air. Research conducted at Southwest Research Institute by Callahan *et al*, on direct water injection experiments on a lean-burn natural gas engine concluded that injecting water near TDC with a water/fuel ratio of 0.80 was effective in reducing NOx by approximately 24% [67]. This will not provide the order of magnitude reduction sought by the ARES program for lean-burn engine out emissions.

2.3.3.2 Cooled exhaust gas recirculation

Spark ignited engines can now take advantage of cooled EGR technology used in diesel engines [68]. A cooled EGR system takes a measured quantity of exhaust gas, then passes it through a heat exchanger before mixing it with the incoming air charge to the cylinder. NOx emissions are reduced [34].

2.3.3.3 Homogeneous Charge Compression Ignition (HCCI)

With HCCI the air/fuel charge autoignites at a point near top dead center. The heat release is controlled using intake manifold temperature or EGR under constraint of a fixed compression ratio. The point of combustion is difficult to manage, and research in this area is still in its infancy. Fuel composition, particularly the higher hydrocarbon content (ethane, propane, and butane) of the fuel is of primary concern [69].

2.3.4 Evaluation of competing emissions reduction technologies

A study was conducted by the U.S. Air Force to evaluate available NOx reduction technologies [70]. The authors devised a numerical rating system to evaluate the merits of

competing technologies. The system was divided into five criteria for a total of 100 points based on emissions reduction capability (25 points), cost (25 points), reliability and maintenance (20 points), deployability (20 points) and fidelity of data (10 points). Three pre-combustion and three post-combustion NOx reduction technologies were evaluated.

Only the emissions reduction capability of each technology is discussed in this report. Technologies that achieved greater than 90% reduction over all loads earned maximum points, followed by those achieving reductions in the 70 to 80% range. Points were prorated for systems with greater than 69% that varied with load and systems with less than 69% NOx reduction scored 0. Each technology was further evaluated on increase in carbon monoxide (CO), particulate matter (PM), hydrocarbons (HC), or secondary emissions. Furthermore, the technologies had to be deployable on or before 2000.

Pre-combustion NOx reduction technologies

- Water-in-Fuel Firing (WFF) – water was emulsified with the fuel to act as a detergent and injected into the engine thereby lowering the combustion temperature to reduce NOx formation.

- Oxygen-Enriched Air (OEA) – Intake air was enriched with oxygen up to 21% to improve combustion.

- Dual-Fuel Firing (DFF) – Natural gas was used as a second fuel in a diesel engine and was injected into the intake manifold. Natural gas was chosen since it has lower NOx production than diesel fuel.

Post-combustion NOx reduction technologies

- Selective-Catalytic Reduction (SCR) – Ammonia was used as a reductant on a vanadia-coated titanium honeycomb catalyst.

- NOx-Sorbent Filtering (NSF) – A granular activated carbon material was used to adsorb NOx from cooled exhaust gas.

- Non-Thermal Discharge (NTD) – An electrically driven process that used high dielectric fields and a chemical agent to promote the conversion of NOx into NO_2. The NO_2 was then cooled and a scrubber was used to remove the water soluble compounds from the exhaust gas.

The evaluation criteria for emissions reduction capability with numerical ratings are shown in Table 6 [70]. It was concluded in the study that, based on the criteria of emissions-reduction, cost, reliability, maintainability, deployability, the Water-in-Fuel Firing method, Selective-Catalytic Reduction, and NOx-Sorbent Filtering technologies are viable to attain overall environmental compliance. However, the study mentions that these three systems are not turnkey solutions, and therefore need further development.

Table 6. Numerical ratings for emission reduction technologies [70]

Rating Element	**Technology**					
	DFF	NTD	OEA	SCR	WFF	NSF
NOx Reduction	0	6	0	5	10	8
Impact on CO	0	1	2	3	1	3
Impact on PM	3	1	3	1	3	1
Impact on HC	0	2	3	2	0	3
Secondary Emissions	2	2	2	1	3	3
Deployment Schedule	3	0	1	3	3	2
Total: Emissions reduction (25)	8	12	11	15	20	20

The NOx-Sorbent Filtering (NSF) method was one of the highest scored under the emissions reduction category in this review [70] and received 8 out of 10 for NOx reduction. In this method the exhaust gas was first cooled using an air-to-air heat exchanger and then filtered to remove PM. In the next step the NOx was physically adsorbed on to a filter containing granular activated carbon material. The NSF system used in this study was similar to the first two steps in the Selective NOx Recirculation (SNR) system discussed below in this report. However, the SNR system adds further steps, where NOx is desorbed from the carbon material and recirculated back into the engine for decomposition.

2.4 *ARES proposals for future NOx reduction strategies*

The Advanced Reciprocating Engine Systems (ARES) consortium was launched by the US Department of Energy (DOE) to develop a new class of cost effective gas fueled internal combustion engines by 2010 for stationary power generation applications. The ARES program is a multiple participant arrangement involving DOE, three US engine manufacturers, national laboratories and universities. The engine output range targeted by ARES is approximately 500 to 6500 kW for power generation applications [71]. Under the ARES program, special attention was given to research on advanced materials, unique fuel and air handling systems, advanced ignition and combustion systems, catalysts, lubricants, and technologies that are compatible with existing transmission and distribution systems.

The ARES program consists of three phases, each with specific targets to reach the program's overall goals. Phase 1 was completed during the 2004 - 2005 timeframe, while the final phase III is expected to be completed during 2009 - 2010. ARES goals for advanced gas engines are listed below in Table 7 [1].

Table 7. Overview of ARES goals by 2010 [1]

Installed Costs	$400-$450 per kW
Maximum Efficiency	50% Thermal, 80+% with CHP
NOx Emissions	0.1 g/bhp-hr
Maintenance Cost	$0.01 per kW-hr
Major Service Interval	Annually
Operator Training	100 hours

The Selective NOx Recirculation technology presented in this report was funded under the ARES program to achieve high NOx reduction.

2.4.1 Proposal from Cummins Inc. for NOx reduction

The current ongoing innovations at Cummins include the advanced lean-burn gas project under the ARES Program that investigates a cost effective method to reduced NOx

emissions using an after-treatment system, improved engine efficiency by reducing parasitic losses, extend maintenance intervals in improving ignition systems and reduced initial cost by increasing BMEP [72].

The phase I goals of 44% brake thermal efficiency and 0.1 g/bhp-hr of NOx emissions were reached and made ready for field testing [73]. The key strategies for improving engine efficiency were by increasing effective expansion ratio, improving air handling, using advanced engine controls, and reducing friction on lean-burn spark ignition engines. This was a 7% improvement in brake thermal efficiency (BTE) from the 2001 baseline level. NOx emissions target was achieved by using a SCR system [73].

To reach the phase II goal of 47% BTE Cummins Inc. proposes further improvement in the combustion system on a stoichiometric-burn engine operation mode. A stoichiometric engine using cooled EGR with a TWC aftertreatment system is projected to be the most cost effective solution to reduce NOx below 0.1 g/bhp-hr without the use of a urea-based SCR system [73].

Phase III goal of 50% brake thermal efficiency may be achieved by through HCCI that does not require an aftertreatment system to further reduce NOx emissions [74].

2.4.2 Proposal from Caterpillar Inc.

The phase I goal of developing a lean-burn natural gas engine with 44% efficiency and 0.50 g/bhp-hr of NOx emissions was introduced in 2004. Their approach was to improve the lean-burn open chamber combustion system, increase pressure of the single stage turbocharger, reduce engine friction, and use a Caterpillar in-cylinder air/fuel ratio controls. NOx emissions were limited by the use of a SCR system [75].

A significant stride towards reaching phase II goals is to use a High Efficiency Advanced Turbocharger (HEAT), which has 65 – 68% turbocharging efficiency and pressure ratios above 4.5 [76]. To reach the NOx target Caterpillar Inc. is developing a high BMEP stoichiometric combustion concept utilizing EGR and a passive 3-way catalyst (SC-3: Stoichiometric, Clean exhaust induction, 3 way catalyst) while simultaneously reducing CO and HC emissions to low levels [75]. The SC-3 system would use 20-30% EGR for a

stoichiometric engine with up to 2% efficiency penalty and would emit ultra low emissions of 0.1 g/bhp-hr of NOx, 0.1 g/bhp-hr of CO, and 0.15 g/bhp-hr THC [77].

The prime path options to reach phase III goals are to utilize open chamber HCCI combustion and reformed fuel open chamber combustion that does not require an aftertreatment system to reduce NOx. A summary of phase III option paths are listed in Table 8 [76].

Table 8. Caterpillar Inc. prime path options for NOx reduction [76]

Combustion Options	**NOx Aftertreatment Options**
HCCI	Not required
SC-3	Passive three way catalyst
Reformed fuel open chamber	Not required
Dual fuel concepts	To be determined
Lean-burn with miller cycle	Advance SCR

2.4.3 Proposal from Waukesha Dresser Inc.

Waukesha Engine Company has been manufacturing natural gas stoichiometric and lean-burn engines from 1985. The current VHP product line stoichiometric engines carry 33% efficiency and 0.15 g/bhp-hr NOx (with catalyst) and lean-burn engines of 35% efficiency with 0.7-1.25 g/bhp-hr NOx [78]. Their VGF product line carries stoichiometric engines with 35% efficiency and Lean-Burn with 39% efficiency. The technical challenges they face to meet ARES program goals are improving ignition systems, friction reduction, sensors, and exhaust after-treatment [79],[80]. This company also proposes a cooled-EGR stoichiometric engine with a TWC as an aftertreatment system.

2.4.4 Proposal from National Laboratories

2.4.4.1 Oak Ridge National Laboratory (ORNL)

A Lean NOx Trap system for lean-burn natural gas engines was proposed by Parks *et al*, ORNL [81]. The catalyst stores NOx during lean conditions and needs regeneration under rich conditions. The sorption chemistry was described as [81]:

$$2NO + O_2 + Pt + K_2CO_3 \longrightarrow KNO_2 + KNO_3 + Pt + CO_2 \quad (13)$$

The regeneration of the LNT required hydrocarbons and was described as [81]:

$$KNO_2 + KNO_3 + Pt + HC \longrightarrow 2KOH + N_2 + CO_2 + Pt + H_2O$$

$$2KOH + N_2 + CO_2 + Pt + H_2O \longrightarrow K_2CO_3 + N_2 + 2H_2O + Pt$$

Total NOx reduction of over 90% was demonstrated, and no additional reductants were needed in this LNT system. There was a narrow operating temperature of this system where hydrocarbon oxidation is best at temperatures greater than 450˚C and the NOx storage capacity is high at temperatures lower than 550˚C. The fuel penalty was 1- 5% for the Oak Ridge dual chamber system.

2.4.4.2 Argonne National Laboratory (ANL)

A NOx reduction method by nitrogen enrichment of the air intake was presented by researchers at ANL [82]. An air separation membrane was proposed to filter out a portion of the O_2, CO_2 and H_2O from the incoming air and allow N_2 through the membrane into the air intake of the engine. This increased the inert combustion temperature resulting in lower NOx emissions. Initial tests were conducted using nitrogen injection, and this showed NOx reduction success.

2.4.5 Summary

"Through 2020, natural gas will remain the energy source of choice to meet industrial end users' needs, by providing increased value relative to other energy sources in energy efficiency, productivity, environmental performance and innovative uses" [83].

Although historically diesel engines have been popular for power generation applications, due to diesel emissions concerns natural gas fueled spark ignited engines are gaining popularity for the higher duty-cycle stationary power market of over 500 hr/yr [84]. As an added advantage with stationary natural gas engines, waste heat can be recovered from the hot engine exhaust and from the engine cooling systems to produce either hot water or low pressure steam for combined heat and power (CHP) applications [84].

The emissions of natural gas spark ignited engines have been reduced significantly in the last decade through better air handling, mixing and control of the combustion processes, and through use of exhaust gas catalysts. However, a catalyst of an IC engine that employs a TWC, SCR, or a LNT may become deactivated due to chemical poisoning and thermal breakdown. This process is commonly known as catalyst aging. In some cases cleaning procedures can remove contaminants from the catalyst, usually restoring catalytic activity.

The ARES consortium brings together leading engine manufacturers, US national laboratories, universities, and other research organizations under the US Department of Energy sponsorship. These parties are cooperating to achieve 50% thermal efficiency and NOx emissions of 0.1 g/bhp-hr by 2010. The ARES goals represent improvements of 30% and 95% in efficiency and emissions respectively from present day averages. Various strategies have been explored in the ARES program, and there are proposals to use stoichiometric combustion in the future for low NOx emissions.

2.6 Selective NOx Recirculation

Selective NOx Recirculation is a NOx reduction aftertreatment system designed for lean-burn reciprocating engines. SNR involves NOx removal from lean exhaust gas by NOx adsorption and subsequent selective external re-circulation of NOx back into the combustion chamber and decomposition of NOx during the combustion process. Unlike conventional EGR, a high concentration of NOx is recycled into the engine intake, rather than post-combustion air as with EGR.

The SNR system can be implemented as a single adsorber system or as two parallel adsorbers in the exhaust. With a single adsorber system the exhaust from the engine bypasses the system when the adsorber is in desorption mode. In a parallel system, one adsorber acts in adsorption mode while the other in desorption mode, so that continuous operation is possible. A control valve is provided to separate the exhaust from one line to the other.

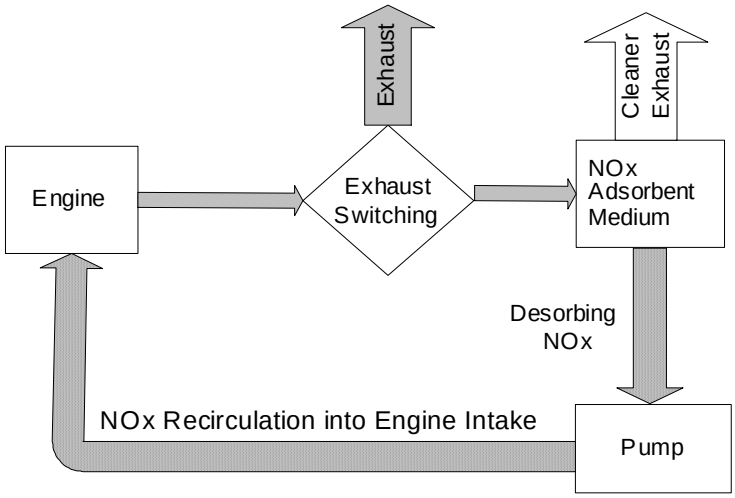

Figure 7. Single adsorber SNR system

The SNR process has no consumables (other than sorbent replacement) nor does it have any byproducts or secondary emissions, but instead uses the nature of the combustion itself to decompose the recirculated NOx.

There are two major focus areas involved with SNR. First is to understand and maximize the NOx decomposition phenomena within the combustion chamber and second is to research the behavior of suitable NOx adsorbent materials that can hold sufficient quantities of NOx from lean exhaust gas and desorb the NOx with relative ease. System design is also required.

2.6.1 Decomposition Process

NOx decomposition or re-burning process is a method which is already used in coal fired plants to control its NOx emissions. The NOx re-burn process starts by creating a

secondary combustion or re-burn zone downstream from the main burner. The combustion gases that result from main combustion zone move to the re-burn zone where a fraction of fuel, usually natural gas, is injected over the burners. The injection of additional fuel creates a fuel-rich zone in which the NOx formed in the main combustion zone is converted to nitrogen and water vapor. Also, any unburned fuel leaving the re-burn zone is subsequently burned to completion in a downstream burnout zone where additional air is injected. Methane combustion for NOx reduction was initially suggested for re-generable flue gas clean up processes. Yet et al. [85] showed that in large coal fired power plants NOx emissions were reduced by injecting natural gas and air into the hot flue gas that comes from coal combustion.

2.6.2 Experimental Results by Daimler-Benz and Johnson Matthey-1998

Researchers from Daimler-Benz and Johnson Matthey conducted experiments on two types of diesel engines and a gasoline engine - a naturally aspirated engine equipped with a pre-chamber and a turbocharged engine operating on direct fuel injection and a gasoline engine operating under slightly rich to lean conditions [86].

The experimental tests were conducted by injecting NOx from gas cylinders into the intake air of the engines. The degree of engine NOx decomposition was evaluated by comparing the NOx concentration in the exhaust with and without feeding NOx in relation to the NOx in the intake air. The equation used to evaluate decomposition efficiency is as follows:

$$\eta_{NOx} = 1 - \frac{NOx_1 - NOx_2}{NOx_{feed}} \tag{20}$$

NOx_1 and NOx_2 represent the NOx concentration with and without NO injection respectively, and NOx_{feed} is the quantity of NO injected.

They noted that the diesel engines had a similar decomposition pattern. Decomposition efficiency increased with an increase in load while engine speed had less influence on NOx decomposition. The NOx decomposition efficiency for the naturally aspirated engine was 10 - 40% and for the turbocharged engine it was 20 - 50%.

Their 2.2 liter naturally aspirated SI engine experiments were conducted at air/fuel ratios that ranged from λ = 0.96 – 1.14. The engine was operated at loads from 2 – 8 bar and speeds from 1000 - 5000 rpm. The highest decomposition percentage was about 90% at 8 bar and 1000 rpm. This was because of the high combustion temperature at a higher load and more residence time of the injected NOx in the combustion chamber influenced the NOx decomposition. They also noted that the CO in the exhaust was reduced and HC was not affected by NOx injections. They also concluded that the NOx decomposition efficiency was almost independent of the injected NOx concentration in the intake air. However, they observed that the air/fuel ratio had a great impact on the NOx decomposition. At stoichiometric and slightly rich conditions the destruction efficiency was observed to be 55 to 90%, and at lean conditions it was about 20%.

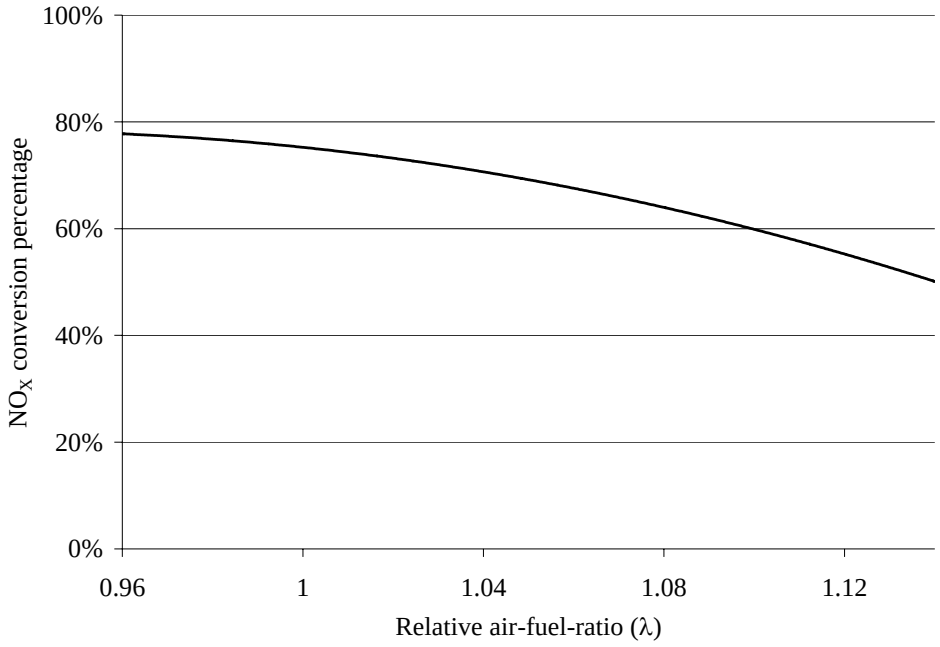

Figure 8. NOx decomposition vs. λ in a SI engine [86]

2.6.3 NOx Storage Materials

The researchers at Daimler-Benz and Johnson Matthey have investigated suitable storage materials to adsorb NOx under lean-burn condition [87]. These catalyst materials are namely barium aluminates, barium tin perovskite, and Barium Y-zeolites where they

adsorbed NOx selectively and store it as nitrate or nitrite species. NOx was stored at low temperatures and the regeneration was done by heating the adsorber.

2.6.3.1 Barium Aluminates

Barium aluminates were tested for their adsorption and desorption capabilities by Chaize *et al*. [87]. It was observed that the adsorption temperature for the washcoat was between 80°C and 200°C and that NOx was completely desorbed at 500°C. The adsorption capacity of NOx was 2.1% of the weight of the catalyst.

2.6.4.2 $BaSnO_3$ Perovskite

Perovskite was formed into a solid material and was tested for NOx storage and release capabilities. Its adsorption temperature range was 80 - 280°C and the desorption temperature range was 450 - 550°C. The NOx Adsorption capacity of perovskite was between 1.4 – 1.9% of its weight [87].

2.6.4.3 Ba-Y Zeolite

Chaize et al. exposed the Ba-Y zeolite adsorber to a gas mixture of equal amounts of NO and NO_2. The temperature was raised from 100 to 560°C in the adsorber and the effects were monitored. It was noted that at 100°C to 200°C the adsorber was capable of reducing one third of the concentration and at 227°C the Ba-Y zeolite started desorbing the NOx [87].

2.6.4.4 Activated carbon

Activated carbon is capable of removing substances from a fluid through an adsorption process. Usually, certain particles or elements are bound to an adsorbent particle surface by either chemical or physical attraction. Activated carbon is mostly derived from charcoal and may consist of a mixture of carbonized materials such as coconut shells, nut shells, and wood. Once the mixture is activated it constitutes a material with an exceptionally high surface area and includes a large number of micropores. For example,

activated carbon sample OVC4x8 manufactured by Calgon Carbon Corporation has a surface area of 1200 m^2 per gram of carbon granules [88].

Activated carbon and carbon fibers have been used to convert NOx into N2 in the presence of NH3 or its oxidation into NO_2 and NO_3 and trapped onto water [89].

2.6.3 Experimental results by Sorbent Technologies, Inc.

The overall SNR scheme researched by Sorbent Technolories was similar to the concept developed by Daimler-Benz AG, but without the sulfur sensitivity of the NOx trapping materials that Daimler-Benz employed. With the Sorbent Technologies material, NOx adsorption occurred only at low temperatures, from ambient to about 200˚F. Therefore, an exhaust gas cooler was added to avoid excessive heat. Their findings are summarized below [90].

A sorbent bed was constructed to handle exhaust flow rates of 100 – 400 acfm that passed gas horizontally through a vertical rectangular bed of sorbent material. A special type of sulfur tolerant carbon granule was used to adsorb the NOx. Experiments were conducted to examine NOx adsorption onto the carbon material, desorption from the carbon, and decomposition in the combustor.

To evaluate the relative NOx adsorption, fixed-bed adsorption runs were performed by injecting 100 and 500 ppm NO and NO_2 concentrations at a variety of temperatures. The results from these tests are shown in Figure 9. For the initial run, 80% of NO_2 was adsorbed by the carbon compared to 40% of NO adsorption at up to 40˚C (105˚F). However, it was concluded that after the first desorption cycle the sorbent material showed similar behavior towards NO and NO_2 at approximately 100˚F. It can be seen that exhaust gas temperature played a major role in adsorber efficiency.

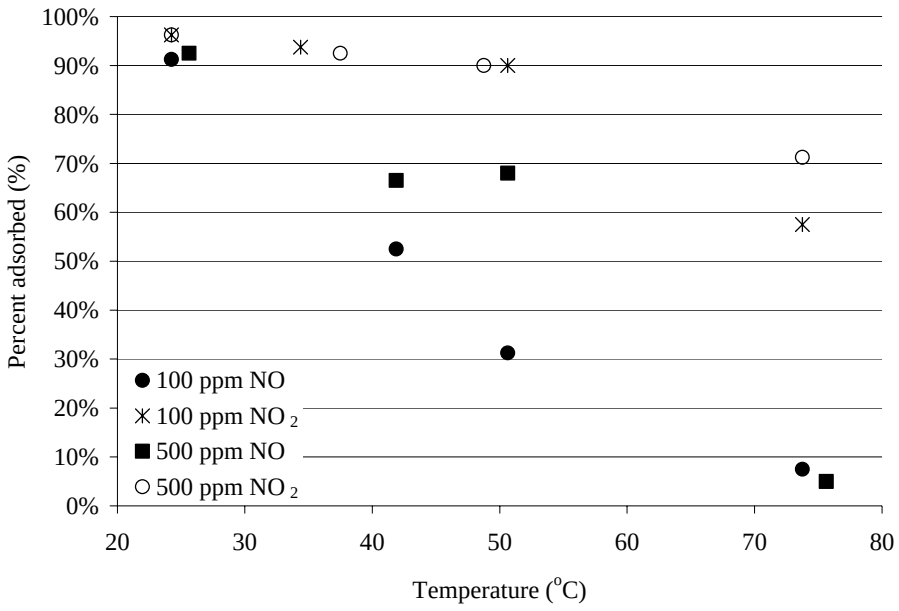

Figure 9. Percent adsorbed as a function of the gas temperature for concentrations of NO and NO_2 [90]

NOx desorption was evaluated by conducting two independent series of tests by exposing the bed to 1000 ppm of NO and then to 1000 ppm of NO_2. Results from these tests are summarized in Figure 10.

This particular adsorber setup was able to adsorb 2.0 weight percent of NO in the first cycle before breakthrough had occurred. When subjected to a hot air stream at 300˚C the bed was able to desorb 90% of the stored NO. The consequent adsorption and desorption runs on NO and NO_2 showed similar results.

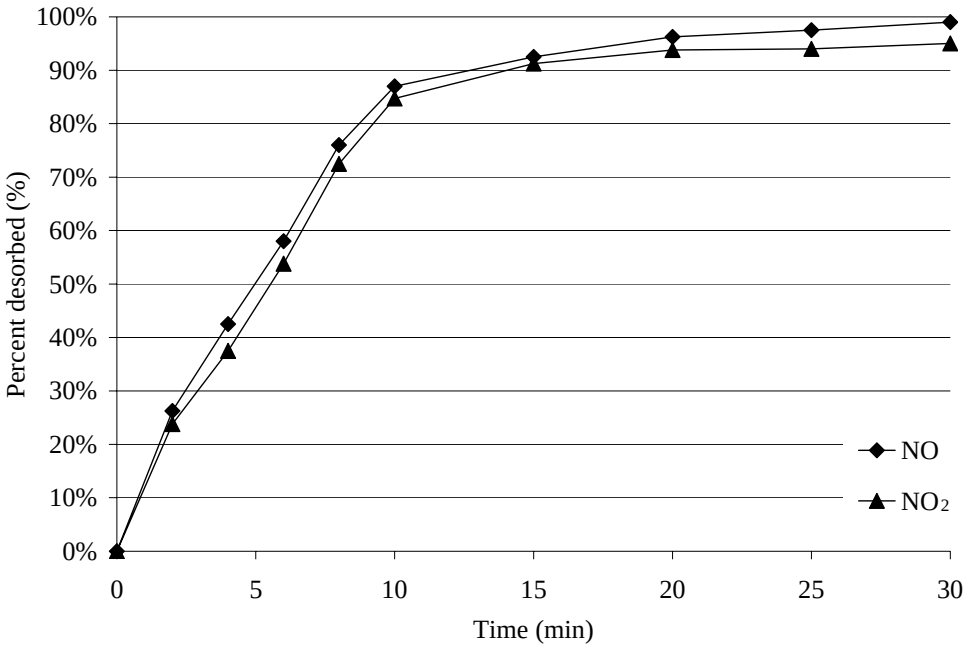

Figure 10. Desorption efficiency as a function of desorbtion time for NO and NO_2, from research conducted by Sorbent Technologies, Inc. [90]

They achieved NOx decomposition efficiencies of over 80% for compression ignition engines using fuels other than diesel and for a prototype diesel fueled spark ignition engine.

2.6.5 Effect of Sulfur on NOx Storage Materials

The researchers from Daimler-Benz and Johnson Matthey also studied the effect of sulfur content on NOx storage materials [87]. It was noted that the performance of NOx storage materials was reduced by the sulfur content in the exhaust. Under lean conditions the alkali and alkaline earth metals form stable sulfates [87]. In order to know the effect of sulfur on NOx adsorbers the researchers used two fuels which had different sulfur contents. They used less than 10 ppm (parts per million) (Sweden quality) and 370 ppm (general European market quality) fuel [87]. It was noted that the NOx storage efficiency was reduced from 80 to 55% when exposed to 370 ppm sulfur fuel level [87]. There was no decrease in the NOx storage efficiency when the adsorbers were exposed to less that 10 ppm sulfur fuel.

3. Selective NOx Recirculation

3.1 Introduction

This section describes the experimental procedure, instruments used and results obtained relevant to the SNR method for NOx reduction. The experiments were conducted at the Center for Alternative Fuels, Engine and Emissions (CAFEE) Research Center at West Virginia University.

The engine runs consisted of three experimental campaigns as described in Table 9.

Table 9. Summary of experimental test engines and their controlled variables

Campaign	Engine	Test Description	Variables
I	1993 Cummins L10G	Lean with no EGR	Speed, load and injection quantities
II	1998 Cummins L10G, and 1998 Honda GX390 as Ad-hoc experiment	Slightly rich with limited EGR control on Cummins engine	Speed, load
III	1998 Cummins L10G	Rich to stoichiometric with full EGR control, in-cylinder pressure measurement	Speed, load, EGR%, and injection quantities

The first experimental campaign tests were conducted on the 1993 Cummins L10G natural gas engine during lean-burn combustion. It was observed that the air/fuel ratio, injected NO quantity and engine operating points affected NOx decomposition rates in the engine. A highest NOx decomposition rate of 27% was measured from this engine. At the end of campaign I, chemical kinetic behavior of the combustion was modeled using the CHEMKIN software package from Reaction Design. This software package was used to model natural gas engine spark ignition combustion characteristics, and HCCI combustion and emissions [91]-[93]. These predictions were performed to relate the experimental data with the established rate and equilibrium models. NOx decomposition rates from 35 - 42% were estimated using the CHEMKIN software for the lean-burn case. This provided insight on how to maximize NOx decomposition rates for a natural gas engine.

The second experimental campaign was performed to acquire both stoichiometric and slightly rich-burn NOx decomposition rates. Prior to using the 1998 Cummins L10 engine in a rich-burn fashion, the smaller 0.389 liter Honda gasoline engine (Table 12) was used as an ad-hoc experiment to obtain NOx decomposition rates at higher in-cylinder temperatures. This data complemented the results obtained from the newer Cummins engine when operated at slightly rich-burn conditions. Although external EGR was added to the Cummins engine, it was not varied independently at each operating point. Decomposition rates of up to 92% were demonstrated. Additionally, in-cylinder pressure was measured to calculate engine indicated mean effective pressure (IMEP) changes due to NOx injections and EGR variations, and to confirm conditions in the cylinder.

The third experimental campaign gathered NOx decomposition data at 800, 1200 and 1800 rpm with EGR managed in an external loop from 0% to point of misfire. The air/fuel ratio was set at stoichiometric and slightly rich conditions and NOx decomposition rates were calculated for each set of runs. Modifications were made to the engine exhaust manifold to record individual exhaust temperature data.

3.2 Experimental equipment and approach

3.2.1 Test engines

A 1993 Cummins L10-240G natural gas lean-burn engine was used during the initial stages of the research. A 300 hp Mustang Eddy current dynamometer was used to absorb power output from the engine. It was controlled by a DYN-LOC IV Digital Dynamometer Controller. The fuel injection system of the engine consisted of a mechanical fuel metering system with no feedback control. This had limitation in changing the air/fuel ratio and emissions stability. The engine characteristics are shown in Table 10.

Table 10. 1993 Cummins L10G test engine specifications

Engine serial #	34683888
Displacement	10 liters
Number of cylinders	6 (in-line)
Firing order	1-5-3-6-2-4
Fuel Introduction	Carburetor
Aspiration	Turbocharged

Bore	125 mm (4.921 in)
Stroke	136 mm (5.354 in)
Compression ratio	10.5 : 1
Rated power	240 bhp
Rated speed	2100 rpm
Torque	750 ft-lb
BMEP	12.8 bar

Due to limitation in air/fuel ratio control of this engine a newer 1998 Cummins L10G engine was used procured from Bell Power Systems with the assistance of Cummins Engine Company. The engine specifications are given in Table 11. The injection system of this new engine consisted of an electronic fuel injection system with closed-loop control. This provided a more stable air/fuel ratio and improved repeatability of the tests. The engine was connected to a 300 hp alternating current (AC) motoring dynamometer.

Table 11. 1998 Cummins L10G test engine specifications

Engine serial #	34933223
Displacement	10 liters
Number of cylinders	6 (in-line)
Firing order	1-5-3-6-2-4
Fuel Introduction	Electronic Fuel Valve/Mixer
Aspiration	Turbocharged
Bore	125 mm (4.921 in)
Stroke	136 mm (5.354 in)
Compression ratio	10.5 : 1
Rated power	280 bhp
Rated speed	2100 rpm
Torque	900 ft-lb
BMEP	15.3 bar

In addition to using these two engines some exploratory work on stoichiometric-burn NOx decomposition was performed using a gasoline engine. The intent was to evaluate the NOx decomposition at higher in-cylinder temperatures and lower available oxygen concentrations before proceeding with similar research on the 1998 natural gas engine. The research was not performed to extend the study to gasoline technology. The engine specifications are given in Table 12. This engine was part of a Hercules brushless 6.5 KW generator and load was added through a panel of electrical loads.

Table 12. 1995 Honda gasoline engine specifications

Manufacturer/Model	Honda GX390
Displacement	0.389Liters (389cc)
Number of cylinders	1
Bore	88mm (3.5in)
Stroke	64mm (2.5in)
Horsepower	13 bhp

3.2.2 Full flow dilution tunnel and critical flow venturi

A dilution tunnel was used for the emissions sampling used in this program. In the tunnel the full flow of exhaust was mixed with dilution air, which was filtered. Directing raw hot exhaust gas into a dilution tunnel lowers the dew point temperature of the exhaust gas to prevent condensation in the gas analyzer sampling lines. The tunnel was 18 inches in diameter, 20 feet in length and was constructed of stainless steel. It incorporated a 10 inch diameter mixing orifice located 3 feet from the entrance of the tunnel to ensure mixing of the air and raw exhaust. Sample probes for the gas analyzers were located 15 feet from the entrance of the tunnel, which were over 10 diameters downstream of the orifice. This particular dilution tunnel meets the requirements of CFR Title 40 part 86 subpart N [94].

A constant volume sampler (CVS) was used to draw the diluted exhaust through the dilution tunnel. The CVS system operated based on the theory of critical flow nozzles, wherein a critical flow venturi (CFV) was placed upstream of a blower and diluted exhaust mixture was pulled at a constant mass flow rate through the sonic venturi. Under choked flow (Mach number equal to 1) the flow rate through the venturi was proportional to the diameter of venturi throat and upstream absolute pressure and temperature. Two critical flow sonic venturis with a nominal flow of 1000 scfm each and another with 400 scfm were used to set a nominal flow of 2400 scfm in the dilution tunnel during testing of the Cummins engines. The tunnel flow was calculated using the following relationship:

$$V_{mix} = \frac{K \cdot P}{\sqrt{T}} \tag{21}$$

where V_{mix} is the dilution tunnel flow, K is the venturi coefficient found during calibration, P is the pressure at the venturi throat, and T is the absolute venturi throat temperature.

3.2.3 Gaseous emissions and air flow measurement systems

A part of the mixture of dilute air and engine exhaust was measured and supplied to the analyzers. Heated sample lines were used to carry the samples to the analyzers to prevent condensation. Each sample line was maintained at different temperatures and they are discussed briefly in this section. The emission measurement analyzer bench was configured to measure HC, NOx, CO, and CO_2. A list of gas analyzers along with their detection method and manufacturers are listed in Table 13.

Table 13. Exhaust gas analyzers

Gas	Detection Method	Manufacturer
THC	Flame ionization	Rosemont Analytical
NOx	Chemiluminescent	Rosemont Analytical
CO	Non-dispersive infrared absorptiometry	Horiba Instruments
CO_2	Non-dispersive infrared absorptiometry	California Analytical and Horiba

The gas analyzers were calibrated with ± 1.0% accuracy research grade calibration gases. The Rosemount Analytical Chemiluminescent Model 955 NO/NOx analyzer used had an accuracy of ± 0.5% of full scale. Since the NOx concentrations encountered were mostly over 50% of full scale measurement this yielded an overall NOx measurement accuracy of ± 2.0%. The root sum of squares (RSS) method of calculating experimental error is shown as follows:

$$\Delta V_{mix} = \sqrt{\left(\frac{\partial V_{mix}}{\partial K}\Delta K\right)^2 + \left(\frac{\partial V_{mix}}{\partial P}\Delta P\right)^2 + \left(\frac{\partial V_{mix}}{\partial T}\Delta T\right)^2} \tag{22}$$

This yielded an uncertainty of ± 0.5% for the tunnel flow when accounting for pressure and temperature measurement device inaccuracies. Using the RSS method of final time yielded an inaccuracy of ± 2.5% for the NOx measurements. A detailed uncertainty analysis of the CAFEE emissions testing laboratory's measurement systems was conducted by Hoppie *et al*. [95]. The engine intake air flow rate was measured using a Meriam Instruments laminar flow element (LFE). The differential pressure across the element, along with the absolute pressure and temperature of the air at the inlet, were measured.

3.2.4 NOx injection system

To simulate the NOx recirculation process into the engine a NOx injection system was utilized. The system consisted of a cylinder of compressed NO of 98.8% purity and a mass flow controller capable of injecting up to 1.5 liters per second. Since the majority of NOx from natural gas engines consists of NO, as discussed below, the gas used for this research was NO alone. Figure 11 shows the NOx injection system integrated with the engine and analyzers.

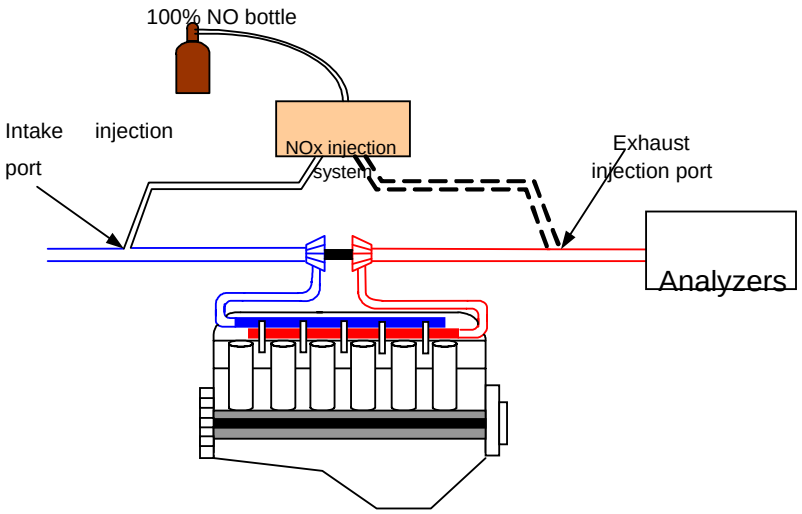

Figure 11. NOx injection system setup

During the runs, NO was injected for 20 seconds during each mode to avoid excessive consumption of NO. The analyzer response was averaged for the central 10 seconds of

each injection. For each engine operating point, NO was injected at the exhaust line (as a reference), as well as at the intake line upstream of the turbocharger. The mass controller flow rate value was later used to infer the concentration of NO in the intake. It was assumed that the exhaust flow was too cold to react significantly with the NO injected directly into the exhaust, so that this served as an accurate representation of the NO quantity entering the engine. Note that this approach improves accuracy of percentage reduction calculation in comparison to a mass balance.

The fraction of injected NO that was decomposed during the combustion process was calculated for each operating condition as follows: The amount of NO injected into the exhaust line was the average detected peak NOx_{PE}. The amount of NO seen by the NOx analyzer due to the injection after decomposition had occurred during the combustion was designated as NOx_{PI}. The average of the baseline NOx emissions, NOx_B, for a given mode was subtracted from the values. The decomposition efficiency (η) was calculated as a fraction of NO decomposed at each load as shown in the following equation [87].

$$\eta = 1 - \frac{\left(NOx_{PI} - NOx_B\right)}{\left(NOx_{PE} - NOx_B\right)} \tag{23}$$

This efficiency is presented as a percentage in the discussion below. In discussing SI engine exhaust, the NOx is primarily NO, which account for 90 - 95% of the total, the remainder being NO_2 [13],[96]. Research conducted at Colorado State University on a large-bore natural gas engine operating at 300 rpm stated that NO_2 was relatively a small amount of the total NOx emitted from the engine [97]. The NO percentage of the 1998 Cummins L10G engine was 91% of the total NOx. Therefore, it was concluded that the NO_2 to NO ratio was small for most engines.

3.2.5 EGR system

EGR was introduced into the intake air of the 1998 Cummins engine by controlling the pressure in the exhaust piping through a butterfly valve maintaining 9kPa positive back pressure. The EGR flow-rate was controlled with a valve placed in the recirculation pipe connecting the main exhaust line downstream of the turbocharger outlet to the intake

duct upstream of the turbocharger intake. This setup is referred to as a Low Pressure EGR arrangement. The EGR piping was long enough to allow sufficient cooling to maintain the intake air temperature between 33 and 42°C before the turbocharger. The engine and EGR setup diagram is shown in Figure 12.

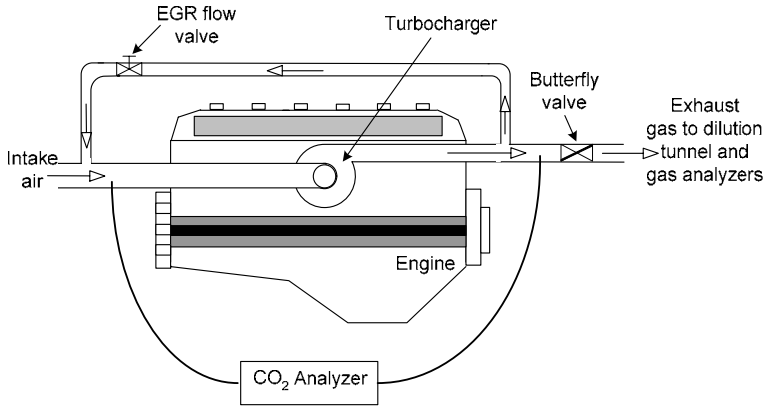

Figure 12. Engine and EGR system setup with two channel CO_2 analyzer

To find the maximum useable EGR quantity, EGR was increased until engine misfire occurred. The EGR percentage was calculated by taking the ratio of the CO_2 concentration measured in both the raw exhaust and the intake manifold, using a two channel California Analytical CO_2 analyzer. EGR was used to control in-cylinder temperatures to avoid knocking and avoid thermal problems during the rich-burn conditions.

3.2.6 Air/fuel ratio control

The 1998 Cummins engine employed closed loop control, with an NGK air/fuel ratio sensor in the exhaust. The investigators did not have direct authority over the engine control unit to alter air/fuel ratios. To operate the engine at alternate air/fuel ratios a circuit was designed that employed a NGK universal exhaust gas oxygen sensor control unit [98]. The output from this circuit was connected to the engine control unit (ECU) enabling control of air/fuel ratio by the researchers. The relative air/fuel ratio was defined by the following equation [96].

$$\lambda = \frac{(A/F)_{actual}}{(A/F)_{stoichiometric}} \tag{24}$$

3.2.7 In-cylinder pressure measurement system

In-cylinder pressure was measured using a Kistler Type 6067C precision cylinder pressure sensor (serial # 1369396), installed in-cylinder number one.

3.2.8 Net heat release calculation

The net heat release rate was calculated using the in-cylinder pressure data. The equation used for the calculation is as follows [96].

$$\frac{dQ_{net}}{d\theta} = \frac{\gamma}{\gamma - 1} P \frac{dV}{d\theta} + \frac{1}{\gamma - 1} V \frac{dP}{d\theta} \tag{25}$$

where γ is the specific heat ratio, P is the in-cylinder pressure, V is the displaced cylinder volume, θ is the crank angle. Q_{net} is the net heat released representing combustion heat release minus the wall heat transfer and ring blow-by flow losses. The value for γ was assumed to be 1.32.

3.3 Test procedure

The engines were run in stock configuration to determine their baseline emissions. After measuring the engine's full load versus speed trace (engine map or lug curve), a steady state test matrix was created. The controlled variables were engine speed, load, air/fuel ratio, NOx injection flow rates, and added external EGR quantity. The three experimental campaigns are described in this section. Campaign I tests conducted on the 1993 Cummins L10G engine achieved NOx decomposition rates of 27% during lean-burn operation. This implied that it would be necessary to run the engine at stoichiometric or slightly rich conditions for maximum NO decomposition. Therefore, campaigns II and III were dedicated to running the engine at optimized NOx decomposition set points. The fact that rich-burn air/fuel ratios facilitate more NOx decomposition was also predicted by chemical kinetic modeling data presented later in this paper.

3.3.1 Campaign I

In order to determine the effect of load, speed and concentration, two different types of NO injections were employed. During the first test, varying concentrations of NO were injected at an engine speed of 800 rpm and load of 400 ft-lb, as shown in Table 14. The engine was allowed to stabilize at 400 ft-lb and then NO was injected at rates varying from 0.39 to 1.82 g/s for 20 second periods into the engine air intake upstream of the fuel mixer (gas carburetor). Table 14 represents NO injection quantities at each engine operating point.

Table 14. Varying injection quantities of NO at constant engine speed and load

Speed (rpm)	Load (ft-lb)	NO injected (g/s)	NO in intake (ppm)	Engine intake flow (slps)
800	400	0.39	5,100	62
800	400	0.78	10,000	62
800	400	1.17	15,000	62
800	400	1.56	20,000	62
800	400	1.96	25,000	62

On the second set of tests, engine speed and intake NO concentrations were kept constant, while varying the engine load, as seen in Table 15. At constant engine speed and varying loads, it was clear that the intake airflow rate fluctuates. To keep the percentage of NO in the intake air constant, the injected NO mass flow was altered accordingly. This held the molar fraction of NO in the intake constant for varying loads, which gave insight as to how conversion rates vary with temperature and pressure, knowing that higher loads lead to higher in-cylinder temperatures and pressures.

Table 15. Varying engine load at constant speed and NOx injection quantities

Speed (rpm)	Load (ft-lb)	NO injected (g/s)	NO in intake (ppm)	Engine intake flow (slps)
800	100	0.64	25,000	21
800	175	1.13	25,000	36
800	250	1.44	25,000	47
800	325	1.8	25,000	57
800	400	1.94	25,000	62

3.3.2 Campaign II

During the second campaign experiments, the engine was operated at 800, 1300, and 2100 rpm and the EGR percentage was not controlled. Emphasis was placed on running the engine slightly rich and closer to stoichiometric for this set of runs because previous lean-burn tests from the first campaign demonstrated low NOx decomposition percentages. Injected NOx amounts were one order of magnitude larger than the baseline NOx emissions for the natural gas engine, because it was believed that the SNR approach would concentrate the exhaust NOx before it was returned to the engine for decomposition . One of the test matrices is shown in Table 16.

Table 16. Test matrix from campaign II

Speed (rpm)	Load (ft-lb)	NO Injected (g/s)	Air/fuel Ratio λ
800	50 - 550	2.0	0.94
1300	50 - 800	2.0	0.95
2100	150 - 600	2.0	1.02

3.3.3 Campaign III

For the third campaign, the engine was run at 800, 1200, and 1800 rpm, with full control over EGR percentage directed into the intake. These sets of runs focused on understanding the effects of EGR, as well as the injected NOx quantity, on decomposition. Four operating points were chosen, denoted by runs A, B, C, and D as shown in the test matrix in Table 17. The percentage of NOx in the intake air was

calculated by taking the ratio of the NOx injection mass flow rate and the total intake air flow rate measured using the LFE. Once again an emphasis was placed on running the engine slightly rich and stoichiometric for λ values that ranged from 0.94 - 1.02.

Table 17. Test matrix from campaign III

Run ID	Speed (rpm)	Load (ft-lb)	NOx% of intake volume flow	EGR Variation
A	800	200	1.22, 3.02, 4.12	0 – 16%
B	800	550	0.55, 1.36, 1.96	0 – 20%
C	1200	550	0.37, 0.91, 1.29	0 – 20%
D	1800	600	0.22, 0.51, 0.74	0 – 18%

4. NOx Decomposition Results and Discussion

4.1 Campaign I experiments

Baseline emissions were taken for HC, NOx, CO and CO_2, at operating conditions shown in Table 18. These emissions data were taken one day prior to the NO injection tests that were performed. These operating conditions were chosen to mimic reaction time scales associated with low speed large stationary engine operation. The sampling rate for the gas analyzers was set to 1 Hz. Engine operating conditions were set and then allowed to stabilize for 60 seconds before acquiring the data. The emissions were then averaged over 50 second modes for each operating condition. Data designated as NOx_1 and NOx_2 were taken from two separate NOx analyzers at the same time to verify the accuracy of the NOx readings. A relative difference between the two analyzers was less than 0.015 for each engine operating condition. Minimizing variation in the relative air/fuel ratio (λ) was considered important, because it affected NOx production and decomposition amounts.

Table 18. 1993 Cummins engine baseline emissions - HC, CO, CO_2, and NO_X at varying loads

	100 ft-lb 800 rpm	175 ft-lb 800 rpm	250 ft-lb 800 rpm	325 ft-lb 800 rpm	400 ft-lb 800 rpm
HC (g/bhp-hr)	3.60	3.43	2.92	2.83	3.17
CO (g/bhp-hr)	2.59	1.79	1.52	1.43	1.38
CO_2 (g/bhp-hr)	670	573	498	440	413
NOx (g/bhp-hr)	1.82	0.68	0.61	0.84	1.09
NOx_2 (g/bhp-hr)	1.75	0.64	0.59	0.80	1.07
HC (g/s)	0.0158	0.0250	0.0317	0.0388	0.0519
CO (g/s)	0.0114	0.0130	0.0165	0.0196	0.0227
CO_2 (g/s)	2.93	4.17	5.41	6.04	6.76
NOx (g/s)	0.0080	0.0049	0.0066	0.0115	0.0178
NOx_2 (g/s)	0.0076	0.0047	0.0064	0.0110	0.0175
Lambda (λ)	1.26	1.36	1.40	1.41	1.40

Figure 13 and Figure 14 show the results for the two tests matrices in Table 14 and Table 15. From these data it was clear that NOx was decomposed during the combustion process at varying loads and injection quantities. Note that in these tables and figures the "exhaust" data represent the amount of NO injected, before decomposition occurred. The "intake" data show the NOx levels after decomposition.

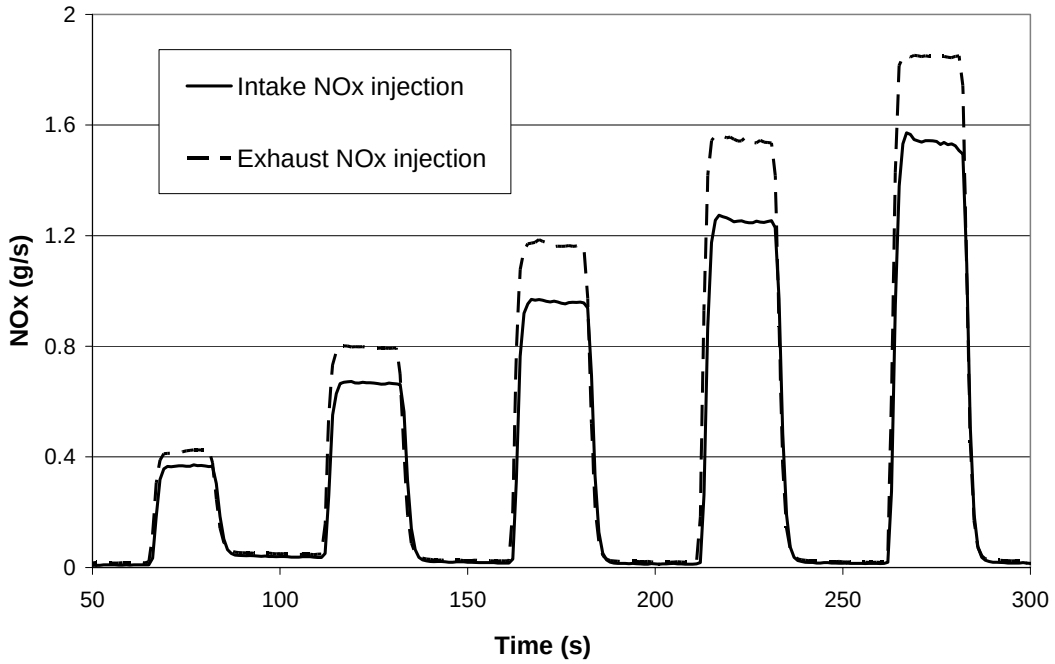

Figure 13. Lean combustion, at 800 rpm and 400 ft-lb, with varying NO injection quantities

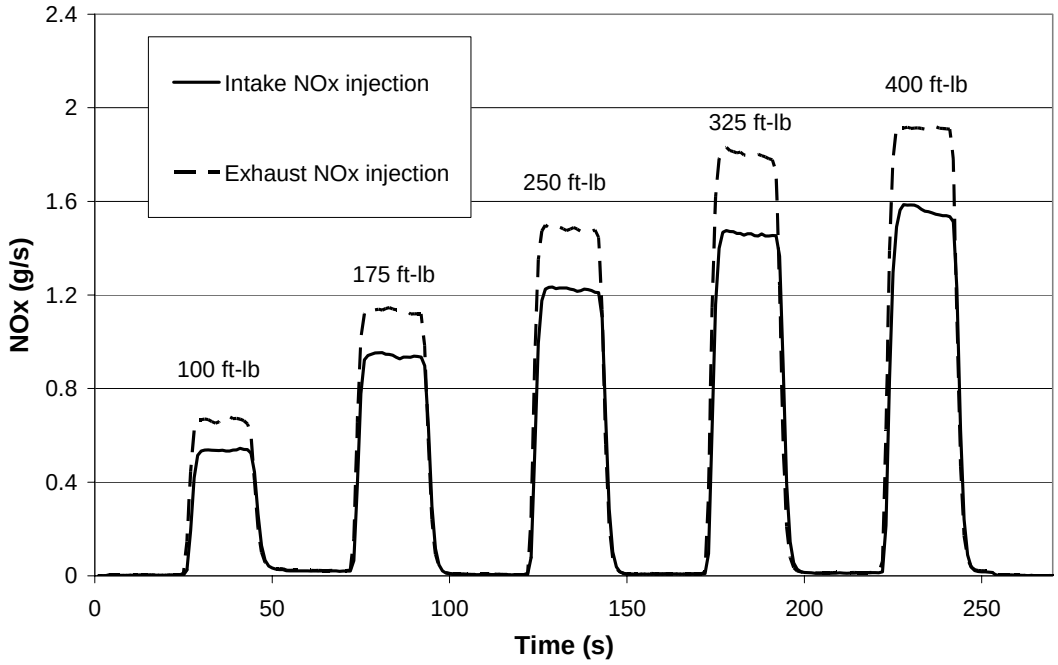

Figure 14. Lean combustion at 800 rpm and intake air NOx concentrations of 25,000 ppm

The percentage of injected NOx that was decomposed during the combustion process was calculated for each operating condition. These values, presented in the tables below, showed good correlation with the values from the mass flow controller for both the varying and constant concentration cases. They also showed that an insignificant percent of NOx is being reduced in the exhaust line and dilution tunnel measurement system.

Table 19. Mass flow controller and NOx values for the varied concentration experiment

Speed (rpm)	Load (ft-lb)	NOx_{PE} - NOx_B analyzer reading (g/s)	Mass flow controller (g/s)	Percent difference (%)
800	400	0.42	0.39	6.0
800	400	0.79	0.78	1.2
800	400	1.16	1.17	0.9
800	400	1.55	1.56	1.1
800	400	1.85	1.96	5.6

Table 20. Mass flow controller and NOx values for the varied load experiment

Speed (rpm)	Load (ft-lb)	NOx_{PE} - NOx_B analyzer reading (g/s)	Mass flow controller (g/s)	Percent difference (%)
800	100	0.66	0.65	1.9
800	175	1.13	1.13	0.3
800	250	1.48	1.48	0.2
800	325	1.79	1.80	0.1
800	400	1.91	1.94	1.3

The NOx decomposition percentages for the data given in Table 19 and Table 20 are shown in Figure 15 and Figure 16, respectively. Error bars represent ± 2.5% inaccuracy in the NOx measurement, which sums to ± 5.0% overall inaccuracy when subtracting these values as shown in Equation 20. It was observed that the NOx conversion rates varied between 14 - 20% as seen in Figure 15 for varying injection quantities, and between 18 - 23% for a constant 25,000 ppm NOx concentration at 800 rpm and varying loads, as seen in Figure 16.

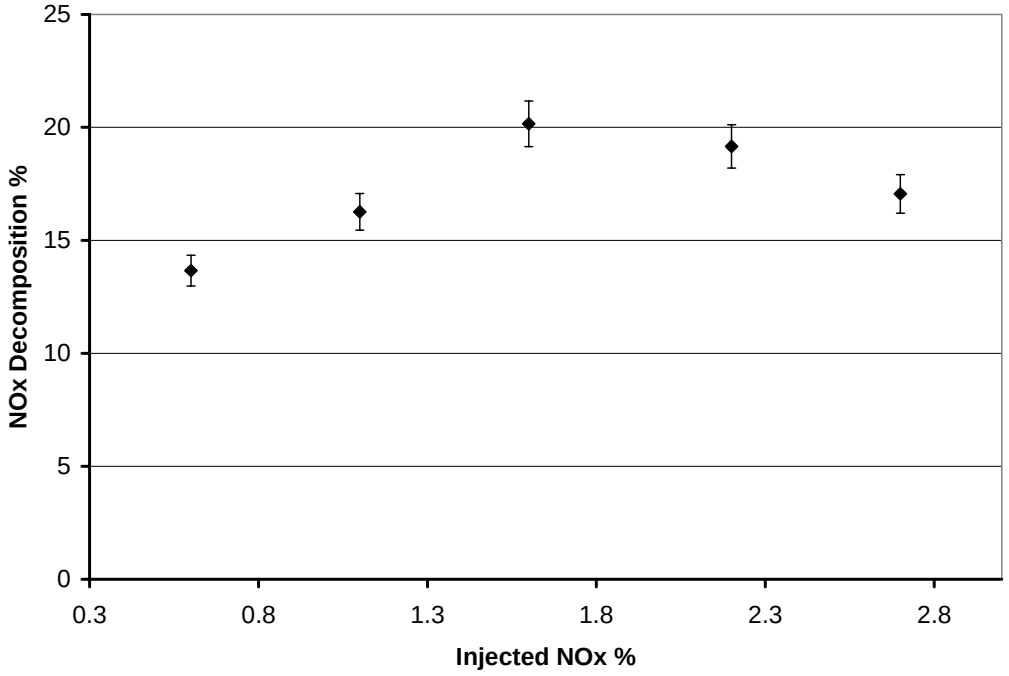

Figure 15. NOx decomposition for varying NOx quantities at 800 rpm and 400 ft-lb, 2.5% error bar

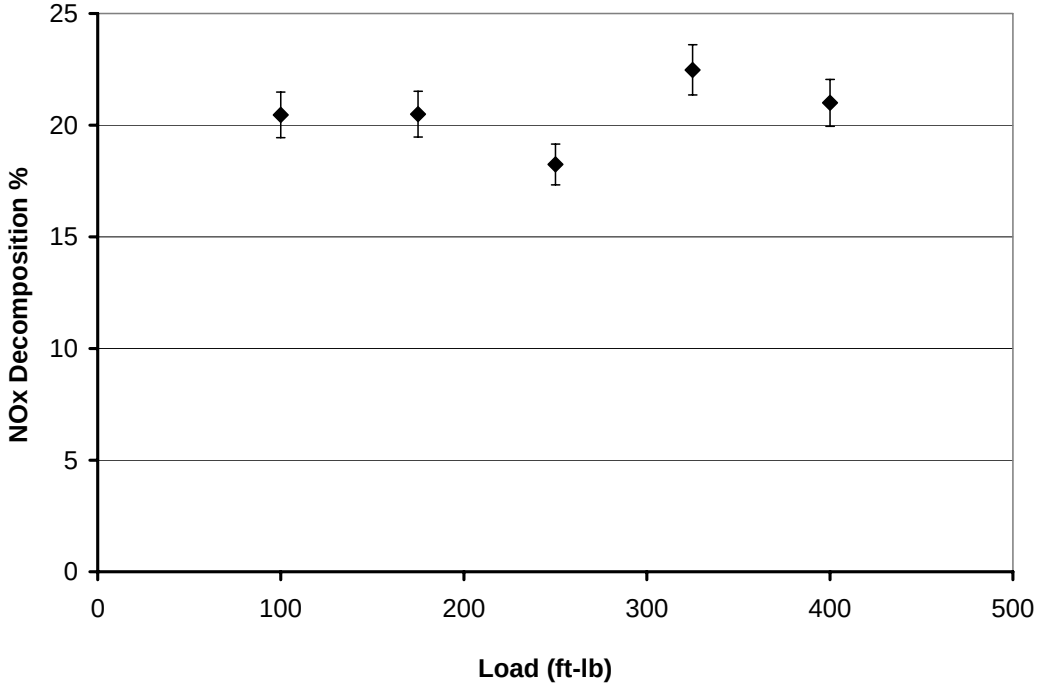

Figure 16. NOx decomposition vs. engine load for constant concentration and engine speed, 2.5% error bar

The results shown in Figure 16 suggest NOx decomposition is unrelated or weakly related to engine load. The inability to hold the air/fuel ratio constant at the 100 and 175 ft-lb load levels may have skewed these results. NOx injection effects on other emissions are represented in Figure 17. These results show 20% reductions in HC emissions and a slight decrease in CO emissions during NO injections.

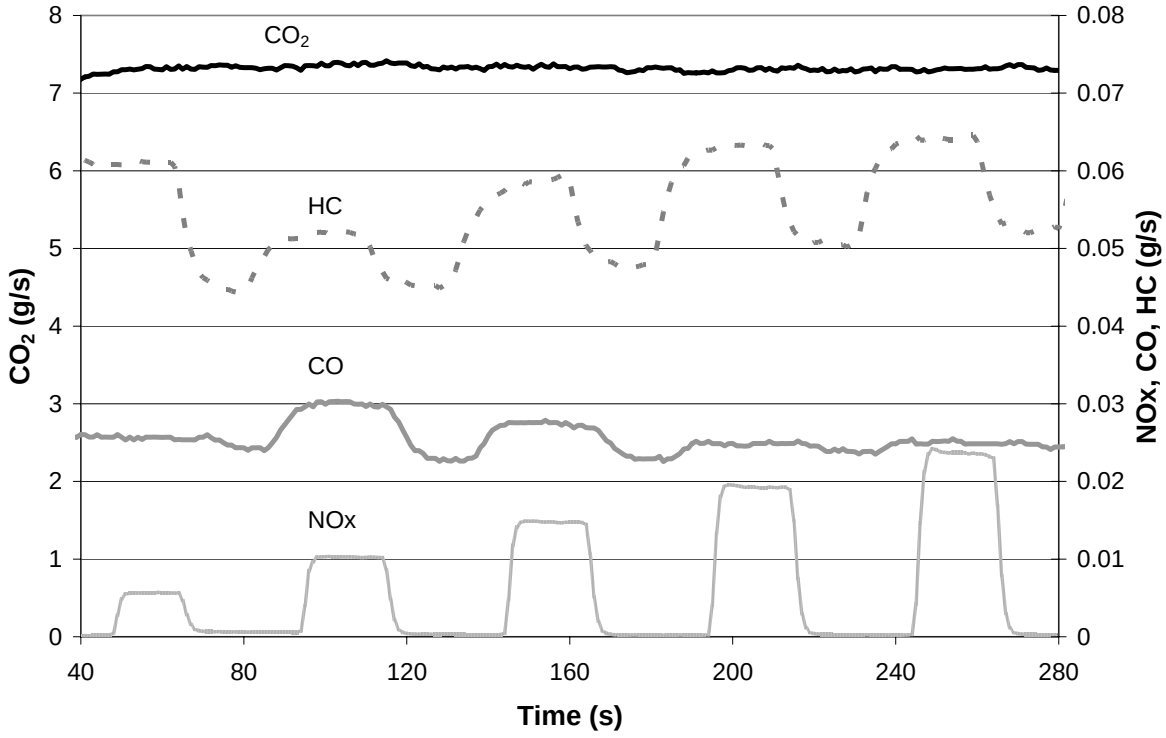

Figure 17. Varying concentration NO injections on other emissions at 800 rpm and 400 ft-lb

4.1.1 Repeatability tests

Figure 18 shows the 800 rpm 400 ft-lb engine set point data for each of the NOx injection experiments shown in Figure 13 and Figure 14. The Exhaust 1 and Intake 1 data represent the varied NOx concentration test, and Exhaust 2 and Intake 2 represent the constant NOx concentration test. This set point was chosen to show repeatability, because the same quantity of NOx was injected in each separate test on different test days. The air/fuel ratio variation for the 5 experiments (baseline and exhaust and intake injections for each NO injection experiment) was 1.38 to 1.42. Therefore, the percentage variation in

the NOx decomposition efficiency due to day-to-day testing variations should not exceed what is shown here for any other test points.

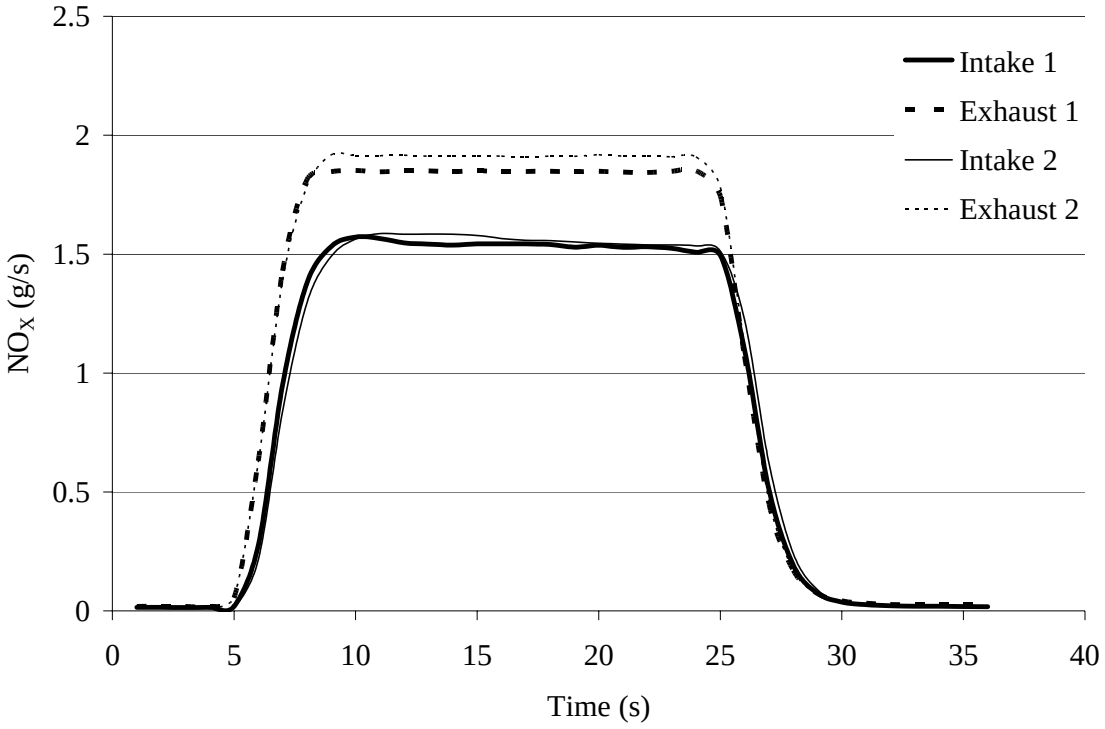

Figure 18. Two sets of NOx injections at 800 rpm and 400 ft-lb load on different test days

4.2 Chemical kinetic modeling

A chemical kinetic solver software package CHEMKIN, developed by Reaction Design, was used to simulate the NOx decomposition process and to guide the experimental program. Since the lean-burn operation yielded only modest NOx decomposition, the researchers elected to use modeling to identify a more fruitful operating region for decomposition before conducting additional experimental studies.

A closed homogeneous batch reactor model was designed to simulate the concentration of NO versus time for an initial mixture containing NO, O_2, N_2, and CH_4 for λ values between 0.9 and 1.4. CH_4 was used as fuel since it is the primary constituent (84 – 91% by mass) of natural gas [99]. An initial NO concentration of 25,000 ppm (or 0.0233 mole

fraction) was used in the initial mixture. A zero-dimensional model was used to predict the NO decomposition quantities of the natural gas engine for combustion temperatures ranging from 1300 to 1750°C. This range was set by examining the theoretical flame temperature and rates of reaction. In 1998, Dodge *et al.* [100] found that a zero-dimensional model predicted the NOx emissions well from lean-burn natural gas engines. The mole fraction of NO in the combustion products was predicted for periods approximating the duration of normal combustion. A time step of 5 microseconds was used as the time base. This modeling produced estimates for the percentage of NO decomposed locally during the combustion process. These percentages were then compared with empirical values, which were acquired from the test engine.

To estimate the temperature and pressure at which NO reactions may occur, an adiabatic flame temperature calculation was performed. The compression stroke was modeled as an isentropic compression. The gases, at an initial temperature and pressure of 25°C and 1 bar (assuming no boost pressure), were compressed to a temperature of 410°C and pressure of 23.9 bar accounting for the engine compression ratio of 10.5 with boost pressure. To allow for valve timing, a 90% volumetric efficiency was assumed. This calculation yielded a pressure of 21.5 bar, before reactions have occurred. Detailed description of flame temperature calculations, energy balance performed and enthalpy values taken from JANAF tables [101] are described in a previous publication by the researchers [102].

4.2.2 Modeling results

Modeling was conducted in six stages that included rich-burn (with no EGR, 10% EGR, and 20% EGR), stoichiometric burn, and lean-burn (with no EGR, and 20% EGR). Replacing excess air with EGR not only reduces NOx in a natural gas engine [34], but may also enhance NO decomposition because it is heated to a lower equilibrium temperature.

Predicting NOx concentration on large time scales of the order of minutes during steady-state operation confirmed that the NOx decomposition phenomenon was rate-limited rather than equilibrium-limited as long as the combustion temperature was maintained.

Since the process was rate limited, the combustion temperature played a significant role in NO decomposition.

Figure 19 and Figure 20 show NO mole fraction as a function of time for lean-burn and rich-burn cases. In Figure 19, the reaction rate for the 1750°C mixture reached equilibrium faster than for the reaction at 1300°C, as expected. After the initial rapid drop in NO mole fraction for each temperature profile, the rates of reaction slowed down until equilibrium was reached at around 0.014 mole fraction.

In Figure 20, all variables were kept constant expect the λ value which was changed from 1.4 to 0.9. A similar trend was seen in the rich-burn case, but the equilibrium was reached at a much lower (0.006) NO mole fraction level than in the lean-burn case. From Figure 19 and Figure 20 it can be concluded that a richer air/fuel ratio lowered the NO equilibrium level and decomposed a higher percentage of NO during combustion.

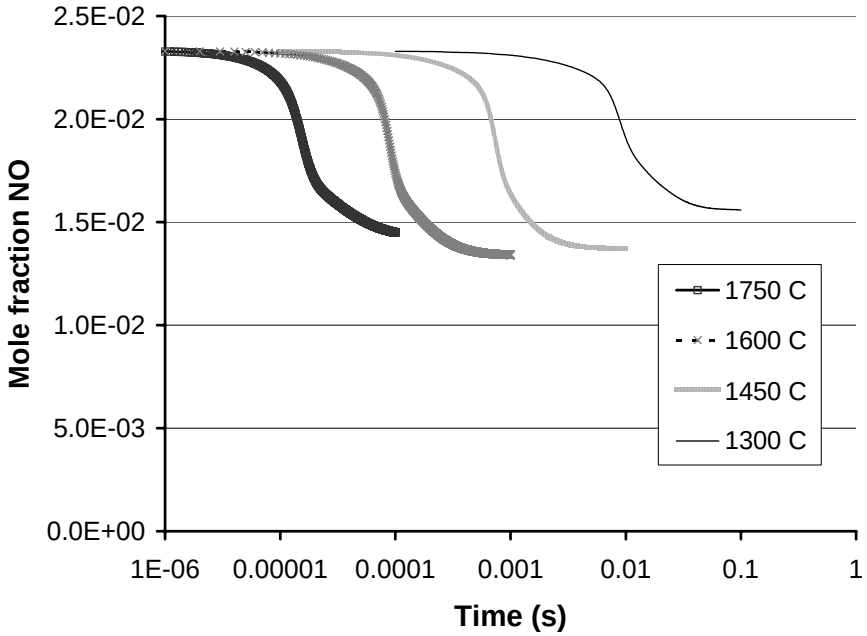

Figure 19. Lean-burn λ=1.4 with no EGR.

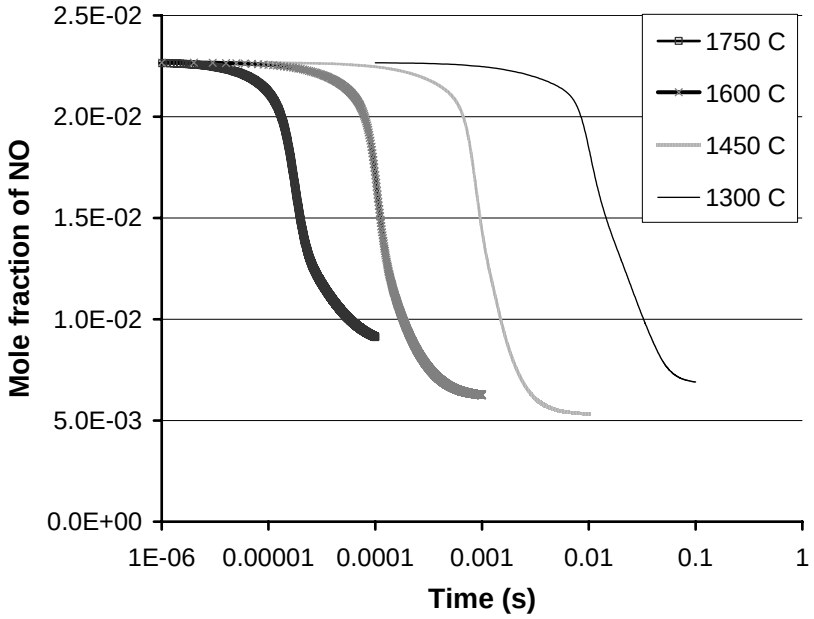

Figure 20. Rich-burn λ=0.90 with no external EGR.

Since a full engine model was not used, a time measure was needed to assess the percentage of NO reduction. In one case, the decomposition rate was estimated based on the amount of fuel consumed. It was assumed that when 98% of the CH_4 was consumed, the reactions would not progress much further and that NO was no longer being converted. The CH_4 burn out rate was also modeled for each case to use for this metric.

This value of 98% was chosen because it was a conservative estimate to the percent of fuel that was consumed in the test engine, although it is admitted that an average fuel efficiency may not apply to the individual packets of gas that are being modeled, it was a necessary assumption. The NO decomposition values obtained from this assumption can be considered as an absolute minimum. Therefore, by choosing a 99% CH_4 burn out rate or by limiting the high reaction rate to a time frame where combustion occurs during a 20° window at top dead center (TDC) could yield a higher NO decomposition rate.

The time frame for CH_4 to be consumed varied with temperature. Therefore, by calculating the NO decomposition for this period gave a reasonable estimate of NO decomposition rates occurring in the cylinder. A summarized version of NO

decomposition rates for varying combustion temperatures are shown in Figure 21 for all the six cases mentioned above.

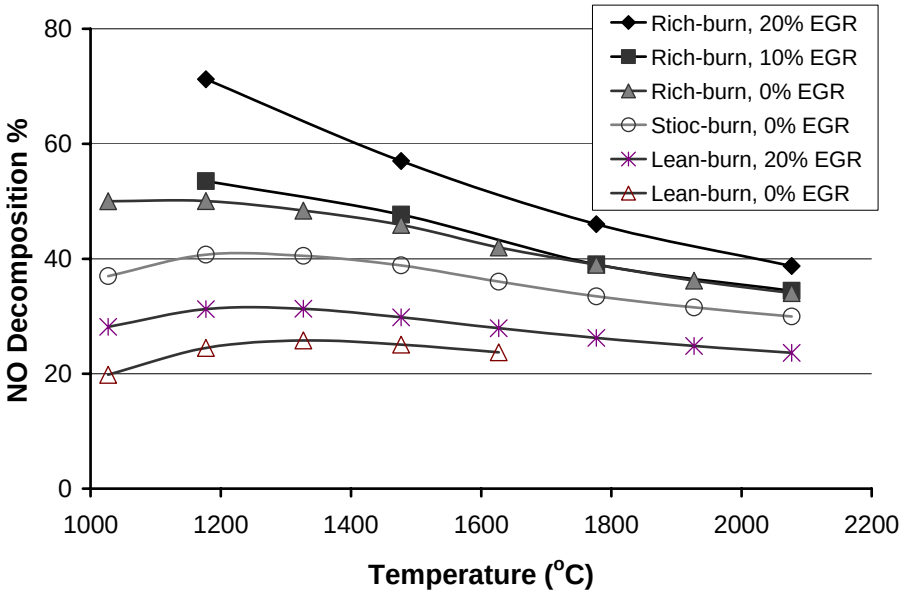

Figure 21. Decomposition percentages at various temperatures after 98% of CH_4 has burnt out

Based on percentage mass decomposition, the overall CHEMKIN model predicted decomposition rates that varied between 20 and 30% for the lean-burn case and 31 to 72% for the rich-burn and stoichiometric cases, highlighting that rich-burn operating conditions has more potential for higher in-cylinder NO decomposition rates. The researchers also used the 20 degree crank window as a measure of time, and this yielded higher percentages of decomposition.

The modeling data emphasized that further experimental research on decomposition should focus on stoichiometric (or rich) combustion, and that decomposition percentages under stoichiometric conditions were likely to support the use of SNR with natural gas engines. However, it was also recognized that for lean-burn engines the air/fuel ratio would need to be richened during decomposition phases.

4.3 Campaign II experiments

4.3.1 Exploratory work

Encouraging CHEMKIN modeling predictions that indicated a higher NOx decomposition in rich-burn engines led to exploratory work on a stoichiometric-burn gasoline engine. This work was accomplished very rapidly and the intent was to confirm NOx decomposition at higher in-cylinder temperatures and lower available oxygen concentrations before proceeding with the 1998 Cummins natural gas engine research.

The gasoline engine had a much lower intake air flow rate (6.5 standard liters per second) than the natural gas engine. The NOx injection system was used to inject up to 70% of NOx in the intake air. The first run kept the intake NOx concentration constant at varying engine loads as shown in Table 21. The second run was conducted at 75% engine load while varying the intake NOx concentration from 1 to 5% shown in Table 22. Figure 22 and Figure 23 show NO injections into the exhaust and intake corresponding to Table 8, and Table 9.

Table 21. Varying engine load at constant NOx concentration

Speed (rpm)	Load (ft-lb)	NOx Injected (g/s)	NOx in Intake (ppm)	Intake Flow Rate (slps)
3600	1.0	0.27	50,000	4.4
3600	3.9	0.30	50,000	4.8
3600	7.8	0..36	50,000	5.8
3600	9.8	0.40	50,000	6.4

Table 22. Varying injection quantities of NOx at constant engine load

Speed (rpm)	Load (ft-lb)	NOx Injected (g/s)	NOx in Intake (ppm)	Intake Flow Rate (slps)
3600	9.8	0.12	10,000	4.8
3600	9.8	0.21	20,000	4.8
3600	9.8	0.30	30,000	4.8
3600	9.8	0.41	40,000	4.8
3600	9.8	0.50	50,000	4.8

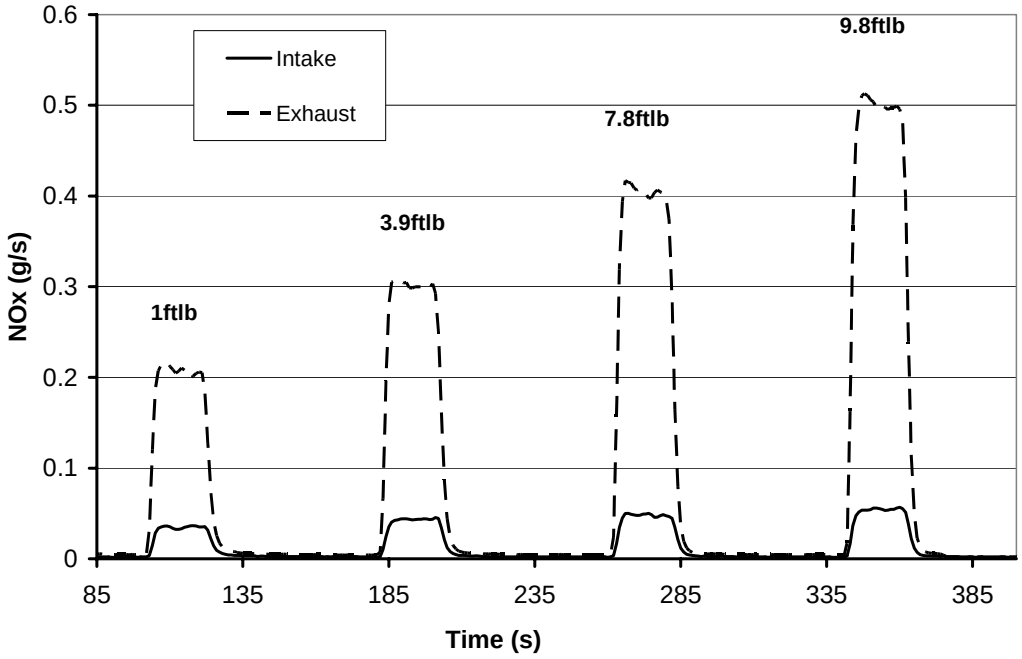

Figure 22. Varying loads at constant NO concentration: Table 21

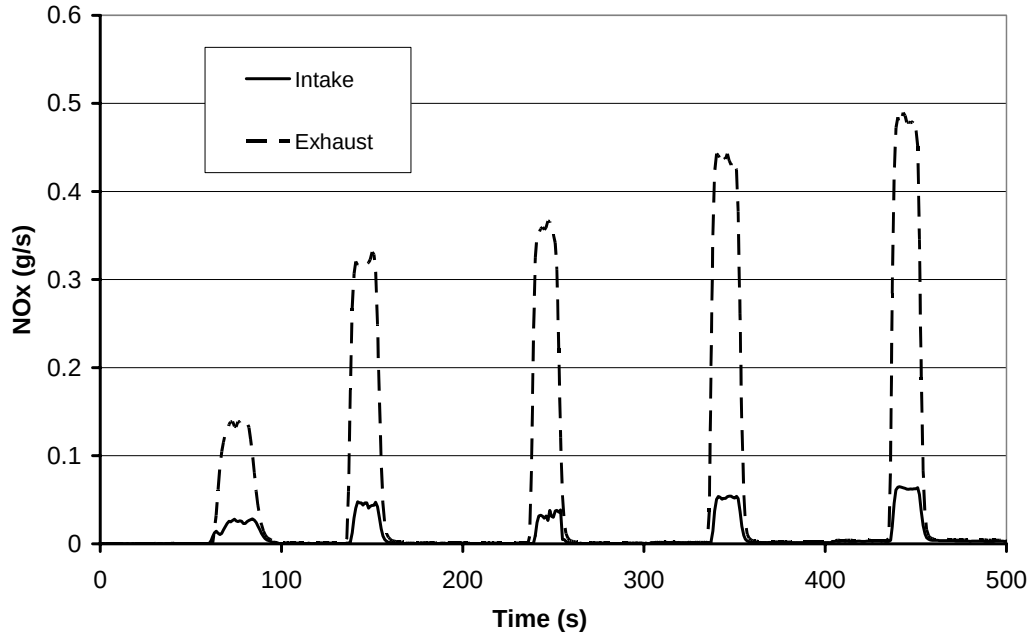

Figure 23. Varying injection quantities at constant engine speed and load from Table 22.

Further results were obtained for higher intake NOx concentrations that ranged from 1 - 70% of the intake air at constant speed and load (Figure 24). It was noted that the effect of intake NOx concentration on decomposition efficiency had no significant effect on the

gasoline-fueled engine when compared with the lean-burn natural gas engine data from the first experimental campaign. This result was further confirmed when intake NOx concentrations were increased from 5 - 70% of the intake air.

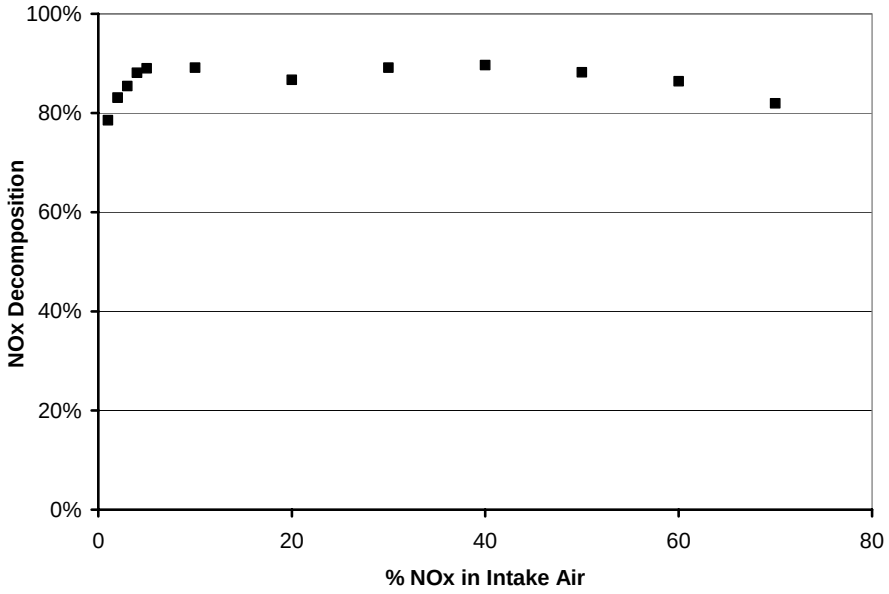

Figure 24. NO decomposition percentage vs. the amount of NO injected

It is noted in this report that NOx decomposition in a gasoline engine cannot be extended directly to NOx decomposition in a natural gas engine because natural gas is acknowledged to be less reactive than gasoline. However, results obtained from these tests were encouraging for lower air/fuel ratio research. Exhaust gas temperature on the gasoline engine showed a significant rise during the NOx injection time period. As seen in Figure 25 the temperature raised 75 - 100˚F during NOx injections. It is known that a typical gasoline spark ignited engine lies close to stoichiometric operation or on the slightly rich side [96]. The success of these runs paved the path for continued research on stoichiometric-burn natural gas operation for maximum NOx decomposition.

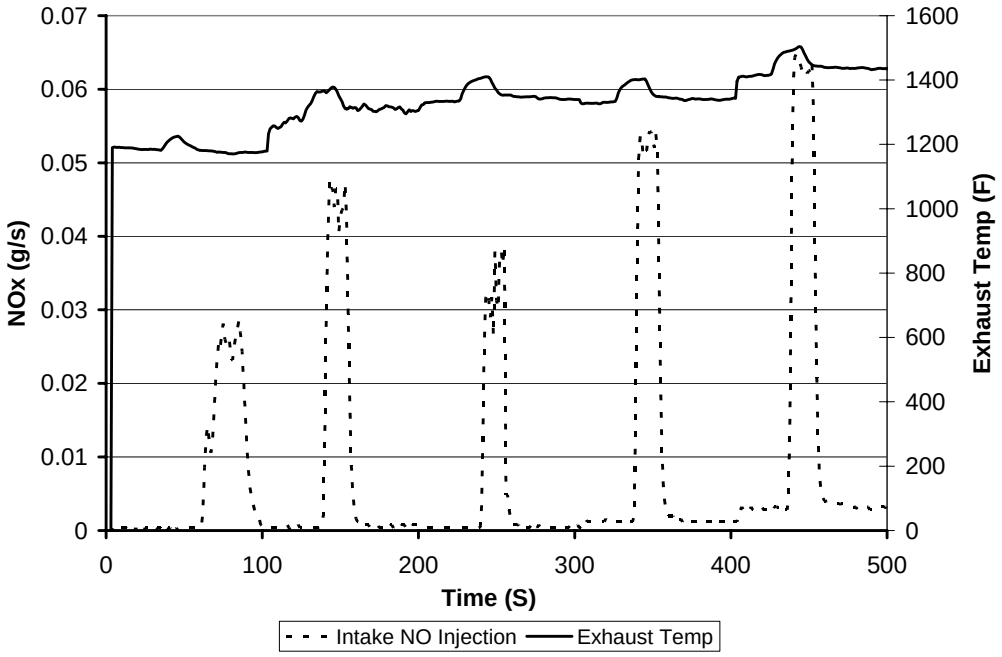

Figure 25. Exhaust gas temperature during intake NO injections

4.3.2 1998 Cummins L10G engine rich-burn results

Figure 26 shows NOx injections into the 1998 Cummins engine intake line and exhaust line at different engine speeds and loads during the second campaign. For this set of runs the NOx injection amount was held constant at 2.0 g/s for 20 seconds and the air/fuel ratio was held constant at 0.97. Figure 27 shows NOx decomposition percentages plotted against increasing load.

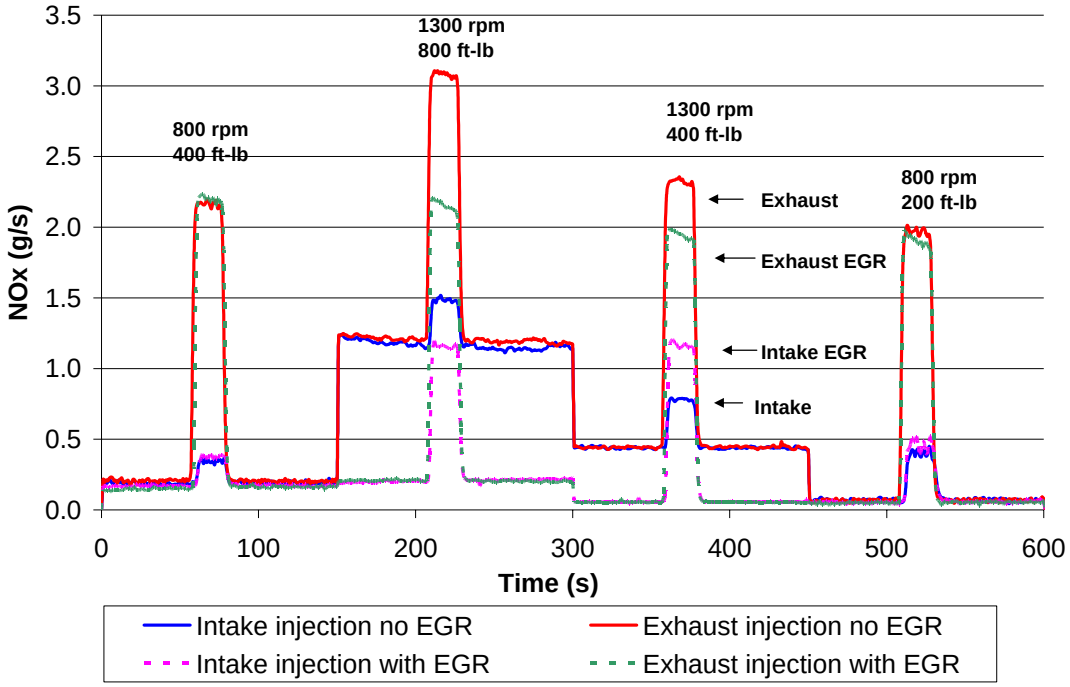

Figure 26. NOx injection runs during second campaign

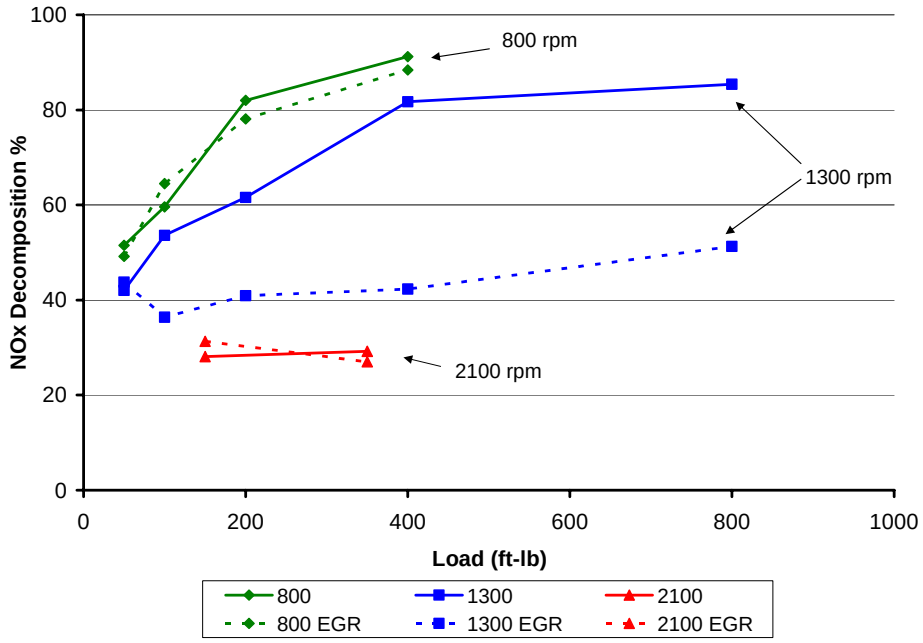

Figure 27. NOx decomposition percentages for the second campaign

As shown in Figure 27, the overall NOx decomposition rates were between 28 and 92% when the engine was operated at a λ value of 0.97 (slightly rich). The maximum decomposition percentage of 92% was achieved at 800 rpm and at 400 ft-lb load and the lowest percentage of 28% was at the 2100 rpm (rated speed) level. These decomposition rates confirm the trends that were corroborated with CHEMKIN modeling data, for stoichiometric or slightly rich operation. Since the highest NOx decomposition was achieved at low engine speed and high load operating points, it can be speculated that high in-cylinder temperature and a high available period for reaction (low engine speed) aided thermal NOx decomposition. It was observed that at a particular engine load the engine speed had a negligible effect on NOx decomposition.

In the runs shown in Figure 27, the EGR quantity was not varied independently. Campaign III experiments addressed variable EGR rates and are discussed in the next section.

4.4 Campaign III experiments

For the third campaign, the engine was run at 800, 1200, and 1800 rpm, with full control over the EGR percentage directed into the intake. Campaign III runs focused on understanding the effects of EGR, as well as the injected NOx quantity, on decomposition. Four operating points were chosen, denoted by runs A, B, C, and D as shown in the test matrix in Table 17. Since higher NOx decomposition was seen at lower speeds and higher engine loads, more attention was given to these operating points as it may mimic behavior in large-bore engines. Five EGR quantities were chosen and for each EGR quantity three NOx concentrations were injected. Once again an emphasis was placed on running the engine slightly rich and stoichiometric for λ values that ranged from 0.94 to 1.02.

Figure 28 shows the NOx decomposition rates of runs A and B (see Table 17), which included injecting three different concentrations of NOx. It can be concluded that NOx decomposition rates weakly depended on the quantity of NOx injected at low EGR rates. There was a trend of lower NOx decomposition values as EGR ratio was increased. The

EGR will affect in-cylinder gas composition, but more importantly will lower in-cylinder temperature and affect the mixture burn rate.

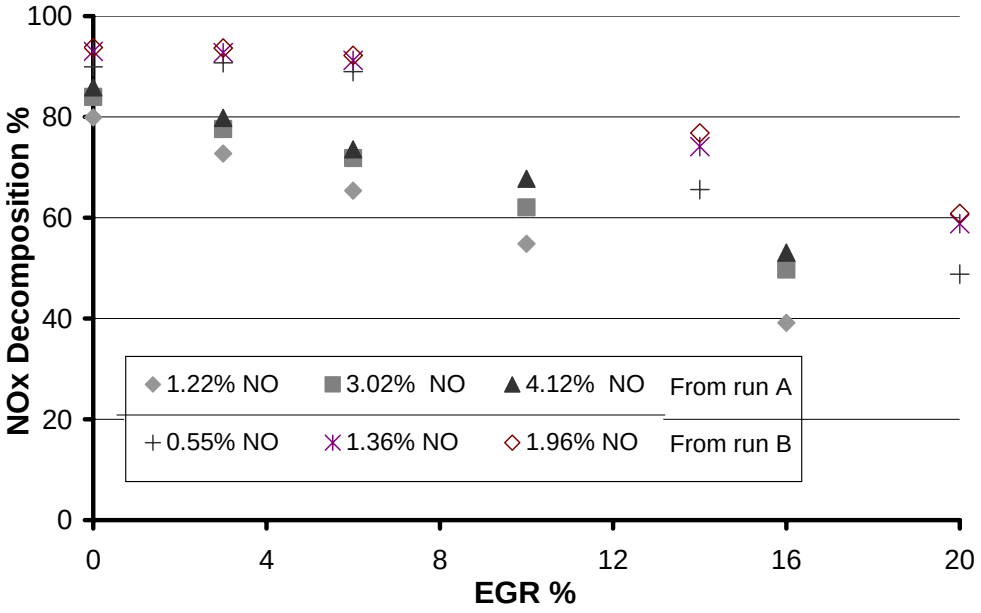

Figure 28. Effects of EGR and NOx concentration on decomposition, from runs A, B, Table 17

The exhaust gas temperature measured at each exhaust port on the 1998 Cummins engine showed a rise during the NOx injection time period. A further increase in temperature was observed as the intake NOx concentration was increased, as shown in Figure 29 and Figure 30. Since the engine was run at stoichiometric conditions or on the slightly rich side ($0.94 \leq \lambda \leq 1.02$), it can be speculated that the disassociation of NOx into nitrogen and oxygen. This would alter the effective air/fuel ratio, alter the combustion rate, and might have raised the combustion temperature. The cylinder to cylinder combustion variation may detract from optimal NOx decomposition.

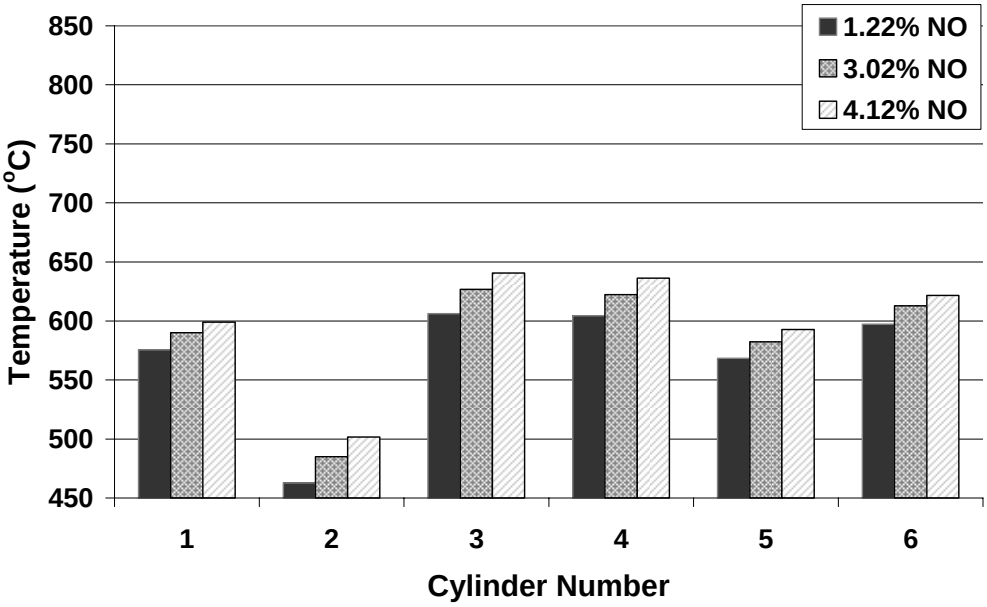

Figure 29. Exhaust gas temperature recorded during NOx injections from run A, Table 4

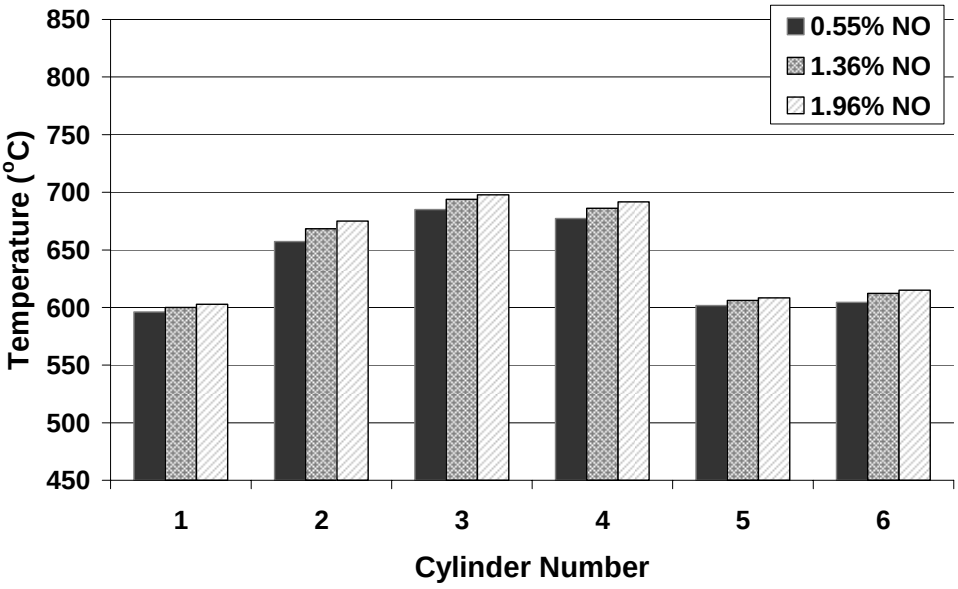

Figure 30. Exhaust gas temperature recorded during NOx injections from run B, Table 4

In addition to NOx emissions data, emissions data for CO, CO_2, and THC were recorded. An example is shown in Figure 31, taken from run B. Even though NOx injections were occurring (as shown by the three excursions on the NOx trace), the corresponding values

for CO, and CO_2 were not affected. However, it can be seen that THC level fluctuated during the run, perhaps due to cylinder-to-cylinder O_2 concentration variation [103].

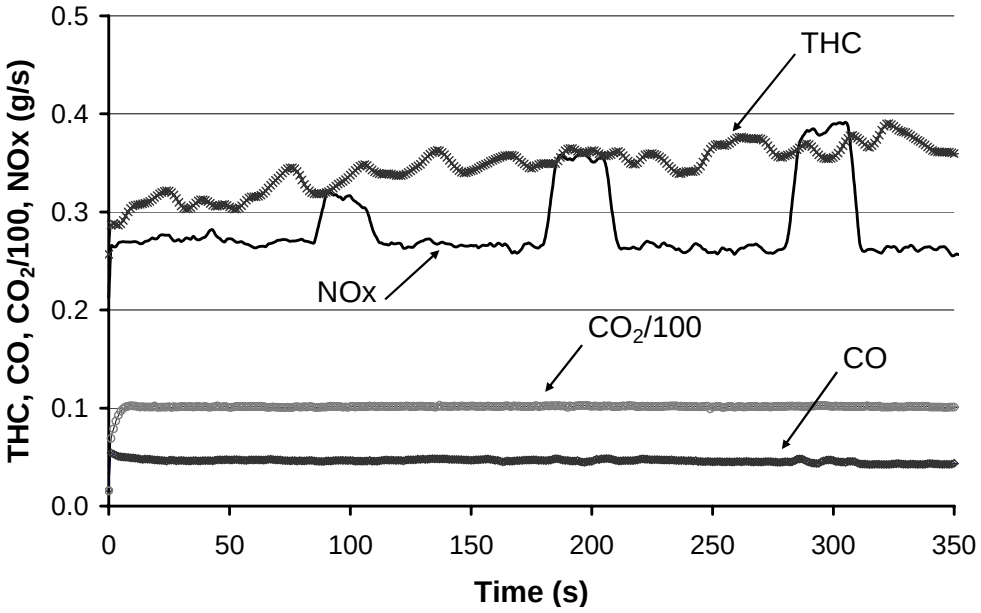

Figure 31. NO injection effects on THC, CO, and CO_2

In-cylinder pressure was recorded during each run to monitor any variations in peak pressure due to NOx injections. In-cylinder pressures from runs A and B shown in Figure 32 and Figure 33 are averages of 140 pressure peaks. For each averaged pressure trace, net heat release rate was calculated using Equation 23.

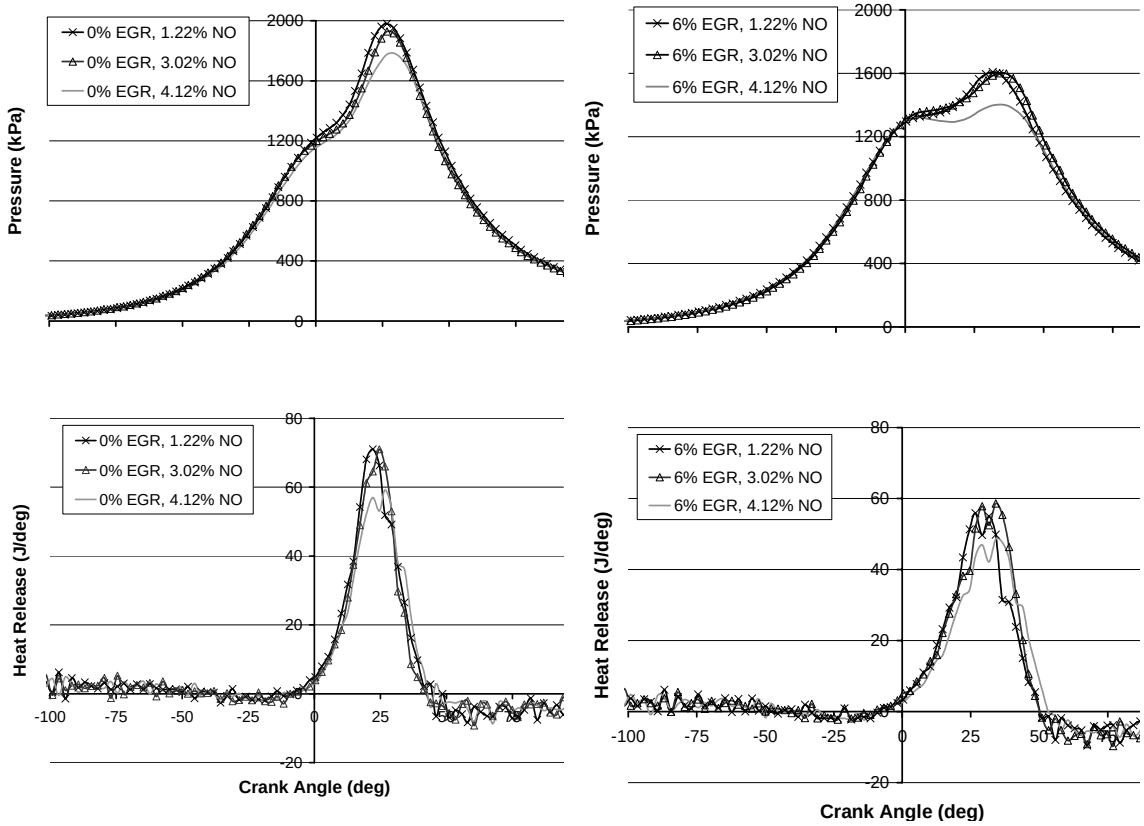

Figure 32. Run A (800 rpm, 271 Nm), no EGR and 6% EGR with three NO injections

A weak trend of reducing peak pressure was observed with increasing concentration of NO in the intake air in run A (800 rpm and 200 ft-lb). By adding 6% EGR the peak pressure dropped from 1900 kPa to 1600 kPa as expected, since EGR reduced the available oxygen content available for combustion and thereby lowered the peak in-cylinder temperature. EGR may also have reduced the flame speed. This trend was almost negligible during run B when the load was increased to 550 ft-lb. In summary, the NO injections did not cause substantial changes to the combustion or to other emissions from the engine.

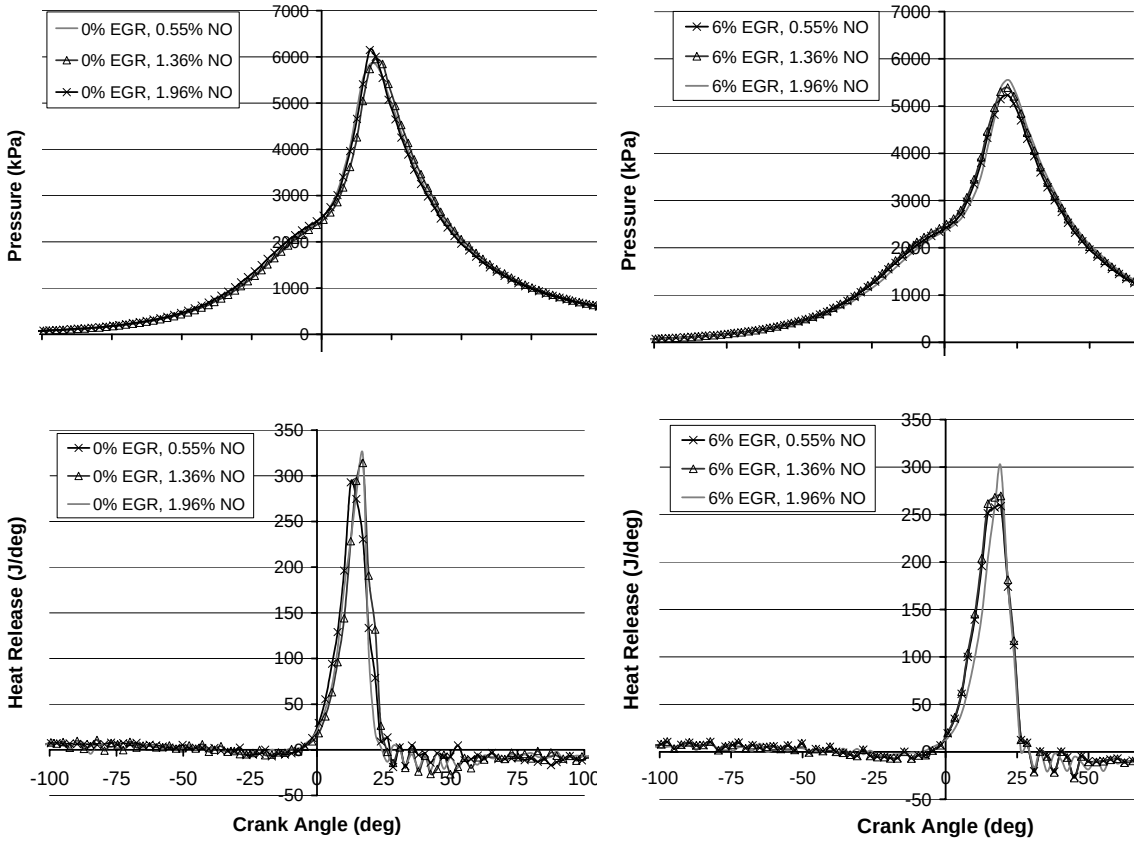

Figure 33. Run B (800 rpm, 745 Nm), no EGR and 6% EGR with three NO injections

5. Benchtop study on NOx adsorption and desorption process

5.1 NOx Adsorption System

In order to quantify the NOx adsorption/desorption characteristics of the sorbent material, a benchtop adsorption system was constructed and instrumented with thermocouples.

The NOx adsorption chamber was 27″ long and 1 3/8″ diameter stainless steel pipe, capable of holding one pound of adsorbent material (Figure 34). Temperatures were measured at 10″ and 20″ from the inlet side of the cylinder by thermocouples. NO was introduced into the bed at one end and the output concentration of the bed was measured using a Rosemount Analytical, Model 955 NOx analyzer. NO at a concentration of 510 ppm was chosen to load the adsorber to test the adsorption/desorption capabilities of the sorbent material.

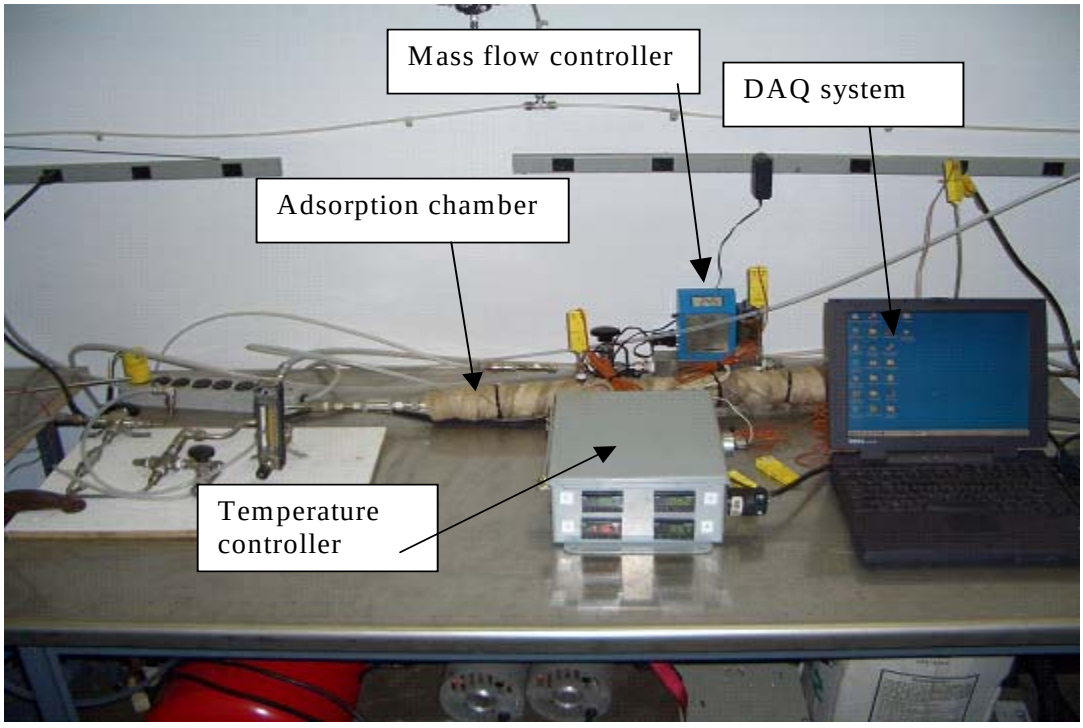

Figure 34. Benchtop setup

5.1.1 Adsorption phase

Two different types of activated carbon materials were evaulated for SNR applications with natural gas engines. Centaur 4X6 activated carbon marketed by Calgon Carbon Corporation (properties shown in Table 23) and a proprietary carbon batch supplied by Sorbent Technologies were used in the experiments. The experimental research did not seek to optimize carbon formulation for the purpose of adsorption, but rather characterized the ability of these available carbon products to adsorb.

Table 23. Properties of Calgon Carbon Corporation's activated carbon, OVC4X8

Property	Value
Ash, wt%	3.0
Moisture, wt%	3.0
Hardness No.	97
Apparent density, g/cc	0.5
Average particle size, mm	3.7
Surface Area, m^2/g	1,200

During an initial adsorption experiment the carbon bed was first preheated to 100˚F and a 7 lpm flow of 510 ppm NO was directed into the chamber. Data were collected until NO breakthrough had occurred and approximately 80% of the NO injected was actually being adsorbed. Operation at high breakthrough rates was not of interest because this operation would not be suited to engine exhaust NOx abatement.

Figure 35 shows the adsorption properties of the two carbon samples. Additional research on the NO adsorption using these two carbon types was undertaken as part of this program, and the results have been presented in the thesis of Zimmerman at West Virginia University. The additional research included an evaluation of the changes in adsorption properties when the carbon was employed for repeated NO adsorptions. Further runs were conducted using Calgon Centaur 4X6 activated carbon. The NO to CENTAUR® 4x6 activated carbon granules weight ratio during the experiments was 0.13%.

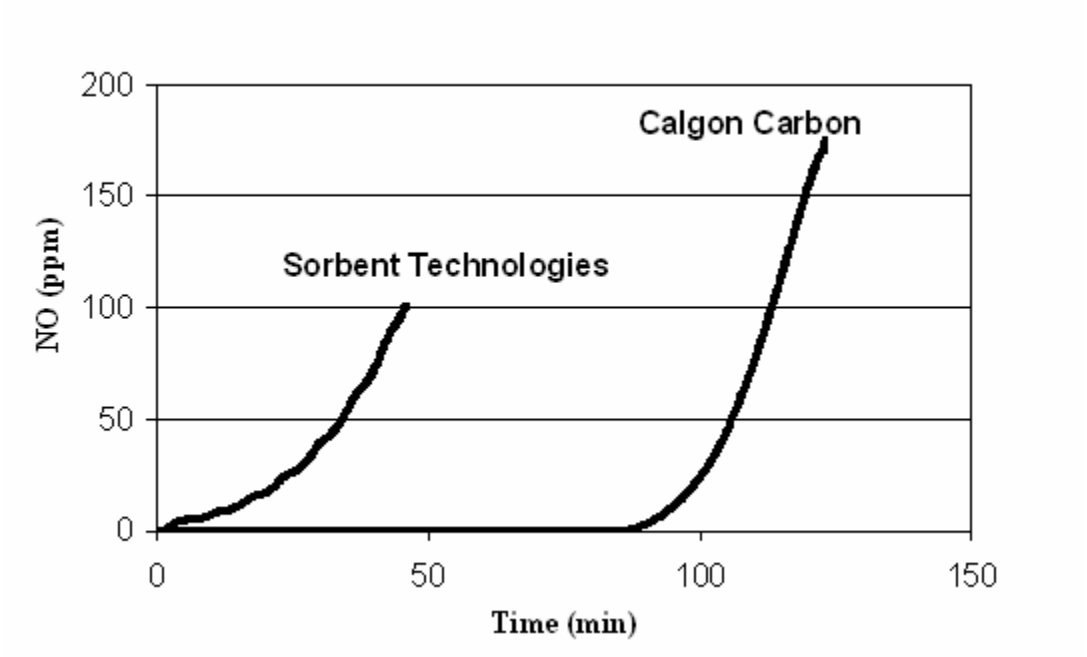

Figure 35. Adsorption breakthrough for Calgon and Sorbent Technologies, Inc. carbon

It was necessary to find the most efficient yet practical adsorption temperature of the carbon at a flow rate of 7 lpm and 510 ppm of NO. An electrical heater coil was wrapped around the chamber to heat the sorbent material to a predetermined temperature. The temperatures chosen for the adsorption runs were 100˚F, 150˚F, 200˚F, and 300˚F respectively. A fresh batch of carbon was used for each adsorption run in order to ensure a constant composition medium eliminating any unknown changes to the carbon during the desorption phase.

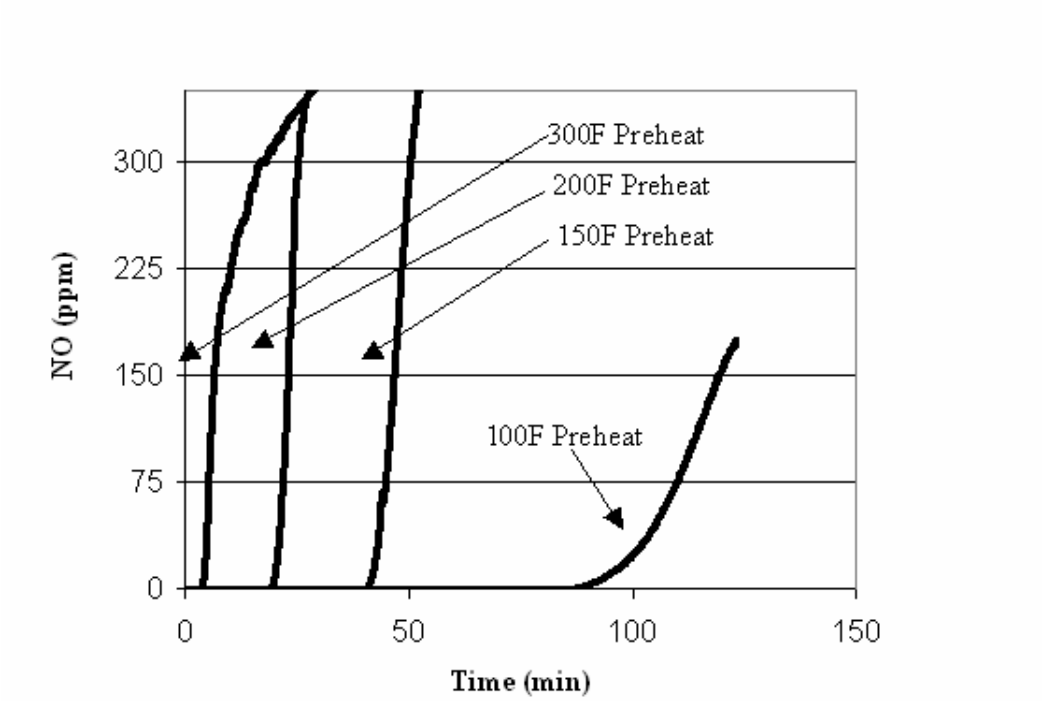

Figure 36. Centaur 4X6 carbon used in adsorption runs to find ideal adsorption temperature

As shown in Figure 36, increasing the temperature of the carbon caused an earlier breakthrough of NO, therefore, the cooler the bed the better the adsorption process, as expected. A temperature of 100˚F was chosen as a standard to preheat the bed for all remaining adsorption runs. It was supposed that the engine exhaust temperature could be lowered to 100˚F in most regions of operation, but this would be exceeded in using air cooling in some climates.

5.1.2 Adsorption of real exhaust

The researchers were concerned that the adsorption performance found in the benchtop dry NO experiments was far lower than the performance suggested by previous research using engine exhaust. In particular, during initial experimental work at WVU using a Cummins natural gas engine, and a full-scale adsorber with carbon supplied by Sorbent Technologies, Inc., adsorption mass was an order of magnitude higher than for the benchtop experiments. At the conclusion of the benchtop experiments, to evaluate the difference between the dry NO (benchtop) and real exhaust NOx adsorption, a slipstream

of a Detroit Diesel Series 60 (diesel fuel) engine's exhaust was cooled and drawn with a pump through the benchtop adsorber set at a temperature of 100°F at a rate of 7 lpm. The diesel exhaust was used because no natural gas engine was installed in the test cell at the time of the experiment. Concentrations of NOx in the diesel engine were sufficiently similar to concentrations in the lean-burn experimental engines used in the NOx decomposition campaigns. The Detroit Diesel engine was set at a speed of 1200 rpm and load of 203 Nm to produce an average level of NOx on the order of 520 ppm. The NO/NOx ratio for this engine was supposed to be approximately 95%. The adsorber completely adsorbed the NOx for approximately 6.5 hours before breakthrough began to occur. The carbon bed continued to adsorb the NOx from the exhaust for a total of 14.3 hours at which point in time the test was ended with 52 ppm out of 520 ppm of NOx breaking through the adsorber. A total of 3.67 grams of NOx was adsorbed onto 567 grams of carbon during this run corresponding to 0.65% (3.67 g of NOx/567 g of carbon*100) mass percentage of NOx to arbon. Figure 37 shows the adsorption data of the diesel engine exhaust compared to the bench test data.

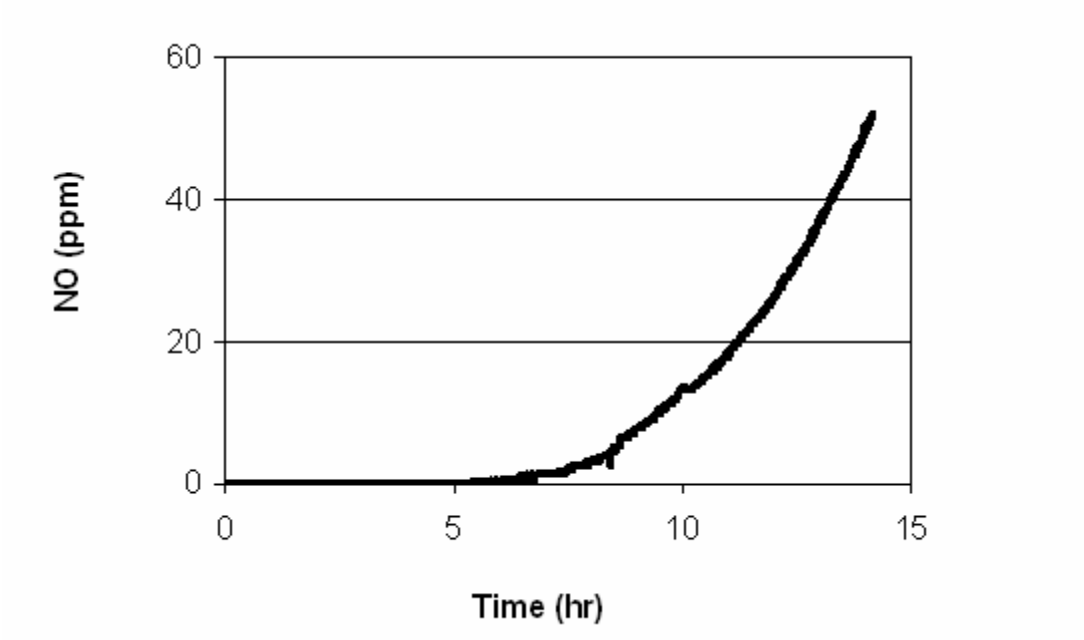

Figure 37. Diesel exhaust adsorption.

A direct comparison of the benchtop dry NO adsorption and diesel exhaust NOx adsorption can be found in Figure 38.

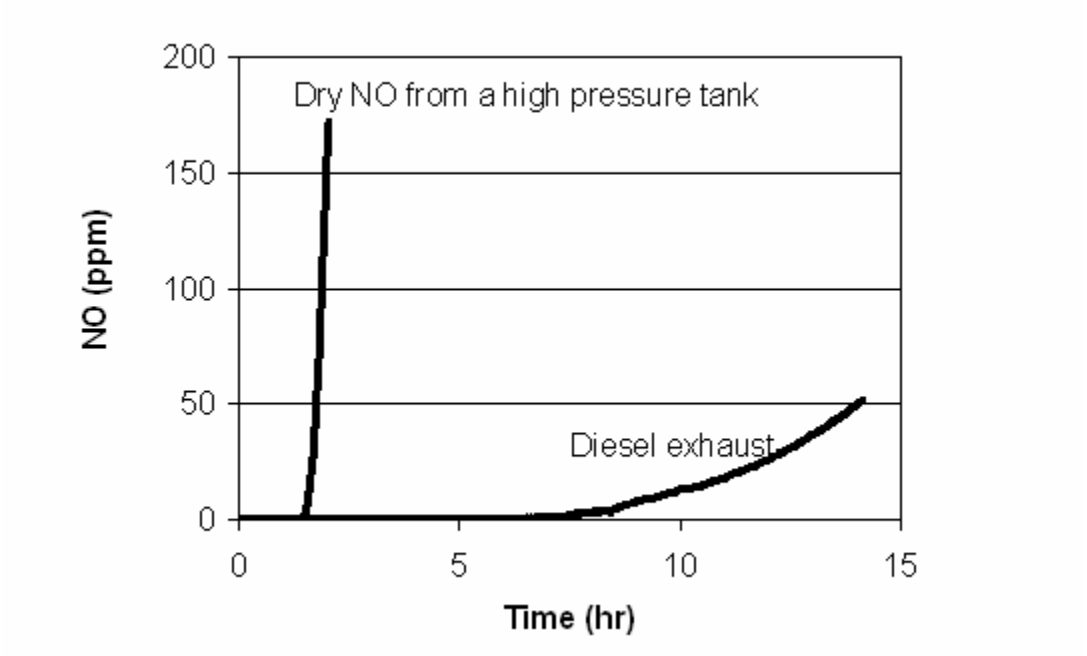

Figure 38. Direct comparison of NO injected from a high pressure tank and diesel exhaust adsorption

Using the breakthrough data for the diesel engine exhaust the following equation was generated to represent the break through curve: $Y= 0.7431X^2 + 0.6833X$ (where X is time in hours and Y is the amount of NOx breakthrough in ppm). Using this equation, if the bed were allowed to adsorb for 18.2 hours after breakthrough had occurred, 258 ppm of NOx would be passing through the bed, corresponding to about 50 percent efficiency. An additional 3.96 grams of NOx would be adsorbed after breakthrough had occurred. A total of 5.66 grams of NOx would be adsorbed onto 567 grams of carbon corresponding to a 1% mass percentage of NOx to Carbon. While extrapolation of this kind is uncertain, the researchers believed that adsorption loadings of 1% were feasible for design considerations. This real exhaust research also spurred the adsorption measurement effort described in Secion 5.1.3 below.

5.1.3 Adsorption with added water

From the data presented in the previous section, it can be seen that an actual exhaust stream adsorbed onto the carbon far longer than the simulated model. The difference in the engine test data compared to the bench test data was suspected to be due to the presence of water vapor and/or oxygen in the engine exhaust stream, which could affect the adsorption capabilities of the sorbent material. In order to investigate the cause of this difference, benchtop experiments were repeated, but the NO was passed through a water bubbler system to simulate the effects of moisture found in the exhaust stream.

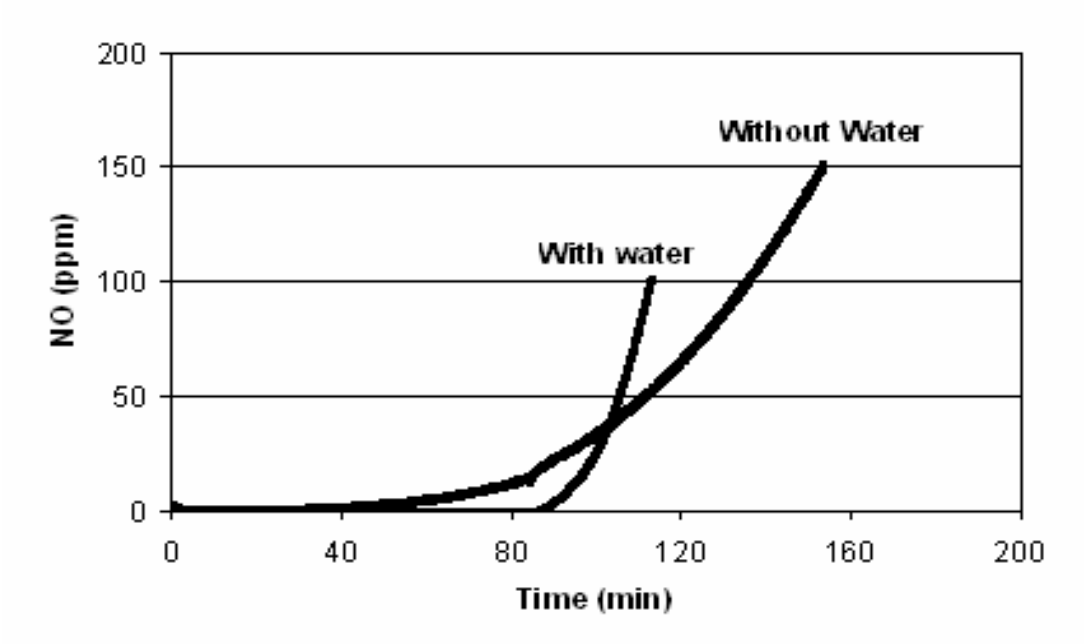

Figure 39. Adsorption onto 567 grams of Calgon Carbon with and without water

For a baseline run, NO was first injected through the carbon without added water at a rate of 7 lpm and a concentration of 510 ppm. During this run, after a breakthrough time of approximately 90 minutes, a total of 0.476 grams of NO were adsorbed onto 567 grams of carbon corresponding to 0.084 weight percent of NO to carbon. NO was next injected through a bubbler system at a rate of 5.5 lpm and concentration of 750 ppm. During this second run with water vapor, a total of 0.55 grams of NOx were adsorbed onto 567 grams of carbon corresponding to 0.097 weight percent of NOx to carbon. A comparison of the data with and without water vapor is shown below in Figure 39.

The presence of water vapor allowed for a slight increase in the mass of NOx adsorbed by the carbon, however, this slight increase does not explain the large difference between the dry bench test data and the diesel engine exhaust.

5.1.4 Adsorption with added oxygen

The next step taken to find the difference between adsorption of actual exhaust and the dry NO adsorption was to add oxygen to the NO during a benchtop experiment. NO at a concentration of 3050 ppm was mixed with compressed air through a gas divider. NO was the component set at 30% and compressed air was the balance set at 70%. The carbon bed was filled 566 grams of Calgon Carbon and left at room temperature (80°F). The bed was left at room temperature because there was not an available temperature controller at the time of testing.

The entire run was broken up into six sections. Data were logged as voltage:

0 - 4.92 volts corresponded to 0 – 3050 ppm NO

The injection gave an output of 0.86 volts (530 ppm) to be adsorbed by the carbon: this input concentration remained constant during each section. The only variable that changed during the sections was the flow-rate in order to accelerate the adsorption process. The time and flow-rate for each section is shown in Table 24 below.

Table 24. NO mixed with compressed air adsorption

Section	1	2	3	4	5	6
Duration	1 hr 15 min	4 hr 45 min	4 hr	3 hr	7 hr	7 hr 40 min
Flow-rate (lpm)	7	7.5	7	7 to 14 half way through	13	13

Near the end of Section 6 measurable breakthrough began to occur. Section 6 was ended with 0.5% or 15.5 ppm breakthrough occurring. A total of 10.93 grams of NOx was adsorbed onto 566 grams of carbon corresponding to 1.93 weight percent NOx to carbon at the start of break-through. The data for the entire run, along with data without adding compressed air and data from the diesel exhaust tests, is shown in Figure 40.

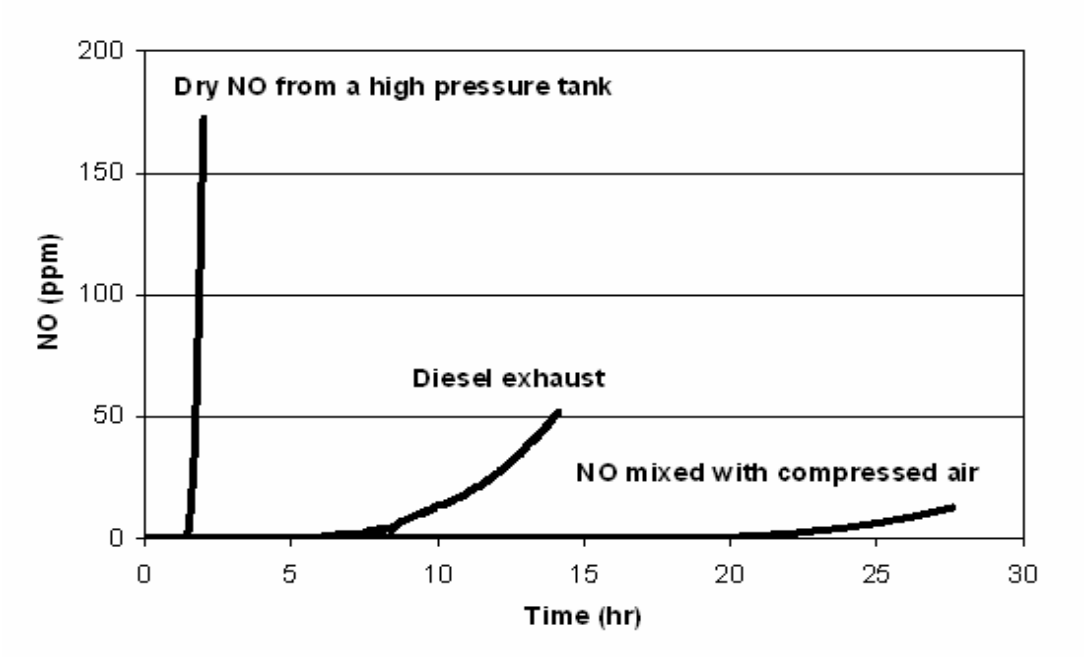

Figure 40. NO, NO mixed with compressed air, and diesel exhaust adsorption

As can be seen for this test, the addition of oxygen (accomplished by mixing NO with compressed air) significantly extended the time to breakthrough between 15 and 20 times longer than the NO (balance nitrogen) tests, with a weight percent adsorbed increase of approximately 25 times. If testing were continued until the concentration of NO breaking through was allowed to reach levels at which testing was stopped in the benchtop and diesel exhaust tests, even higher adsorbed mass levels would be achieved. This data were comparable and slightly better than the diesel exhaust data, demonstrating the effect that the presence of oxygen has on adsorption. However, the reduced adsorption temperature of 80°F would also improve adsorption. Increases in the breakthrough time and adsorbed amounts compared to the diesel engine exhaust could also be due to different constituents found in the exhaust stream such as particulate matter and hydrocarbons also adsorbing onto the carbon.

Figure 41 represents NOx weight that can be adsorbed onto the Calgon carbon material. Calgon Corporation stated that at 76°F the carbon material is capable of adsorbing approximately 2 % of its weight in NOx [104]. Experimental tests conducted with a benchtop model using 566 g of activated carbon granules adsorbed 10.93 g of NOx at

80°F. Adsorbed NOx weight was lower as the adsorbtion temperature was increased. At 100°F, 2.8 g of NOx was adsorbed into the carbon granules in the benchtop adsorber that contained 500 g of carbon. A similar reduction in NOx adsorbtion due to elevated temperatures was observed in experiments conduced by Sorbent Technologies, Inc. using similar type of activated carbon granules [90].

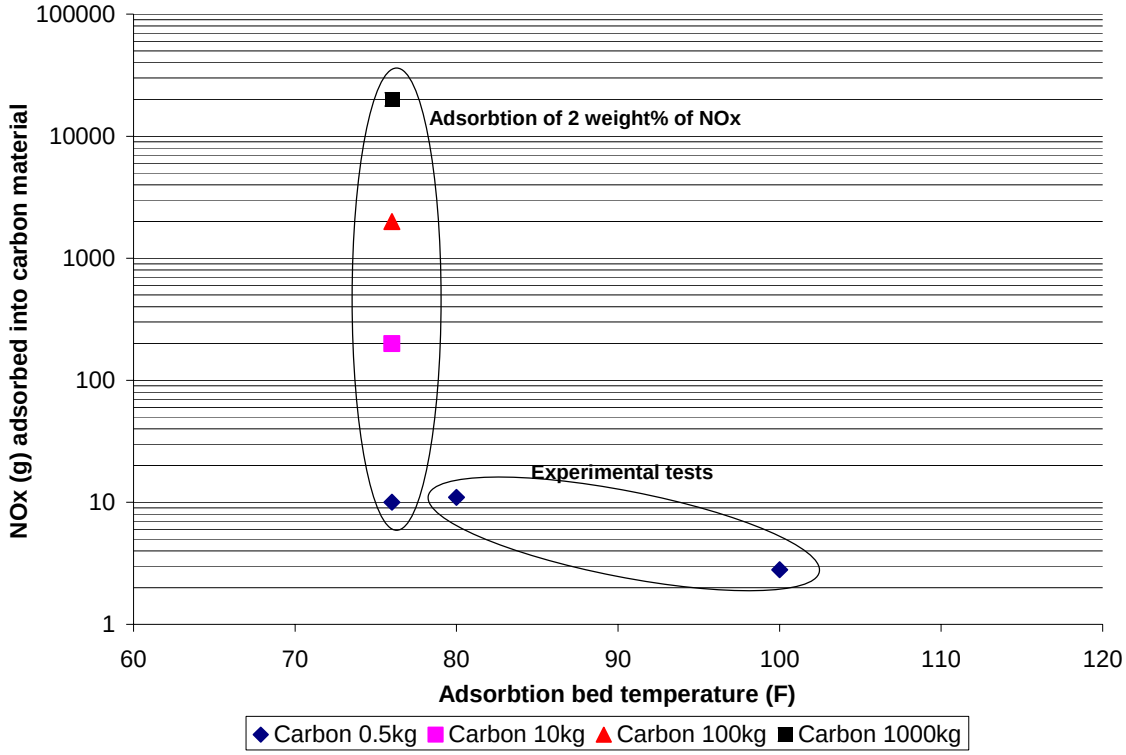

Figure 41. Amount of NOx adsorbed into carbon vs. bed temperature

The difference between the adsorption of NO with and without oxygen present can be explained by the adsorption mechanism. The researchers reviewed physical chemistry research and a literature review published by Kong and Cha [110] that supports the present conclusions. It is likely that the NO is oxidized to NO_2 as part of the adsorption process, and that this oxidation reaction is not possible when the balance of gas is nitrogen. For lean-burn engines, oxygen would be available to facilitate the reaction. The researchers have discussed this issue in greater detail in reference [105].

Desorption Phase

It was also desired to find the most practical and efficient desorption temperature for the carbon. The carbon bed was first adsorbed with 510 ppm of NO. To simulate an exhaust flow, an inline heater was used to heat air entering the bed to a temperature of 800˚F. The first desorption peak occurred at an inside bed temperature of 300˚F. There was also a larger quantity of NO release centered around 450˚F. Temperatures above 450˚F had no effect on the release rate of NO. Clearly the desorption process is complex because it involves heat and mass transfer, as well as the desorption process itself.

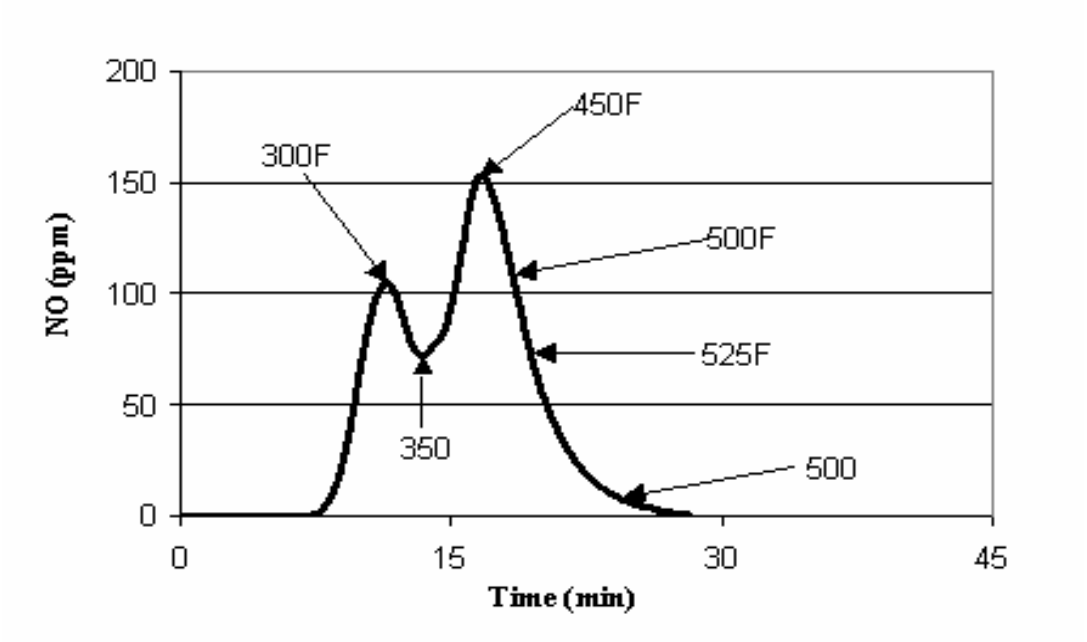

Figure 42. Desorption runs at a varying inside bed temperature

The greatest quantity of NO was released at a temperature of 450˚F. Temperatures below 300˚F were unsatisfactory for NO desorption. These data may imply that there are two different types of NO bonding within the carbon, and it is not certain how the NO_2 plays a role in the desorption dynamics.

5.2.1 Desorption of NO with added oxygen

It was desirable to find the amount of NO which was converted to NO_2 in the presence of oxygen as the mixture adsorbed onto the carbon surface. The NO (balance air) adsorption run was followed by a desorption run, while measuring both NO and NO_2 concentrations exiting the carbon bed. A flow rate of 7 lpm of ambient air was passed through the carbon bed at an inside bed temperature of 300°F. The desorption continued for a period of 14 minutes at which point in time the test was stopped since too much moisture was exiting the bed in order to ensure a proper reading on the NOx analyzer. From the data obtained, however, it was found that approximately 54% of the NO injected was converted to NO_2 as it adsorbed onto the carbon while 46% remained as NO. Dr. Mridul Gautam of West Virginia University suggested to the researchers that this level of NO_2 may have saturated the catalytic NOx converter of the analyzer. If this is the case, the NO_2 fraction will have been underestimated.

6. System Model and Sizing

6.1 Overview

Present day stationary natural gas engines produce NOx levels in the range of 0.9 – 1.3 g/bhp-hr. Therefore, to reach the ARES NOx target of 0.1 g/bhp-hr, a reduction of 88 – 92% is required. The overall SNR system design and implementation on a stationary natural gas engine has two main aspects.

The first is the feasibility of directing NOx-laden air into the engine for its decomposition. The objective is to achieve high NOx reduction from the engine with minimum engine modification. Possible options are discussed, along with benefits and drawbacks for each implementation, below.

The second aspect of incorporating SNR into a production engine is the variability of the adsorption system configuration. The researchers considered one, two or three adsorption chamber setups, the system size with respect to the engine with which it is integrated, and auxiliary power requirements for the gas cooling system.

6.2 Engine NOx decomposition options

CHEMKIN modeling and experimental engine data discussed in this report showed that for NOx decomposition, the engine must be operated with a stoichiometric or slightly rich fuel mixture. However, stoichiometric operation implies high in-cylinder temperatures, leading to concerns over engine longevity and excessive NOx production. The solution is to combine the stoichiometric operation with the exhaust gas recirculation (EGR), to provide a combustible mixture that encourages NOx decomposition chemically, and is also at an acceptable temperature. The desired in-cylinder temperature must be low enough to discourage a high NOx equilibrium, but high enough to promote a fast rate of decomposition, as CHEMKIN model data have shown. The in-cylinder temperature must also not chellenge the materials of construction of the engine or reduce engine longevity. The basic system design must therefore allow for the addition of EGR while operating the engine at a stoichiometric setting, even though the engine would

normally operate with a lean mixture. It was noted that excessive EGR can lead to slow and incomplete combustion, with high carbon monoxide and hydrocarbon emissions [34].

With mixer-equipped engines, the researchers assumed as a first approximation that the excess (i.e., in excess of the stoichiometric requirement) air in the intake should be replaced with exhaust gas. However, for very lean engines, where effects of full EGR replacement of excess air would be unacceptable, the intake must be throttled as well as augmented with exhaust gas during the decomposition. For engines with feedback control of air/fuel ratio, it would be necessary to intervene between the wide range oxygen sensor and controller to cause the controller to operate the engine stoichiometrically during the decomposition phase. This type of operation has already been demonstrated with the electronically managed Cummins L10G engine used in this research.

The researchers also considered the option of running only one cylinder of the engine in stoichiometric mode, and returning all of the desorbed NOx to that cylinder. Table 25 explains the proposed system configurations along with the benefits and challenges for each configuration.

Table 25. Possible system configurations for engine NOx decomposition

Benefits	Challenges
Return NOx stream to whole engine, during lean-burn operation	
No engine control intervention Simple plumbing for adsorber hookup	Need to operate at low speed, high load for high percent decomposition, or large adsorbers with high recycle are needed Need to desorb rapidly to maintain NOx concentration in intake
Return NOx stream to whole engine, during intermittent stoichiometric burn operation	
The same fueling control is applied to the whole engine A wide operating range is possible for adequate NOx decomposition It is readily implemented on most electronically controlled engines A reducing catalyst could be used for additional NOx cleanup	Affects turbochargers because mass flow must be reduced Concern over engine thermal management and knock Transient may occur during changeover from lean-burn Complex controls and fueling on mixer-type engines Need to desorb rapidly to maintain NOx concentration in intake Intermittent loss of thermal efficiency
Return NOx stream to one cylinder, during lean-burn operation	
Concentration of NOx in-cylinder aids rapid decomposition	Need to operate at low speed, high load for high percent decomposition, or large adsorbers with high recycle are needed Need to raise desorbed stream to intake runner pressure
Return NOx stream to whole engine, during intermittent stoichiometric burn with EGR operation	
The same control is applied to the whole engine A reasonable operating range is possible for adequate NOx decomposition If EGR replaces excess air, control of mixer-type engines is simplified Reducing catalyst could be used for additional NOx cleanup	Transient may occur during changeover from lean-burn to stoichiometric burn EGR mass must match desorption requirements Plumbing can be more complex
Return NOx stream to one cylinder, during intermittent stoichiometric burn operation	
A wide operating range is possible for adequate NOx decomposition Concentration of NOx in target cylinder aids decomposition Total engine flow changes little, few	Engine alteration required to separate one cylinder, ie. separate intake runner Concern over engine thermal management on one cylinder More complex controls and fueling on

transient concerns Small effect on thermal efficiency	mixer-type engines
Return NOx stream to one cylinder, during intermittent stoichiometric burn with EGR operation	
A reasonable operating range is possible for adequate NOx decomposition Concentration of NOx in target cylinder aids decomposition Total engine flow changes little, few transient concerns Small effect on thermal efficiency	Engine alteration required to separate one cylinder More complex controls and fueling on mixer-type engines

6.2.1 Single Adsorber NOx Reduction

The baseline NOx and decomposition values were directed into a NOx adsorption and desorption phase model which was based on the current experimental NOx saturation condition of the adsorber.

Assumptions for a single adsorber case were as follows:

- Exhaust gas from engine is normally directed to an adsorber
- Engine baseline NOx mass emissions are constant
- During the desorption period the major portion of exhaust gas from engine bypasses the adsorber into the atmosphere in a single adsorber system
- EGR carries NOx for decomposition
- EGR% is constant during decomposition
- Engine baseline NOx emissions are constant for a given operating point: $\dot{m}_{NOx}$
- Adsorber adsorbs NOx at 100°F at an instantaneous constant efficiency: η_a
- Adsorber desorbs NOx at 300°F at a mass rate of $\dot{m}_d$
- Desorption efficiency: η_d
- Mass of NOx in the adsorber at any time: m_a

Consider a cycle of adsorption followed by desorption where:

t_a – adsorption time in seconds

t_d – desorption time in seconds

From these assumptions, it can be deduced that NOx released to the stack after adsorption is:

$$\dot{m}_{out} = \dot{m}_e * \eta_a \tag{26}$$

NOx mass stored in the adsorber is:

$$m_s = (\dot{m}_e - \dot{m}_{out})\, t_a \tag{27}$$

During the desorption period, mass rate of NOx released from the adsorber is:

$$\dot{m}_d = (m_s - m_a)(\eta_d / t_d) \tag{28}$$

If the total mass flow of the exhaust is $\dot{m}_{Te}$, then the mass concentration of NOx in exhaust is:

$$C_e = \frac{\dot{m}_e}{\dot{m}_{Te}} \tag{29}$$

Assuming the total mass flow of the desorption gas $\dot{m}_{Td}$, is related to $\dot{m}_{Te}$ by the fraction of *EGR%*, then the concentration of NOx in the desorption gas is:

$$C_d = \frac{\dot{m}_d}{EGR\% * \dot{m}_{Te}} \tag{30}$$

The total engine exhaust total flow $\dot{m}_{Te}$ is virtually identical to the total mass flow into the engine. Blowby losses are typically 1% by mass. Hence, if during desorption the desorbed stream is directed to the engine intake, then the concentration of NOx in the intake (assuming no background NOx) is given by:

$$C_i = \frac{\dot{m}_d}{\dot{m}_{te}} \tag{31}$$

As an example, consider the following operating point, for the case of a 10 liter engine:

Engine speed = 800 rpm

Engine load = 350 ft-lb

External EGR = 0%

λ = 0.98

Consider the following adsorber characteristics:

Adsorption efficiency = 80%

Adsorber adsorbs NOx at 100°F for 4 hours

Desorbs NOx at 450°F for 1 hour

Engine NOx decomposition = 90%

During desorption engine would operate slightly rich producing 0.11 g/s NOx

The outputs for these conditions are:

Baseline engine NOx rate (lean-burn) = 0.063 g/s

NOx output rate after adsorber = 0.025 g/s after 4 hours

Averaged NOx out into atmosphere = 0.033 g/s

Therefore, the model illustrates a total NOx reduction of 49% for using a single adsorber system for a given operating point (Figure 43).

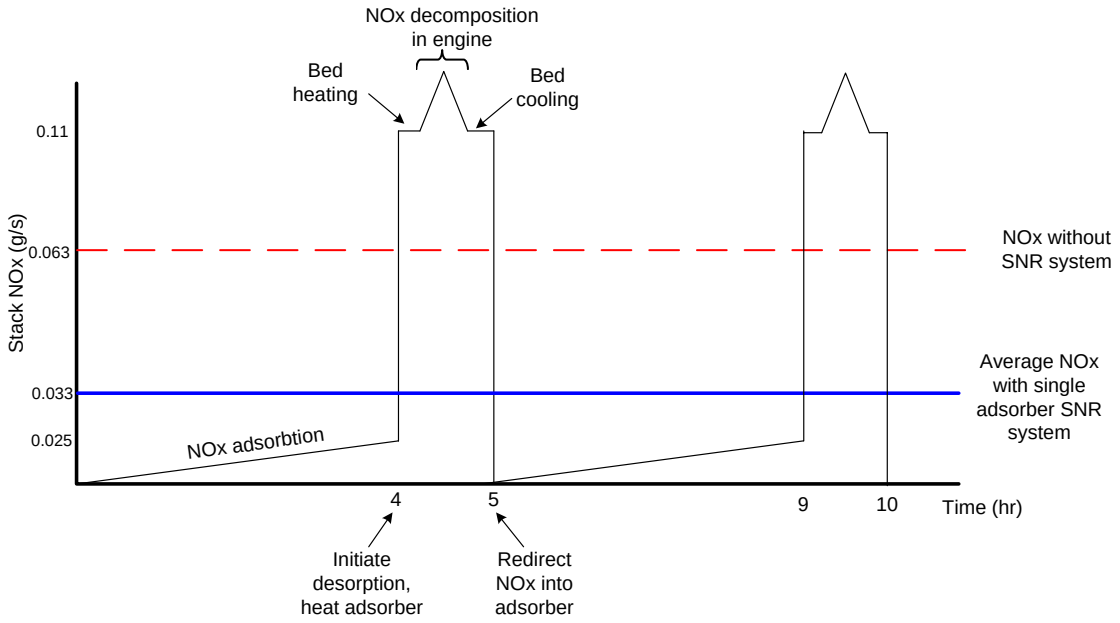

Figure 43. An example run on the overall NOx reduction capability of a SNR system

The model was extended to simulate NOx reduction when two NOx adsorbers were utilized where one operated in adsorbtion mode while the other in desorption mode. The modeling criteria are shown below in Section 6.3 of this report. With a twin adsorber system the average NOx reduction was over 85%.

6.3 Adsorber design configuration

The adsorption should take place from exhaust gas that has passed through a heat exchanger to reduce the temperature and a demister to remove condensed water. The loe carbon to hydrogen ratio of natural gas causes the water level to be higher in natural gas engines than in petroleum-fueled engines. Desorption was considered using a slipstream of hot exhaust gas to minimize energy demands, or by heat exchange with hot exhaust gas.

The sorbent chamber design must consider the heating and cooling rates for the bed at the time that desorption and adsorption phases (respectively) are initiated. If the thermal inertia of the bed prevents rapid heating, the desorbed stream may be low in NOx concentration, leading to poor decomposition rates in the engine. The design must consider a cycle of four modes, namely adsorption, heating, desorption and cooling. In a

twin or triple adsorber system, adequate time is available for heating, desorption and cooling phases between the adsorption phases. Also, there is freedom in determining the cycle time of the adsorbers, which determines adsorber size and heating/cooling behavior.

6.4 SNR arrangement

A most likely arrangement for an SNR application is shown in Figure 44**.** The system uses one of two NOx adsorbers to collect a substantial fraction of the NOx onto the sorbent material by first cooling the engine exhaust gas. Once the adsorber is saturated (which may be determined by breakthrough measurement using sensor inputs or a conservative model), the desorption process recirculates a concentrated stream of NOx into a NOx decomposition system that facilitates thermal NOx decomposition. Figure 44 shows a schematic of an adsorber SNR aftertreatment system, operating in an adsorption mode, coupled to a lean-burn engine. A control valve (V3) in the figure is used to direct the cooled exhaust stream one of the two NOx chambers. A closed loop gas circulating system can be added to increase the concentration of the desorbed gas, but is not shown in Figure 43.

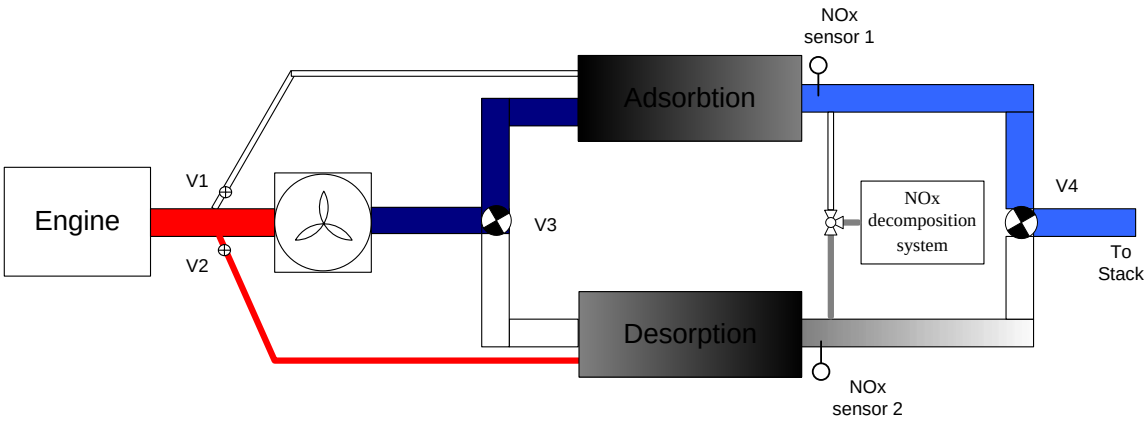

Figure 44. Single adsorber SNR system in adsorption mode

A portion of the hot exhaust gas from the engine is used to heat the sorbent bed to initiate the desorption process. Therefore, it is necessary to conduct a mass and heat demand analysis on the adsorber system. It was of concern to the researchers that, for a given sorbent, a high emissions engine may produce a full sorbent load of NOx in a shorter time than it would take to produce the available exhaust energy needed to heat the bed for desorption, but analysis showed that adequate exhaust energy was available for

desorption for the case of a Cummins QSV91 engine or a Wauhesha APG1000 engine [105].

6.5 Technical and economic analysis

The basis for this analysis is the exhaust flow from a Cummins L10G natural gas engine with the following exhaust gas properties:

Flow of gas = 355 scfm = 7.4795 mol/s = 0.2095 kg/s

NOx loading = 1060 ppm

Gas exhaust temperature = 1100°F (593.3°C)

Power = 240 hp (186 kW)

From the adsorption data presented above and in reference [105], a conservative estimate for the average loading for NO_2 on carbon was taken to be 0.5 wt%.

The design of the absorber should be based on either a cycle time length criterion or on a bed pressure drop criterion. Both of these approaches are given below to determine the limiting condition.

Cycle time criterion

Assuming a cycle time of 8 hours for adsorption using a flow of 355 scfm with a loading of 1060 ppm (NO_2 equivalent), the required amount of carbon per absorber is

$$\text{Required amount of carbon} = \frac{(.2095)(8)(60)(60)(1060\times10^{-6})}{(0.005)} = 1,279\,\text{kg} \qquad (32)$$

The bulk density of activated carbon = 560 kg/m^3

Volume of activated carbon = (1,279)/(560) = 2.284 m^3 (33)

Assuming a length/diameter ratio of the adsorption bed of 3

$$\text{Diameter of Carbon bed} = \sqrt[3]{\frac{4}{\pi}\frac{(2.284)}{(3)}} = 0.99\text{m} \qquad (34)$$

$$\text{Length of Bed} = (0.975)(3) = 2.97\ \text{m}$$

Bed Pressure Drop Criterion

When absorbing the exhaust gas, the total flow rate of gas (less a small slip stream of by-pass gas used for regeneration) must pass through the bed. The pressure drop may be estimated using the Ergun equation:

Exhaust gas through packed carbon bed

$\dot{m} = 0.2095\,\text{kg/s}$

Properties of exhaust gas at T ≅ 50°C are

$\rho = 1.0012\ \text{kg/m}^3$

$\mu = 17.7\times10^{-6}\ \text{kg/m.s}$

$\text{CSA of bed} = \pi D^2/4 = \pi(0.99)^2/4 = 0.769\text{m}^2 \qquad (35)$

$$\text{Superficial gas velocity through the bed, } u_o = \frac{\dot{m}}{\rho}\frac{1}{A} = \frac{(0.2095)}{(1.0012)}\frac{1}{(0.769)} = 0.272\,\text{m/s} \qquad (36)$$

Using Ergun's equation [106], one finds that

$$\Delta P_{bed} = \frac{150\mu u_0}{d_p^2}\frac{(1-\varepsilon)^2}{\varepsilon^3} + \frac{1.75\rho u_o^2}{d_p}\frac{(1-\varepsilon)}{\varepsilon^3} \qquad (37)$$

$$\frac{\Delta P_{bed}}{L} = \frac{(150)(17.7\times10^{-6})(0.272)}{(0.0037)^2}\frac{(1-0.5)^2}{0.5^3} + \frac{1.75(1.0012)(0.272)^2}{(0.0037)}\frac{(1-0.5)}{0.5^3} = 246\,\text{Pa/m}$$

$$\Delta P_{bed} = (246)(2.97) = 730\,\text{Pa (0.11 psi)} \qquad (38)$$

The pressure drop value lies within the boundaries prescribed by Calgon Carbon Corp. for their granular carbon and is not excessive for this cycle time (Figure 44). Therefore, the use of an 8 hour cycle time is taken as the basis for the remaining analysis.

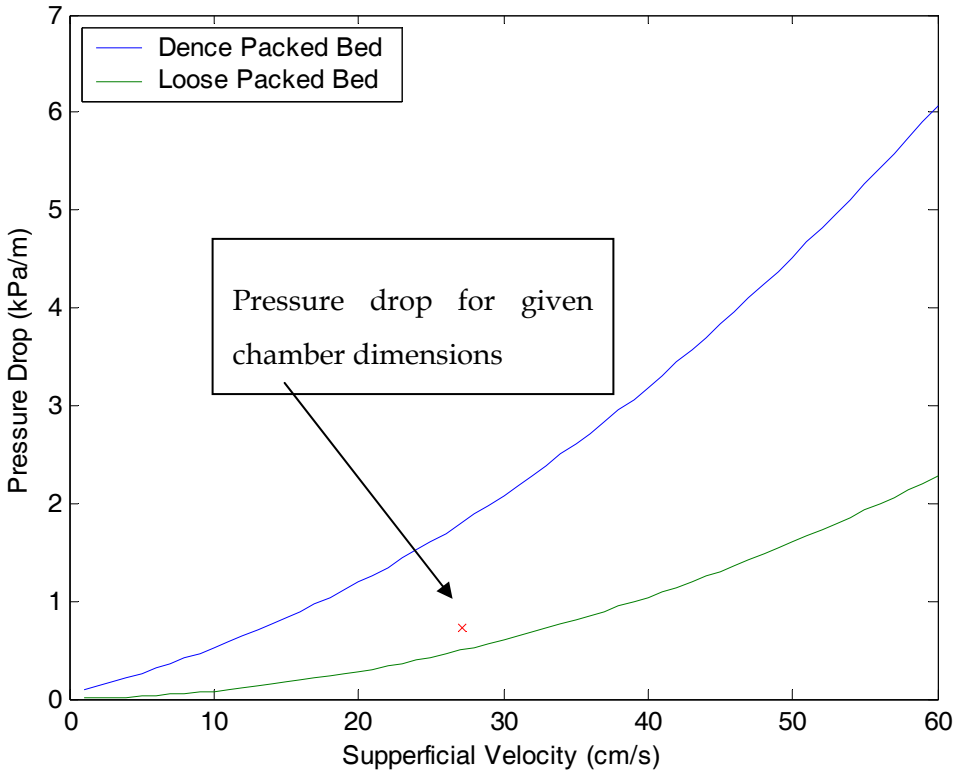

Figure 45. Pressure drop for chamber dimension of Length 2.97 m and diameter 0.99 m

The carbon lifetime is expected to consist of 1000 adsorbtion desorption cycles. Therefore, for the calculated chamber dimension each cycle would last 16 hours where 8 hours dedicated to adsorbtion, 4 hours to heat the carbon material, 2 hours for the desorption phase and 2 hours to cool down to ambient temperature.

Adsorption Cycle

During the adsorption cycle, the exhaust gas is cooled to approximately 120°F (48.9°C) using air at a temperature of 108°F (40°C). The temperature-enthalpy diagram for this heat exchanger is shown in Figure 46.

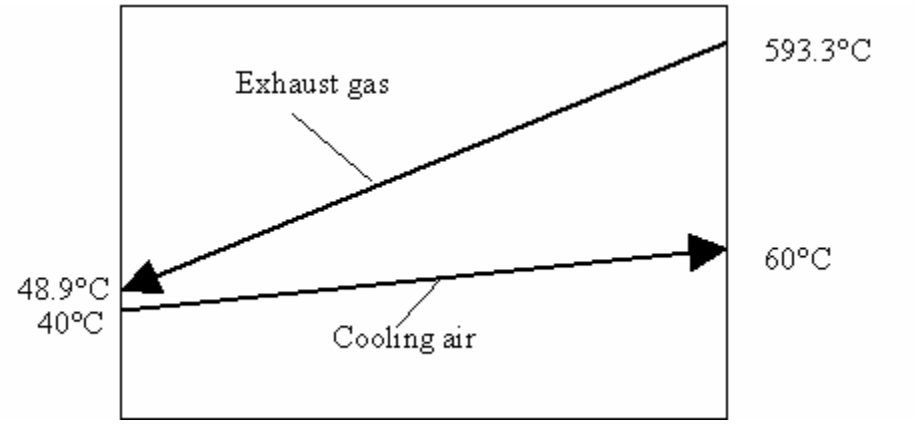

Figure 46. Temperature-enthalpy diagram for exhaust gas exchanger

For this exchanger, the log-mean temperature difference (LMTD) is given by

$$\Delta T_{lm} = \frac{(593.3-60)-(48.9-40)}{\ln\dfrac{(593.3-60)}{(48.9-40)}} = 128.1^{o}C \tag{39}$$

An overall energy balance gives

$$\dot{M}C_p\Delta T = \dot{m}c_p\Delta t$$

$$\dot{m} = \frac{\dot{M}C_p\Delta T}{c_p\Delta t} = \frac{(0.2095)(1084)(593.3-48.9)}{(1005)(60-40)} = 6.14 \text{ kg/s} \tag{40}$$

For this exchanger, assume a fin-fan exchanger in which the exhaust gas flows through the inside tubes and the cooling air stream flows on the outside of the tubes (on the shell side).

The correction factor (F) for the LMTD is found as $F = f(P,R)$, where

$$R = \frac{\dot{m}c_p}{\dot{M}C_p} = \frac{(6.14)(1005)}{(0.2095)(1084)} = 27.2$$
$$P = \frac{t_2 - t_1}{T_1 - t_1} = \frac{(60-40)}{(593.3-40)} = 0.0355 \quad (41)$$

For a cross flow exchanger using these values of P and R, Levenspiel [106] gives $F = 0.95$

The duty for the heat exchanger is 444.9 MJ/h (123.6 kW)

To estimate the overall heat transfer coefficient a trial and error calculation must be used. The results for this calculation are presented below:

Based on the bare outside tube area, the overall heat transfer coefficient = 14.56 W/m^{2}K= (2.564 BTU/hr/ft^2/°F)

Heat exchanger area = $A_o = \frac{Q}{U_o \Delta T_{lm} F} = \frac{(123,600)}{(14.56)(128.1)(0.95)} = 66.3\text{m}^2$ (42)

Assume that the exchanger is made from 1" OD .14 BWG tubes 20 ft in length

Outside area per tube = $\pi D_o L = \pi(20)(1/12) = 5.236$ ft^2 (0.4864 m^2) (43)

Number of tubes required = (66.3)/(0.4864) = 136 (44)

Arrangement is 4 parallel rows of tubes stacked vertically with 136/4 = 34 tubes per row

Using a 2 5/16" (0.05874 m) pitch, width of a tube bank = (34)(0.05874) = 2.0m (45)

CSA of bank = (2.0)(20)(.3048) = 12.2 m^2 (46)

Approx. CSA for air flow = 12.2 – (34)(0.0254)(20)(0.3048) = 6.94 m^2 (47)

Density of ambient air = 1.094 kg/m^3

Approx. face velocity of air = (6.14)/(1.094)/(6.94) = 0.809 m/s (2.65 ft/s) (48)

Required power for fans = (12.5)(12.2)/(100)/(.3048)^2 = 16.4 hp (12.2 kW) (49)

(based on 12.5 hp/100 ft^2)

Use 3 fans (F-101A/B/C) each with a rating of 5.5 hP (4.1 kW)

Check overall heat transfer coefficient

Inside tubes

CSA for flow = $n n_t \pi D_i^2 / 4 = (136)\pi(0.021184)^2 / 4 = 0.04793$ m^2 (50)

average density = 0.698 kg/m^3

average velocity inside tubes = (0.2095)/(0.698)/(0.04793) = 6.26 m/s (51)

average viscosity = 27.66×10^{-6} kg/m/s

$$\mathrm{Re} = \frac{\rho v D}{\mu} = \frac{(0.698)(6.26)(0.02118)}{(27.66\times10^{-6})} = 3,346$$

$$Nu = 0.023\,\mathrm{Re}^{0.8}\,\mathrm{Pr}^{0.33} = (0.023)(3,346)^{0.8}(0.716)^{0.33} = 13.6 \quad (52)$$

$$h_i = Nu\frac{k}{D_i} = 13.6\frac{0.04475}{0.02118} = 28.7\ \mathrm{W/m^2K}$$

Outside Tubes

Fin diameter = 0.0572 m

Number of fins = 10 per inch = 394 per m

Tube pitch = 0.0587 m

D_{eq} = 0.0098 m

$$\mathrm{Re} = \frac{\rho v D_{eq}}{\mu} = \frac{(1.094)(0.81)(0.0098)}{(19.54\times10^{-6})} = 444$$

$$Nu = 0.4\,\mathrm{Re}^{0.6}\,\mathrm{Pr}^{0.33} = (0.4)(444)^{0.8}(0.693)^{0.33} = 13.7 \qquad (53)$$

$$h_o = Nu\frac{k}{D_o} = 13.7\frac{0.02822}{0.0098} = 39.6\ \mathrm{W/m^2K}$$

Combining heat transfer resistances, one finds that

$$\frac{1}{U_o} = \frac{D_o}{D_i h_i} + \frac{t_{wall}}{k_{wall}} + \frac{1}{U_o} = \frac{(.0254)}{(0.02118)(28.7)} + \frac{(0.00211)}{(50)} + \frac{1}{(39.7)} = 0.06702 \qquad (54)$$

$$U_o = 14.9\ \mathrm{W/m^2K}$$

This is sufficiently close to the assumed value of 14. 6 W/m²K to accept the calculations.

Exchanger Design Summary

A summary of the exhaust gas exchanger layout is given in Figure 47.

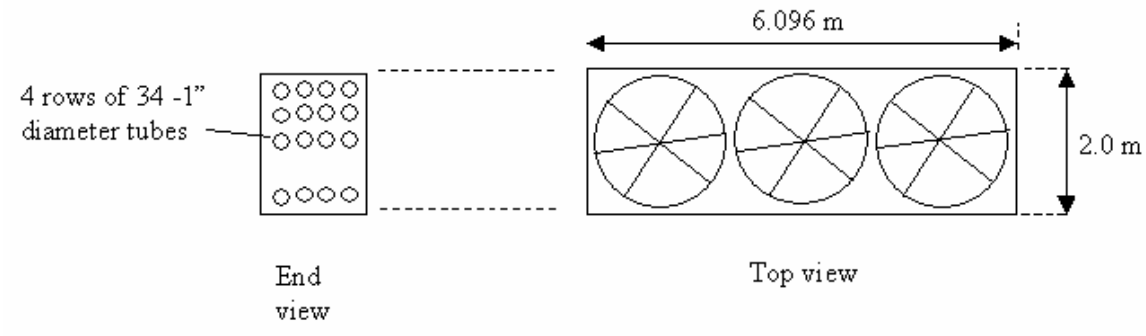

Figure 47. Illustration of the tube and fan layout for the exhaust gas exchanger

Pressure Drop measurements

Exhaust gas through packed carbon bed

From Equation (38) we have

$$\Delta P_{bed} = (246)(2.97) = 730\,\mathrm{Pa}\ (0.11\ \mathrm{psi}) \qquad (55)$$

Exhaust gas through tubes

Re = 3,346

f = 0.01 (assume a smooth tube in turbulent flow – a conservative estimate)

$$\Delta P_f = 2 f \rho v^2 \frac{L}{D} = (2)(0.01)(0.698)(6.26)^2 \frac{(6.096)}{(0.02118)} = 157\text{Pa (0.023 psi)} \qquad (56)$$

Thus the total pressure drop through the bed and exchanger is 887 kPa (0.133 psi). A summary of the conditions for the exhaust gas cooling and adsorption process are given in Figure 48.

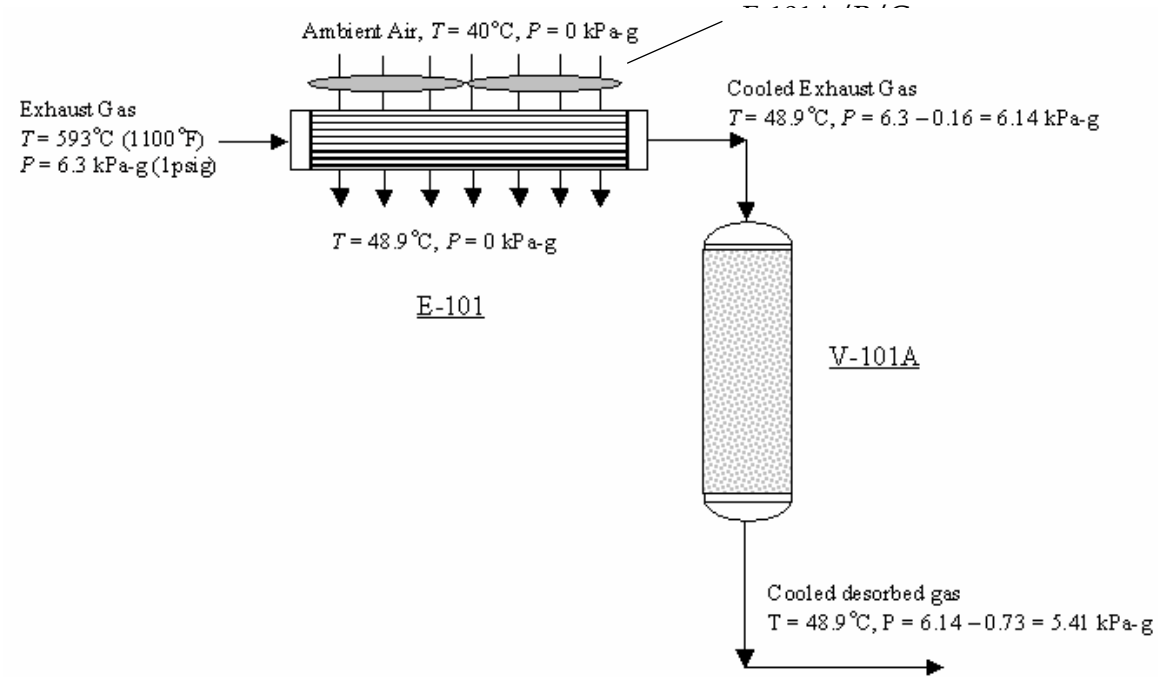

Figure 48. Illustration of conditions during the NOx adsorption cycle

Regeneration/Desorption Cycle

During the desorption cycle, in this design, the bed was assumed to be heated from 48.3°C to 204°C (400°F) using heated air rather than an exhaust gas slipstream. This approach allows the delivery of substantial energy to the bed without a high gas throughout. A high gas throughput would yield a low NOx concentration in the

desorbed gases, and would limit NOx decomposition in the engine. In order to increase the concentration of the NOx in the discharge gas (hot air containing NOx), the air stream is circulated in a closed loop. The layout and important process conditions for the desorption step are illustrated in Figure 49.

It is assumed that the air moves through the packed bed in a flat front and therefore the exit temperature will be at the initial bed temperature of 48.3°C. This assumption will be checked. In addition, the heating of the gas in the compressor is taken into account and is evaluated after a pressure balance is established for the flow loop. A slipstream of exhaust gas is used as the heating medium for the circulating air. In the previous calculation for the exhaust gas cooler the full exhaust stream was used. The lower duty in the exhaust cooler caused by the use of a slipstream will be ignored and thus the exhaust gas cooler will be slightly oversized.

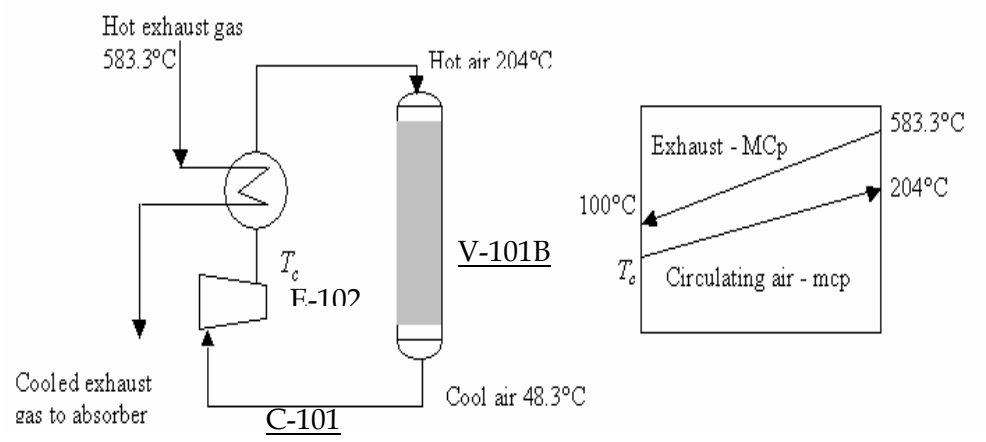

Figure 49. Process conditions for the carbon regeneration and NOx desorption process

As a preliminary estimate, assume that the temperature increase in the compressor is negligible. Therefore, for this exchanger, the log-mean temperature difference (LMTD) is given by

$$\Delta T_{lm} = \frac{(593.3-204)-(100-48.9)}{\ln\dfrac{(593.3-204)}{(100-48.9)}} = 166.6^{o}C \qquad (57)$$

An overall energy balance gives

$$Q_{tot} = M_{carb} C_{p,carb} \Delta T_{carb} = (1279)(709)(204 - 48.3) = 141.2\text{MJ} \quad (58)$$

where Q_{tot} is the total energy to cool the carbon bed assuming that the exit gas leaves at the initial bed temperature of 48.3°C. Assuming a 4-hour heat up period, the required rate of heat transfer is

$$\dot{Q} = \frac{Q_{tot}}{time} = \frac{141.2 \times 10^6}{(4)(60)(60)} = 9.80\,\text{kW} \quad (59)$$

An overall energy balance gives:

$$\dot{M} C_p \Delta T = \dot{m} c_p \Delta t = \dot{Q}$$

$$\dot{m} = \frac{\dot{Q}}{c_p \Delta t} = \frac{(9{,}800)}{(1005)(204 - 48.3)} = 0.0626 \text{ kg/s} \quad (60)$$

$$\dot{M} = \frac{\dot{Q}}{c_p \Delta t} = \frac{(9{,}800)}{(1070)(583.3 - 100)} = 0.0190 \text{ kg/s}$$

The circulating air flow rate is 0.0626 kg/s while the exhaust gas slip steam is 0.0190 kg/s or 9.0 % of the exhaust gas flow rate.

For this exchanger, assume a double-pipe design, with counter current flow

Assume a 2" Sch 10 pipe inside a 4" Sch 10 pipe, therefore

$D_{i,in}$ = 2.157 inch = 0.05478 m

$D_{i,o}$ = 2.375 inch = 0.06033 m

$D_{o\,in}$ = 4.26 inch = 0.1082 m

$D_{o,o}$ = 4.5 inch = 0.1143 m

$D_{o,eq}$ = ($D_{o\,in}$ – $D_{i,o}$) = 0.04787 m

Flow areas for inside and annular side are,

$$A_{in} = \frac{\pi}{4} D_{i,in}^2 = \frac{\pi}{4}(0.05478)^2 = 0.002357 \text{ m}^2$$
$$A_{out} = \frac{\pi}{4}(D_{o,o}^2 - D_{i,o}^2) = \frac{\pi}{4}(0.1082^2 - 0.06033^2) = 0.006336 \text{ m}^2 \quad (61)$$

Heat Transfer Coefficients

Inside coefficient **–** circulating air inside tubes

Assume that there are 2 banks of double pipe tubes operating in parallel

$$\dot{m} = 0.0626 \text{kg/s}$$
$$\rho_{ave} = 0.9109 \text{ kg/m}^3$$
$$v = \frac{\dot{m}}{\rho_{ave} n_{tubes} A_{in}} = \frac{(0.0626)}{(0.9048)(2)(0.002357)} = 14.68 \text{ m/s}$$

$$\text{Re} = \frac{\rho v D_{i,in}}{\mu} = \frac{(0.9048)(14.68)(0.05478)}{(19.5 \times 10^{-6})} = 37,300$$
$$Nu = 0.023 \text{Re}^{0.8} \text{ Pr}^{0.33} = (0.023)(37,300)^{0.8}(0.578)^{0.33} = 87.2 \quad (62)$$
$$h_i = Nu \frac{k}{D_{in,i}} = 87.2 \frac{(0.03459)}{(0.05478)} = 55.1 \text{ W/m}^2 K$$

Outside Coefficient **–** exhaust gas slipstream through annulus

$$\dot{M} = 0.0190 \text{ kg/s}$$
$$\rho_{ave} = 0.698 \text{ kg/m}^3$$
$$v = \frac{\dot{M}}{\rho_{ave} n_{tubes} A_{out}} = \frac{(0.0190)}{(0.698)(2)(0.006336)} = 2.14 \text{ m/s}$$
$$\text{Re} = \frac{\rho v D_{o,eq}}{\mu} = \frac{(0.698)(2.14)(0.04787)}{(27.66 \times 10^{-6})} = 2,590 \quad (63)$$
$$Nu = 0.023 \text{Re}^{0.8} \text{ Pr}^{0.33} = (0.023)(2,590)^{0.8}(0.716)^{0.33} = 11.08$$
$$h_i = Nu \frac{k}{D_{o,eq}} = 11.08 \frac{(0.04475)}{(0.04787)} = 10.35 \text{ W/m}^2 K$$

Overall Coefficient

$$\frac{1}{U_o} = \frac{D_{i,o}}{D_i h_i} + \frac{t_{wall}}{k_{wall}} + \frac{1}{U_o} = \frac{(.06033)}{(0.05478)(55.1)} + \frac{(0.002775)}{(50)} + \frac{1}{(10.35)} = 0.1166 \quad (64)$$

$$U_o = 8.57 \text{ W/m}^2\text{K}$$

Overall heat transfer coefficient = 8.57 W/m²K= (1.53 BTU/hr/ft²/°F)

(based on outside tube area)

Heat exchanger area = $A_o = \frac{Q}{U_o \Delta T_{lm} F} = \frac{(9,800)}{(8.57)(166.6)(1)} = 6.86\text{m}^2$ (65)

Length of tubes, $L = \frac{A_o}{n_{tubes} \pi D_{i,o}} = \frac{(6.86)(2)}{(4)(\pi)(.06033)} = 18.1$ m (6 - 10 ft pipes) (66)

Exchanger Design Summary – multiple pipe arrangement

In summary, the exchanger for the regeneration of the carbon bed consists of two parallel banks of six, 10 ft length pipes using two inch schedule 10 pipes for the inside and four inch schedule 10 pipes for outside. Circulating air flows inside the two inch diameter pipes and the exhaust gas will flow on outside in the annulus formed between two inch and four inch diameter pipes. The arrangement for this exchanger showing the flow of the circulating, regenerating gas stream is illustrated in Figure 50.

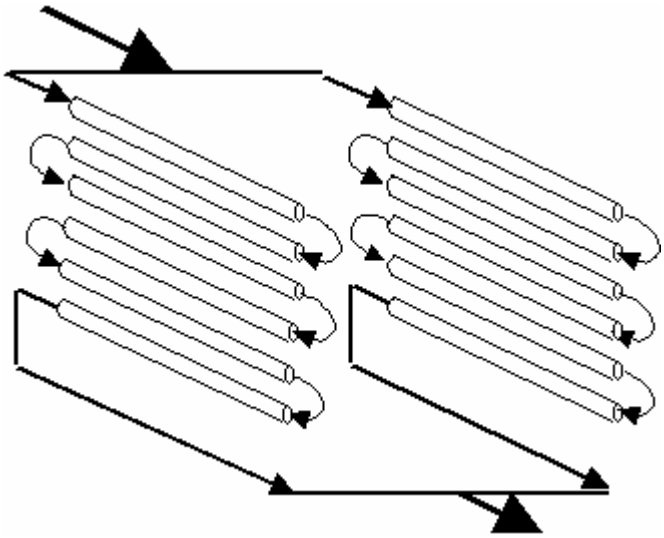

Figure 50. Layout of the regeneration exchanger (E-102) showing the flow of the regenerating air. The exhaust gas flows in the annulus between the 2″ and 4″ pipes but is not shown in this figure

Concentration of Desorbed NOx

The purpose of the circulating desorbing air stream is to concentrate the NOx. The volume of air is a function of the volume of the circulation loop consisting of the blower, carbon bed, multiple pipe exchanger, and associated piping.

The total amount of NOx adsorbed on the carbon bed during the 8-hour adsorption cycle is given by

$$\begin{aligned} &\text{NOx absorbed} = (.2095)(8)(60)(60)(1060\times10^{-6}) = 6.40\,\text{kg} \\ &\text{NOx absorbed} = \frac{6.40}{46} = 0.1390\,\text{kmol} = 139\,\text{mol} \end{aligned} \tag{67}$$

Volume of carbon = 2.284 m^3

Assume that the volume of the circulating air loop is *X* times the volume of carbon in the bed.

Concentration of NOx in the circulating, desorbing gas after an 8-hour cycle is

$$C_{NO_x} = \frac{(139)(22.4)}{(2.284)X(1000)+(139)(22.4)} = \frac{1.3632}{1.3632+X} \tag{68}$$

The resulting end-of-cycle concentrations of NOx in the regenerating air stream as a function of the volume of regenerating gas is shown in Table 26.

Table 26. Concentration of NOx in the regenerating air stream at the end of the cycle as a function of the volume of recirculating gas expressed as X, ratio of the gas volume to the volume of carbon in the bed

C_{NOx}	57.7%	40.5%	21.4%	12.0%
X	1	2	5	10

A volume of circulating gas equal to approximately 11.4 m^3 (or five times the volume of carbon in a single absorber) gives rise to a NO_x concentration of approximately 21.4% at the end of the desorption cycle. To take account of the increase in volume of circulating gas, due to the increase in the number of moles, a purge stream of approximately 20% by volume is required over the course of the cycle. Alternatively, without purging, the pressure in the recicrculating loop increases by approximately 20% (or ~3 psi).

Pressure drops for regeneration cycle

In order to evaluate the size of the circulating air compressor (blower), an estimate of the associated pressure drops around the loop must be made. These are itemized below:

Circulating air through carbon bed

The flowrate of circulating air through the bed during regeneration was given previously as 0.0626 kg/s.

The superficial gas velocity through the bed is found as follows

$$u_o = \frac{\dot{m}}{\rho A} = \frac{(0.0626)(4)}{(0.9109)\pi(0.99)^2} = 0.0893 \text{ m/s} \tag{69}$$

Using Ergun's equation we get

$$\Delta P_{bed} = \frac{150\mu u_0}{d_p^2}\frac{(1-\varepsilon)^2}{\varepsilon^3} + \frac{1.75\rho u_o^2}{d_p}\frac{(1-\varepsilon)}{\varepsilon^3} \tag{70}$$

$$\frac{\Delta P_{bed}}{L} = \frac{(150)(19.5\times10^{-6})(0.0893)}{(0.0037)^2}\frac{(1-0.5)^2}{0.5^3} + \frac{1.75(0.9048)(0.0893)^2}{(0.0037)}\frac{(1-0.5)}{0.5^3} = 52\,\text{Pa/m}$$

$$\Delta P_{bed} = (52)(2.97) = 154\,\text{Pa (0.022 psi)} \quad (71)$$

Circulating air through exchanger

The circulating air is split evenly through the two parallel tube banks each of which contains approximately 60 ft of 2″ sch 10 pipe with 5 – 180°elbows.

Equivalent L/D of tube bank is $(60)(0.3048)/(0.05478) + (5)(75) = 709$ (72)

Re = 37,300

Absolute roughness of drawn tubing, ε = 0.0015 mm

$\varepsilon/D = 1.5\times10^{-6}/0.05478 = 2.74\times10^{-5}$ (73)

The friction factor is given by:

$$\frac{1}{\sqrt{f}} = -4\log\left\{\frac{\varepsilon/D}{3.7} + \left[\frac{6.81}{\text{Re}}\right]^{0.9}\right\} = -4\log\left\{\frac{2.74\times10^{-5}}{3.7} + \left[\frac{6.81}{37,300}\right]^{0.9}\right\} = 13.43 \quad (74)$$

$$f = 0.00555$$

The frictional pressure drop is given as

$$-\Delta P_f = 2f\rho v^2\frac{L_{eq}}{D} = (2)(0.00555)(0.9109)(14.68)^2(709) = 1543\text{ Pa (0.22 psi)} \quad (75)$$

Circulating air compressor

$$\Delta P_{f,loop} = \Delta P_{f,bed} + \Delta P_{f,exchanger} + \Delta P_{f,piping}\,(25\%\text{ of loop}) = \frac{(154+1543)}{(0.75)} = 2,263\text{ Pa} \quad (76)$$

For adiabatic compression, assuming an efficiency of 60%, we have

$$-w_{theor} = \frac{RT_1}{(mw)(k-1)}\left[\left(\frac{P_2}{P_1}\right)^{(k-1)/k} - 1\right] \quad \text{and} \quad \dot{W}_{act} = \frac{\dot{m}w_{theor}}{\varepsilon_{comp}} \tag{77}$$

$$-w_{theor} = \frac{(8.314)(273.2+48.3)}{(0.0291)(1.4-1)}\left[\left(\frac{101.3\times10^3+2263}{101.3\times10^3}\right)^{(1.4-1)/1.4} - 1\right] = 1454\,\text{J/kg}$$
$$\dot{W}_{act} = \frac{\dot{m}w_{theor}}{\varepsilon_{comp}} = \frac{(0.0626)(1454)}{(0.6)} = 151\,\text{W} \tag{78}$$

In practice, a small blower capable of moving 0.0626 kg/s (140 scfm) across a pressure drop of 2,263 Pa (0.33 psi) should be used.

Exhaust gas through exchanger

Re = 2,590 (transition flow)

L_{eq}/D_h = (60)(0.3048)/(0.04787) + (5)(75) = 757 (79)

For laminar flow

$$-\Delta P_f = 2\rho f v^2 \frac{L}{D_h} = 2(0.698)\frac{16}{2590}(2.14)^2(757) = 30\,\text{Pa} \tag{80}$$

For Turbulent Flow

$$\frac{1}{\sqrt{f}} = -4\log\left\{\frac{\varepsilon/D}{3.7} + \left[\frac{6.81}{\text{Re}}\right]^{0.9}\right\} = -4\log\left\{\frac{1\times10^{-6}}{(3.7)(0.04787)} + \left[\frac{6.81}{2,590}\right]^{0.9}\right\} = 9.286 \tag{81}$$
$$f = 0.01077$$

$$-\Delta P_f = 2\rho f v^2 \frac{L}{D_h} = 2(0.698)(0.01077)(2.14)^2(757) = 52\,\text{Pa} \tag{82}$$

Using the turbulent flow relationship (conservative) the friction pressure drop for the exhaust gas slip stream is 52 Pa, which is negligible.

Bed Cooling

The beds are cooled from their regeneration temperature (400°F or 204°C) to their operating temperature (~100°F or 40°C) using a stream of ambient air at 40°C. Since all the NOx that can be desorbed will have been removed during the desorption cycle, the hot air stream leaving the bed may be safely vented to atmosphere. Alternatively, this air stream could be rerouted to the engine inlet and used as combustion air, with little effect on engine operation. The cooling cycle is chosen as two hours, which will leave a two hour window for the bed to sit prior to starting the adsorption cycle again. The required mass flow rate of air will be twice that used in the desorption cycle, namely (2)(0.0626) = 0.1252 kg/s. This will give rise to a pressure drop of approximately (4)(154) = 616 Pa (0.09 psi) through the bed.

A check on the sizing of the compressor was performed:

$$\Delta P_{f,loop} = \Delta P_{f,bed} + \Delta P_{f,piping}\,(25\%\text{ of loop}) = 616 + 525 = 1141\text{ Pa} \tag{83}$$

For adiabatic compression, assuming an efficiency of 60%, one finds that

$$-w_{theor} = \frac{RT_1}{(mw)(k-1)}\left[\left(\frac{P_2}{P_1}\right)^{(k-1)/k} - 1\right] \quad \text{and} \quad \dot{W}_{act} = \frac{\dot{m}w_{theor}}{\varepsilon_{comp}} \tag{84}$$

$$-w_{theor} = \frac{(8.314)(273.2+48.3)}{(0.0291)(1.4-1)}\left[\left(\frac{101.3\times10^3 + 1{,}141}{101.3\times10^3}\right)^{(1.4-1)/1.4} - 1\right] = 736\,\text{J/kg}$$

$$\dot{W}_{act} = \frac{\dot{m}w_{theor}}{\varepsilon_{comp}} = \frac{(0.1252)(736)}{(0.6)} = 154\,\text{W} \tag{85}$$

This is essentially the same as for the circulating air flow for the regeneration case. For this case the flow is approximately 280 scfm.

Summary of Equipment Specifications for Adsorption and Desorption Cycle

The equipment used to adsorb the NOx and to regenerate the carbon beds is shown in Table 27 below.

Table 27. Equipment specifications for NOx adsorption and carbon regeneration process

Equipment No.	Description	Capacity/Dimensions*	Number of Units Required
E-101	Exhaust gas heat exchanger	Area (bare tubes) = 66.3 m^2 (714 ft^2) Air-cooled, fin-fan, cross-flow exchanger	1
E-102	Regeneration heat exchanger	Area (bare tubes) = 6.86 m^2 (74 ft^2) Double-pipe exchanger	1
C-101A/B (include 1 spare)	Blower for regeneration and bed cooling	Capacity = 280 scfm bare module Pressure drop = 2263 PA (0.33 psi)	2
V-101A/B	Vessels for carbon adsorption beds	Vessel Diameter = 0.99 m (3.2 ft) Vessel height = = 2.97 m (9.6 ft)	2
F-101A/B/C	Fan for E-101	4.1 kW (5.5 hP)	3

Economic Analysis

In order to evaluate the effective cost of using an activated carbon adsorption system, capital costs, utilities, operating labor, and raw material costs must be estimated. The "one time" costs associated with the purchase of the equipment can be amortized and combined with the other operating costs in order to establish an equivalent annual operating cost (EAOC). The interest rate used for these calculations is 8% (before tax) and the lifetime used for this economic evaluation is 10 years.

- Due to presence of condensate and NOx, all equipment is designed using 304 stainless steel (SS), which has acceptable resistance to weak nitric acid solutions (<10%) (Turton et al, [107])

Two base cases are presented for the design calculations given above. These base cases represent different operating philosophies for the adsorption and regeneration process. Base Case 1 is presented based on a conservative estimate of operation, which is typical of

the chemical processing industry, and represents a high cost of operation. The key assumptions for this case are listed below:

- All equipment is made of stainless steel to minimize corrosion
- Additional manpower to operate the regeneration unit is estimated at ½ an operator per shift
- Maintenance costs are estimated at 5% of the fixed capital costs

Base Case 2 is presented based on a philosophy of minimizing costs, which is consistent with the automotive industry approach. The key assumptions for this case are listed below:

- All equipment is made of carbon steel (CS)
- Additional manpower to operate the regeneration unit is estimated at 5 hr per week
- Maintenance costs are estimated at 1% of the fixed capital costs

Clearly the equivalent annual operating cost for Base Case 2 will be significantly lower than for Base Case 1 and these two cases represent reasonable upper and lower bounds for the economics of this operation.

Base Case 1

Capital Cost Estimation

The capital cost estimation technique used here is based on the *equipment module costing technique,* which is a common technique to estimate the cost of chemical plants. This technique is generally accepted as the best for making preliminary cost estimates and is based on the approach, introduced by Guthrie [108, 109] in the late 1960's and early 1970's. The purchased costs for all equipment are obtained using the data from Turton et al. [107] This costing technique relates all costs back to the purchased cost of equipment

evaluated for some base conditions. Deviations from these base conditions are handled by using multiplying factors that depend on the following:

a. the specific equipment type,

b. the specific system pressure, and

c. the specific materials of construction.

The results for the equipment shown in Table 27 and are given in Table 28.

Table 28. Purchased and Bare Module Costs for Equipment: Table 27

Equipment No.	Description	MOC	C^0_p* ($1,000)	C_{BM} ($1,000)
E-101	Exhaust gas heat exchanger	SS	51.1	230.0
E-102	Regeneration heat exchanger	SS	4.2	25.1
C-101	Blower for regeneration and bed cooling	SS	8.4	55.3
V-101A/B	Vessels for carbon adsorption beds	SS	11.2	88.6
F-101A/B/C	Fan for E-101	CS	16.2	66.8
Total			91.1	465.8

*C^0_p is the purchased cost for the equipment at the base conditions of carbon steel

The capital investment required to buy and install this equipment is given by the bare module cost, C_{BM}. If the initial cost of the carbon (approx $5,200 at $2.20/kg) is added to this, the initial investment is given as $471,000.

Utility and Carbon Replacement Costs

The utility costs required to run the carbon adsorption and regeneration equipment are minimal and consist of the electric utilities to run the fans (F-101A/B/C) for the air cooler and the blower (C-101) for the circulating regeneration air stream.

Power for F-101A/B/C = 12.3 kW

Power for C-101 (assume a 60% efficiency) = 0.13 kW

Total power = 12.43 kW

Cost of electricity = \$0.06/kWh

Annual cost (assuming 8,000 hours per operating year) = (12.43)(8000)(0.06) = \$5,700/yr

Replacement cost of carbon is estimated on a carbon lifetime of 1,000 cycles. Each cycle lasts 16 hours, so the average life time of the carbon = 16,000 hr or 2 years. Therefore, the equivalent of 1 bed of carbon must be replaced per year.

Cost of carbon replacement = (1,224 kg)(2.2 \$/kg) = \$2,690/yr

Total utility and carbon replacement cost = \$5,700/yr + \$2,690/yr = **\$8,590/yr**

Operating Labor Costs

Assume that the maintenance of the rotating equipment used in the carbon adsorption/regeneration process will require an increment of ½ a person per shift. Based on an 8-hour shift, 1 person per shift is equivalent to 4.5 additional operators [107]. Further assuming a wage rate of \$50,000/yr (including benefits, etc.), the annual cost of operating labor is (2.25)(\$50,000) = **\$112,500/yr**

Maintenance Costs

Assume that the cost of maintenance supplies is 5% of the initial capital investment [107]. This gives an annual maintenance cost of (0.05)(\$466,300) = **\$23,300/y**

Equivalent Annual Operating Cost (EAOC)

The EAOC for the current project is given as follows:

$$EAOC = C_{UT} + C_{OL} + C_{MAIN} + [A/P, i, n]C_{BM} \quad (86)$$

Where the amortization factor, $[A/P,i,n] = \frac{i(1+i)^n}{(1+i)^n - 1} = \frac{(0.08)(1.08)^{10}}{(1.08)^{10} - 1} = 0.149$.

Substituting this in to Equation (y), gives:

$$EAOC = 8,590 + 112,500 + 23,400 + (0.149)(471,000) = \$214,700/yr \qquad (87)$$

Base Case 2

Capital Cost Estimation

The results for the equipment shown in Table 27, using carbon steel throughout, are given in Table 29.

Table 29. Purchased and Bare Module Costs for Equipment given in Table 27 using carbon steel throughout.

Equipment No.	Description	MOC	C^0_p* ($1,000)	C_{BM} ($1,000)
E-101	Exhaust gas heat exchanger	CS	51.1	111.0
E-102	Regeneration heat exchanger	CS	4.2	13.8
C-101	Blower for regeneration and bed cooling	CS	8.4	26.4
V-101A/B	Vessels for carbon adsorption beds	CS	11.2	45.6
F-101A/B/C	Fan for E-101	CS	16.2	66.8
Total			91.1	263.6

*C^0_p is the purchased cost for the equipment at the base conditions of carbon steel

The capital investment required to buy and install this equipment is given by the bare module cost, C_{BM}. If the initial cost of the carbon (approx $5,200 at $2.20/kg) is added to this, the initial investment is given as $268,000.

Utility and Carbon Replacement Costs

The utility costs required to run the carbon adsorption and regeneration equipment are minimal and consist of the electric utilities to run the fans (F-101A/B/C) for the air cooler and the blower (C-101) for the circulating regeneration air stream.

Power for F-101A/B/C = 12.3 kW (88)

Power for C-101 (assume a 60% efficiency) = 0.13 kW (89)

Total power = 12.43 kW

Cost of electricity = $0.06/kWh

Annual cost (assuming 8,000 hours per operating year) = (12.43)(8000)(0.06) = $5,700/yr (90)

Replacement cost of carbon is estimated on a carbon lifetime of 1,000 cycles. Each cycle lasts 16 hours, so the average life time of the carbon = 16,000 hr or 2 years. Therefore, the equivalent of 1 bed of carbon must be replaced per year.

Cost of carbon replacement = (1,224 kg)(2.2 $/kg) = $2,690/yr (91)

Total utility and carbon replacement cost = $5,700/yr + $2,690/yr = **$8,590/yr** (92)

Operating Labor Costs

Assume that the maintenance of the rotating equipment used in the carbon adsorption/regeneration process will require an increment of 5 hr per week. Assuming a wage rate for a 40 hr week of $50,000/yr (including benefits, etc.), the annual cost of operating labor is (5/40)($50,000) = **$6,500/yr**

Maintenance Costs

Assume that the cost of maintenance supplies is 1% of the initial capital investment [107]. This gives an annual maintenance cost of (0.01)($268,800) = **$2,688/y**

Equivalent Annual Operating Cost (EAOC)

The EAOC for the current project is given as follows:

$$EAOC = C_{UT} + C_{OL} + C_{MAIN} + [A/P, i, n]C_{BM} \quad (93)$$

Where the amortization factor, $[A/P, i, n] = \frac{i(1+i)^n}{(1+i)^n - 1} = \frac{(0.08)(1.08)^{10}}{(1.08)^{10} - 1} = 0.149$.

Substituting this in to Equation (y), gives:

$$EAOC = 8,590 + 6,500 + 2,688 + (0.149)(268,800) = \$57,800/yr \quad (94)$$

Therefore, annual operating costs for the adsorption/regeneration system are expected to vary between $57,800 and $214,700 per year. It is instructive to put these numbers into perspective with respect to the cost of fuel to run the engine. For the Cummins L10G, the estimated cost of fuel based on natural gas at $8.00 per MMBTU is approximately $130,000 per year. Thus, the annual operating cost of the adsorption system represents between 44 – 165% of the cost of natural gas to run the engine. It is evident that for a small engine running at low power, the system is not feasible. However, the design can be scaled to larger engines, as discussed below.

Effect of Capacity/Size on Economics

The case developed previously was for a small Cummins L10G natural gas engine. We now consider the case for a Cummins QSV91 natural gas engine with an output of approximately 1750 kW.

The design conditions for this engine are as follows:

Flowrate of exhaust gas = 10,094 kg/h (22255 lb/h)

Temperature of Exhaust = 498 °C (928°F)

NOx in Exhaust = 0.78 g/s (~ 280 ppm)

The same methodology used for the smaller engine given previously is used here. The results are summarized in Table 30, it should be noted that a 24 hour cycle time was chosen for the larger engine due to excessive bed pressure drop for small cycle times.

Table 30. Equipment specifications for NOx adsorption and carbon regeneration process

Equipment No.	Description	Capacity/Dimensions*	Number of Units Required
E-101	Exhaust gas heat exchanger	Area (bare tubes) = 924 m^2 (9,950 ft^2) Air-cooled, fin-fan, cross-flow exchanger	1
E-102	Regeneration heat exchanger	Area (bare tubes) = 19.3 m^2 (207 ft^2) Multiple-pipe exchanger	1
C-101A/B (include 1 spare)	Blower for regeneration and bed cooling	Capacity = 0.2 m^3/s (425 scfm) Pressure drop = 4090 Pa (0.59 psi)	2
V-101A/B	Vessels for carbon adsorption beds	Vessel Diameter = 2.48 m (3.2 ft) Vessel height = 5.0 m (9.6 ft)	2
F-101A/B/C	Fan for E-101	4.15 kW (6.1 hP)	15

The capital cost estimates for the Cummins QSV91 engine were done using the same approach as for the smaller engine. Specifically, two cases were considered. The first case (I) used a conservative estimate using mainly stainless steel as the material of construction and the second case (II) used carbon steel. The results of the capital cost analysis for these two cases are given in Table 31 and Table 32.

Table 31. Purchased and Bare Module Costs for Equipment given in Table 27 for two cases

Equipment No.	Description		Case I		Case II	
		C^0_p* ($1,000)	MOC	C_{BM} ($1,000)	MOC	C_{BM} ($1,000)
E-101	Exhaust gas heat exchanger	179.0	SS	805	CS	388
E-102	Regeneration heat exchanger	8.3	SS	49	CS	27
C-101	Blower for regeneration and bed cooling	8.5	SS	63	CS	30
V-101A/B	Vessels for carbon adsorption beds	64.4	SS	420	CS	222
	Initial Carbon	27.0		27		27
F-101A/B/C	Fan for E-101	349.0	CS	960	CS	960
			Total	$2,325	Total	$1,654

Table 32. Summary of operating cost for Cases I and II

Expense	**Case I ($1,000)**	**Case II ($1,000)**
Bare Module Cost	2,298.0	1,654.0
Utility	30.3	30.3
Carbon Replacement	9.0	9.0
Maintenance	114.9	16.5
Operating Labor	112.5	6.5
Total operating costs	266.7	62.3
Equivalent Operating Cost	**$609.1**	**$308.7**

Therefore, annual operating costs for the adsorption/regeneration system for the Cummins QSV91 natural gas engine are expected to vary between $309,000 and $609,000 per year. These numbers represent 26 – 51% of the cost of natural gas to run the engine.

6.6 Conclusions

A research study was completed to address the feasibility of reducing NOx from lean-burn natural gas engines using SNR. In this process, the NOx is first adsorbed from cooled exhaust gas in a bed of carbon, subsequently desorbed thermally, and then

decomposed by pasasing it through the engine combustion process again. The decomposition of NOx, the adsorption and desorption of NOx, and the arrangement and economics of the system were investigated separately.

NO decomposition studies were performed using two Cummins 10 liter engines. A campaign of NO injections into the first engine demonstrated that decomposition was insufficient under lean-burn conditions. Reaction modeling confirmed that stoichiometric burn was desirable for high decomposition rates, and two campaigns with the second engine confirmed the high decomposition, as well as the effects of using EGR with stoichiometric burn. Combustion (as in-cylinder pressure) was not substantially affected by the NO injections.

From a benchtop study it can be concluded that activated carbon is suitable medium for adsorbing NOx, but there was no attempt to optimize the type or size of carbon used. It is important to note that the adsorption process was highly dependent on the presence of oxygen in the exhaust, and the adsorption studies using NO with balance nitrogen yielded data with low adsorption potential that were not representative of real engine operation. The adsorption probably took place as a result of converting NO to NO_2. A cooler inside bed temperature provided for a superior NOx loading of the bed, which is to be expected. Water was not determined to have a significant effect of the adsorption process. The greatest amount of NOx adsorbed onto the carbon during the NO mixed with compressed air run equaling 1.93 mass percent of NOx to carbon. Based on these data, a conservative value of 0.5 mass percent was used for design calculations. The carbon bed must reach a temperature of at least 450°F in order to ensure proper desorption. At least 54% of the NO injected converted to NO_2 in the presence of oxygen according to the benchtop experimental work using NO with balance air.

Arrangements for returning the desorbed NOx to the engine were considered, and the option of returning the NOx to a single cylinder of a multi-cylinder engine, and causing that cylinder to run stoichiometrically with EGR, was considered to be superior.,

A system design and economic analysis were performed. The system used three adsorber beds to allow sufficient time for heating and cooling of the beds between the adsorption

and desoorption functions. The desorption was accomplished by heating the bed and circulating desorption gas, rather than using an exhaust slipstream. A major cost was associated with the heat exchangers, both for construction and for air cooling fan operation. It was necessary to assume the life of the carbon, in the absence of detailed data on long term operation. Two cost scenarios were considered, one with an industrial level of maintenance and operation, and one less expensive, more automated operation strategy. It was evident that economies of scale and a high degree of automation would favor the SNR operation. The SNR cost was found to represent 26% of the fuel cost for operation of a 1,750 kw engine over ten years. It is likely that stoichiometric operation would be preferred for a new 0.1 g/bhp-hr engine installation, but the SNR approach was technically feasible and should be considered, with design optimization, as a retrofit technology for lean-burn engines.

References

[1]. Distributed Energy Resources. "Advanced Reciprocation Engines Systems," U.S. Department of Energy, 1000 Independence Ave, SW Washington, DC, February 2001.

[2]. Cackette, T. "Reducing the Impact of Diesel on Air Quality and Public Health," California Environmental Protection Agency, August 20, 2000.

[3]. Mauzerall, D. L., Sultan, B., Kim, N. and Bradford, D. F. "NOx Emissions from large Point Source: Variability in Ozone Production, Resulting Health Damages and Economic Costs," Atmospheric Environment, Paper 39 (2005) 2851- 2866, 2004.

[4]. International Association for Natural Gas Vehicles, "IANGV Emissions Report," March 31, 2000.

[5]. Soliman, A., Jackson, P., Midlam-Mohler, S., Zou, Z., Guezennec, Y. and Rizzoni, G. "Diagnosis of a NOx Aftertreatment Systems," SAE Paper No. 2005-24-004, Warrendale, PA, 2005.

[6]. Callahan, T. J. "Reciprocating Engine Technology - Can We Get There From Here?," Southwest Research Institute, Reciprocating Engines Peer Review, Chicago, IL, April 23-24, 2002.

[7]. Office of Air Quality Planning and Standards, "How nitrogen oxides affect the way we live and breathe," Research Triangle Park, NC 27711, EPA-456/F-98-005, September 1998.

[8]. Thompson, S. A. "Nitrogen Dioxide," Publication issued by the Department of Environmental Quality, Oklahoma Department of Libraries, 2003.

[9]. Clean Air Technical Center (MD-12). "Nitrogen Oxides (NOx), Why and How They are Controlled," U.S. Environmental Protection Agency, Research Triangle Park, NC, 27711, EPA 456-99-006R, November, 1999.

[10]. Encyclopedia Britannica, Volume 16, page 470, William Benton Publisher, 1957.

[11]. Alpha-Gamma Technologies Inc. "Natural Gas-Fired Reciprocating Engines," Emission Factor Documentation for AP-42 Section 3.2, Prepared for U.S. Environmental Protection Agency, Raleigh NC, July 2000.

[12]. Johnson, R. H. and Wilkes, C. E. "Emissions Performance of Utility and Industrial Gas Turbine," American Power Conference, April 23-25, 1979.

[13]. Campbell, L. M., Stone, D. K. and Shareef, G. S. "Sourcebook: NOx Control Technology Data," U.S. Environmental Protection Agency, Research Triangle Park, NC, Document No. EPA-600/2-91-029, 1991.

[14]. Bosh, H. and Jenssen, F. "Catalytic Reduction of Nitrogen Oxides. A Review on the Fundamentals and Technology," Catalysis Today, Volume 2, No. 4, March 1988.

[15]. Chen, S. L. "Influence of Coal Composition on the Fate of Volatile and Char Nitrogen During Combustion," 19th Symposium (International) on Combustion,. Published by Combustion Institute, Pittsburgh, PA, pp 1271-1280, EPA-600/D-83-032 (NTIS PB83-183194), 1982.

[16]. Encyclopedia Britannica, Volume 16, page 162, William Benton Publisher, 1957.

[17]. Tunali, I., Bata, R. and Churchill, R. WVU's NAFTPC - CNG Review.

[18]. Liss, W. E. and Thrasher, W. H. "Natural Gas as a Stationary Engine and Vehicular Fuel," SAE Paper No. 912364, Warrendale, PA, 1991.

[19]. Alternative Control Techniques Document. "NOx Emissions From Stationary Reciprocating Engines," EPA-453/R-93-032, July 1993.

[20]. Klimstra, J. "Interchangeability of Gaseous Fuels – The Importance of the Wobbe Index," SAE Paper No. 861578, Warrendale, PA, 1986.

[21]. Nylund, N. O. "On the development of a low-emission propane engine for heavy-duty urban vehicle applications," Doctoral Thesis, Espoo: Technical Research Centre of Finland, (VTT Publications 260). ISBN 951-38-4798-5, 1955.

[22]. International Association for Natural Gas Vehicles. "CNG city bus engine with optimized part-load efficiency, high mean effective pressure and low emissions," In: Proc. NGV 94, The Fourth International Conference & Exhibition on Natural Gas Vehicles, Toronto: IANGV,1994.

[23]. Jönsson, L. "Volvo THG103 - A Low Emission CNG Engine," In: Proc. NGV 92, The Third International Conference & Exhibition on Natural Gas Vehicles,Gothenburg: IANGV, 1992.

[24]. Clarke, D. P. and Such, C. H. "Development of a medium duty, turbo-charged, lean-burn natural gas engine," In: Proc. NGV 92, The Third International Conference & Exhibition on Natural Gas Vehicles. Gothenburg: IANGV, 1992.

[25]. Weaver, C. S. "Natural Gas Vehicles – A Review of the State of the Art," SAE Paper No. 892133, Warrendale, PA, 1989.

[26]. Shipley, A., M., Green, N., McCormack, K., Li, J. and Elliott, R., N. "Certification of Combined Heat and Power Systems: Establishing Emissions Standards," ACEEE Publications, Report Number IE014, September 2001.

[27]. Manufacturers of Emission Controls Association, "Emissions Control Technology for Stationary Internal Combustion Engines," Status report, 1660 L Street NW, Suite 1100, Wachinton DC 20036, July 1997.

[28]. Johnson Matthey, 3-way Catalysts – non selective catalytic reduction URL: http://ect.jmcatalysts.com/technologies-3way.htm

[29]. Nylund, N. O. and Eklund, T. "Low emission heavy-duty vehicles for urban services," In: Proc. 27 th ISATA/Dedicated Conference on Electric, Hydrid & Alternative Fuel Vehicles and Supercars (Advanced Ultralight Hybrids). Croydon: Automotive Automation Limited, ISBN 0 947719 63 6, 1994.

[30]. Kim, J. W. "Development of the Daewoo dedicated light duty NGV II," In: Proc. NGV 94, The Fourth International Conference & Exhibition on Natural Gas Vehicles. Toronto: IANGV, 1994.

[31]. International Association for Natural Gas Vehicles, IANGV Emissions Report, Match 31, 2000.

[32]. Klimstra, J. "Catalytic converters for natural gas fuelled engines - a measurement and control problem," SAE Paper No. 872165, Warrendale, PA, 1987.

[33]. Varde, K. S. and Cherng, J. C. "Emissions and their control in natural gas fuelled engines. In: Automotive Emissions and Catalyst Technology," SAE Paper No. SP-938, Warrendale, PA, 1992.

[34]. Bhargava, S., Clark, N. N., and Hinlebrand, M. W. "Exhaust gas Recirculation in a Lean-Burn Natural Gas Engine," SAE Paper No. 981395, Warrendale, PA, 1998.

[35]. Cummins Inc. "Mobile off-highway emissions – choosing the right technology," Bulletin 4103672, Rev. 8/04. Columbus, IN 47202.

[36]. Cox, G., DelVecchio, K, Hays, W., Hiltner, J., Nagaraj, R. and Emmer, C. "Development of a Direct- Injected Natural Gas Engine System for Heavy-Duty Vehicles," Final Report, Phase II, Document no. NREL/SR-540-27501, February 2000.

[37]. Little, A. D. "Selective Catalytic Reduction Urea Infrastructure Study, NREL/SR-540-32689, National Technical Information Service, US Department of Commerce, Springfield, VA, 2002.

[38]. Incitec, fact sheet. "Urea," Incitec Ltd, Murarrie, Qld, Australia, 2000.

[39]. Kilford & Kilford. "Garden King Urea," Material Safety Data Sheet, Envirogreen, Penrith, NSW, Australia 1998.

[40]. Makeham, P. and Coffey Geosciences Pty Ltd. "Investigation of implications for the distribution and use of urea to improve diesel vehicle emissions," prepared for Land Transport Environment Committee, August 2004.

[41]. Johnson Matthey, Selective Catalytic Reduction (SCR) deNOx Catalyst. URL http://ect.jmcatalysts.com/applications-ssec-na-products-scr.htm.

[42]. Krishnan, R. "SCR Economics for Diesel Engines," Diesel and Gas Turbine Worldwide, RJM Corporation, Norwalk, CT, July-August 2001.

[43]. Fable, S. and Jackson, M. "Urea Infrastructure Hurdles: Report on TIAX Selective Catalytic Reduction Urea Infrastructure Study," Motor Fuels: Effects on Energy Efficiency & Emissions in the Transportation Sector, October 10, 2002.

[44]. Energy prices published at Bloomberg's media services, real-time financial and market data, http://www.bloomberg.com/markets/commodities/energyprices.html

[45]. Fable, S., Kamakate, F. and Venkatesh, S. "Selective Catalytic Reduction Urea Infrasturcture Study," National Renewable Energy Laboratory, Document no. NREL/SR-540-32689, July 2002.

[46]. Dou, D., Miyaura, S., Dogahara, T., Kikuchi, S. and Okada, K. "NOx-Trap Catalyst Development for Mitsubishi 1.8L GDITM Application," SAE Paper no. 2003-01-3078, Warrendale, PA, 2003.

[47]. Daw, C. S., Chakravarthy, K. and Lenox, K. E. "A simple model for lean NOx adsorber catalysts," Third Joint Meeting of the U.S. Sections of The Combustion Institute, Oak Ridge National Laboratory, Oak Ridge, TN, 2003.

[48]. Erkfeld, S. "Sulphur Poisoning and Regeneration of NOx Trap Catalyst for Direct Injected Gasoline Engines," SAE Paper No. 1999-01-3504, Warrendale, PA, 1999.

[49]. Brogan, M., Clark, A. D. and Brisley, R. J. "Recent Progress in NOx Trap Technology," SAE Paper No. 980933, Warrendale, PA, 1998.

[50]. Fekete, N., Kemmler, R., Voigtländer, D., Krutzsch, B., Zimmer, E., Wenninger, G., Strehlau, W., van den Tillaart, J., Leyrer, J., Lox, E. and Müller, W. "Evaluation of NOx Storage Catalysts for Lean-Burn Gasoline Fueled Passenger Cars," SAE Paper No. 970746, Warrendale, PA, 1997.

[51]. Brogan, M., Clark, A. and Brisley, R. "Recent Progress in NOx-Trap Technology," SAE Paper No. 980933, Warrendale, PA, 1998.

[52]. Dou, D., and Bailey, O. H. "Investigation of NOx Adsorber Catalyst Deactivation," SAE Paper No. 982594, Warrendale, PA, 1998.

[53]. Dearth, M., Hepburn, J., Thanasiu, E., McKenzie, J. and Horne, G. "Sulfur Interaction with Lean NOx-Traps: Laboratory and Engine Dynamometer Studies," SAE Paper No. 982595, Warrendale, PA, 1998.

[54]. Goebel, U., Hoehne, J., Lox, E., Mueller, W., Okumura, A., Strehlau, W. and Hori, M. "Durability Aspects of NOx Storage Catalysts for Direct Injection Gasoline Vehicles," SAE Paper No. 99FL-103, Warrendale, PA, 1999.

[55]. Hodjati, Sh., Semelle, F., Moral, N., Bert, C. and Rigaud, M. "Impact of Sulfur on the NOx-Trap Catalyst Activity-poisoning and Regeneration Behavior," SAE Paper No. 2000-01-1874, Warrendale, PA, 2000.

[56]. Hachisuka, I, Hirata, H., Ikeda, Y. and Matsumoto, S. "De-activation Mechanism of NOx storage-Reduction Catalyst and Improvement of Its performance," SAE Paper No. 2000-01-1196, Warrendale, PA, 2000.

[57]. Asik, J., Meyer, G. and Dobson, D. "Lean NOx-Trap Desulfation Through Rapid Air Fuel Modulation," SAE Paper No. 2000-01-1200, Warrendale, PA, 2000.

[58]. Bailey, O., Dou, D. and Molinier, M. "Sulfur Traps for NOx Adsorbers: Materials Development and Maintenance Strategies for Their Application," SAE Paper No. 2000-01-1205, Warrendale, PA, 2000.

[59]. Ohno, H., Takanohashi, T., Takaoka, N., Kuroda, O. and Iizuka, H. "NOx Conversion Properties of a Mixed Oxide Type Lean NOx Catalyst," SAE Paper No. 2000-01-1197, Warrendale, PA, 2000.

[60]. Iwachido, K., Tanada, H., Wantanabe, T., Yamada, N., Nakayama, O., Ando, H., Hori, M., Taniguchi, S., Noda, N. and Abe, F., "Development of the NOx Adsorber Catalyst for Use with High-Temperature Con ditions," SAE Paper No. 2001-01-1298, Warrendale, PA, 2001.

[61]. Dou, D. and Balland, J. “Impact of Alkali Metals on the Performance and Mechanical Properties of NOx Adsorber Catalysts,” SAE Paper No. 2002-01-0734, Warrendale, PA, 2002.

[62]. Monroe, D. and Li, W. “Desulfation Dynamics of NOx Storage Catalysts,” SAE Paper No. 2002-01-2886, Warrendale, PA, 2002.

[63]. Parks, J., Watson, A., Campbell, G. and Epling, B. “Durability of NOx Absorbers: Effect of Repetitive Sulfur Loading and Desulation,” SAE Paper No. 2002-01-2880, Warrendale, PA, 2002.

[64]. Walkowicz, K., Stephens, D. and Stork, K. “The DOE/NREL Next Generation Natural Gas Vehicle Program – An Overview,” SAE Paper No. 2001-01-2068, Warrendale, PA, 2001.

[65]. Iwamoto, M. "Removal of Nitrogen Monoxide through a Novel Catalytic Process", Journal of Physical Chemistry, 95, pg. 3727-3730, 1991.

[66]. Truex, T. J. "Lean NOx Catalysts", SAE Catalysts and Emission Control TOPTEC, MI, September 1994.

[67]. Callahan, T. J., Dodge, L. G., Roberts, C. E., Stovell, C. H., Bourn, G. D. and Bartley, G. J. “Technical Path Evaluation for High Efficiency Low Emissions Natural Gas Engine,” Interim Report TFLRF No. 363, Contact No. DAAE07-99-C-L053, Southwest Research Institute, San Antonio TX, May 2002.

[68]. Dunn, M. “State of the Art and Future Developments In Natural Gas Engine Technologies,” Cummins Westport Inc. 9th Annual DEER Conference, August 2003.

[69]. Hiltner, J., Agama, R., Mauss, F., Johansson, B. and Christensen, M. “Homogeneous Charge Compression Ignition Operation With Natural Gas: Fuel Composition Implications,” Journal of Engineering for Gas Turbines and Power, Volume 125, Issue 3, pp. 837-844, July 2003.

[70]. Reuther, J. "Evaluation of Air Emissions-Reduction Technologies for Aerospace Ground Equipment," Battelle Research Laboratories, Columbus OH, Document no. AFRL-HEWP-TR-1998-0026, April 1998.

[71]. Haught, D. "Advanced Reciprocating Engine Systems (ARES) Program," Distributed Energy Resources, U.S. Department of Energy, Washington DC, 20585.

[72]. Duggal, V. Cummins Engine Company Inc., California Advanced Reciprocating Internal Combustion Engines Collaborative, Workshop Proceedings, California Energy Commission, July 10, 2001.

[73]. Brandon, L. "Cummins' Technology Strategy for ARES," DOE Distributed Energy Peer Review, Arlington VA, December 13, 2005.

[74]. Lyford-Pike, E. and LaPointe, L. "ARES Technology for High Brake Thermal Efficiency, Low Emissions, Base Load, Prime Power Applications," Presentation at the 3rd annual Advanced Stationary Reciprocating Engines Meeting, June 29, 2006.

[75]. Gerber, G. and Boley, B. "Evolution of the G3500C Engine Design towards ARES Phase I Goals," Presentation at the 2nd Annual ARES – ARICE Conference, Diamond Bar, CA, March 2005,

[76]. Gerber, G. Principal Investigator, Caterpillar Inc. U.S. Department of Energy Cooperative Agreement Number: DE FC02-01CH11079, presentation at ARES Peer Review, Chicago, IL, April 23-24, 2002.

[77]. Baldwin, D. and Gerber, G. "Advanced Reciprocating Engine Systems," DOE Distributed Energy Peer Review, Arlington, VA, December 13 -15, 2005.

[78]. McCormick, M. Waukesha Engine Dresser, Inc., California Advanced Reciprocating Internal Combustion Engines Collaborative, Workshop Proceedings, California Energy Commission Sacramento, CA, July 10, 2001.

[79]. Drees, J. Waukesha Engine Dresser Inc. "Stoichiometric Combustion Advances," ARE/ARICE Contractor Conference, April 14-15, 2004.

[80]. Drees, J. Waukesha Engine Dresser Inc., Advanced Power Generation, DOE Distributed Energy Peer Review, Arlington, VA, December 13 -15, 2005.

[81]. Parks, J., Tassitano, J. and Storey, J. "Lean NOx Trap Catalysis: NOx Reduction for Lean Natural Gas Engine Applications," Oak Ridge National Laboratory, 2nd Annual Advanced Stationary Reciprocating Engines Conference, Diamond Bar, CA, March 15-16, 2005.

[82]. Biruduganti, M., Gupta, S., McConnell, S. and Sekar, R. "Nitrogen Enriched Combustion of a Natural Gas Engine to Reduce NOx Emissions," 2nd Annual Advanced Stationary Reciprocating Engines Conference, Diamond Bar, CA, March 15-16-2005.

[83]. Gas Technology Institute and Energy Solutions Center, Technology Priorities for Industrial Applications, November 2002.

[84]. Energy and Environmental Analysis, Inc. "Industrial Application Guide For Innovative Combined Heat and Power," prepared for Energy Solutions Center,U.S. Department of Energy and Exergy Partners Corp, January 2004.

[85]. Yeh, J. J., Pennline, H. and Drummond, C. "New Strategy to Decompose Nitrogen Oxides from Regenerable Flue Gas Cleanup Processes," 194th ACS National Metting, American Chemical Society, New Orleans, LA 1987.

[86]. Krutzsch, B., Wenninger, G., Weibel, W., Stapf, P., Funk, A., Webster, D., Chaize, E., Kasemo, B., Martens, J. and Kiennemann, K. "Reduction of NO_X in Lean Exhaust by Selective NO_X – Recirculation (SNR -Technique), Part I: System and Decomposition Process," SAE Paper No. 982592, Warrendale, PA, 1998.

[87]. Chaize, E., Webster, D. E., Krutzsch, B., Wenninger, G., Weibel, M., Hodjati, Sh., Petit, C., Pitchon, V., Kiennemann, A., Loenders, R., Monticelli, O., Jacobs, P. A., Martens, J. A., and Kasemo, B., "Reduction of NOx in Lean Exhaust by Selective NOx-Recirculation (SNR-Technique) Part II: NOx Storage Materials," SAE Technical Paper No. 982593, Warrendale, PA, 1998.

[88]. Sales specification sheet, “Coconut activated carbon OVC4x8,”Calgon Carbon Corporation, Pittsburgh, PA, 2005.

[89]. Lim, S., Yoon, S., Shimizu, Y., Jung, H. and Mochida, I. “Surface Control of Activated Carbon Fiber by Growth of Carbon Nanofiber,” American Chemical Society, Langmuir, Volume 20, No. 13, pages 5559 – 5563, 2004.

[90]. Nelson, B. W. “Demonstration of a New Emission Control System for Stationary Diesel and Natural Gas Engines,” Prepared for the California Air Resources Board under Innovative Clean Air Technologies Program, Sorbent Technologies, Inc., Grant No. ICAT00-3, Twinsburgh, OH, March 2004.

[91]. Kong, S. C. and Reitz, R. D. "Application of detailed chemistry and CFD for predicting direct injection HCCI engine combustion and emissions," Proceedings of the Combustion Institute 29:663-669, 2003.

[92]. Kong, S. C. and R. D. Reitz. "Use of detailed chemical kinetics to study HCCI engine combustion with consideration of turbulent mixing effects," Journal of Engineering for Gas Turbines and Power-Transactions of the ASME,” 124(3):702-707, 2002.

[93]. Smith, P., Golden, D., Frenklach, M., Moriarty, N., Eiteneer, B., Goldenberg, M., Bowman, C., Hanson, R., Song, S., Gardiner, W., Lissianski, V. and Qin, Z. “Over view of GRI-Mech,” Internet web site: http://www.me.berkeley.edu/gri_mech, 2004.

[94]. Code of Federal Regulations, Title 40, Part 86, “Emission Regulations for New Otto-Cycle and Diesel Heavy-Duty Engines; Gaseous and Particulate Exhaust Test Procedures,” Washington, DC, 1998.

[95]. Hoppie, J. A. “Defining Drivetrain Losses in Developing a Cycle for Engine and Chassis Dynamometer Test Compliance and Uncertainty Analysis of Emissions Test Facilities,” M. S. Thesis, West Virginia University, Morgantown, WV, 1997.

[96]. Heywood, J. B. “Internal Combustion Engine Fundamentals,” McGraw Hill, Inc. New York, NY, 1998.

[97]. Puzinauskas, P. V., Olsen, D. B. and Wilson, B. D. Mass integration of fast-response NO measurement from a two-stroke large-bore natural gas engine. International journal of engine research, Volume 4, Issue 3, Pages 233-248, 2003.

[98]. Universal Exhaust Gas Oxygen Sensor NGK NTK: NGK Spark Plug Co. Part # TL-7113-A1 manual.

[99]. Wayne, W. S. "A Parametric Study of Knock Control Strategies for a Bi-Fuel Engine," PhD Dissertation, West Virginia University, May 1997.

[100]. Dodge, L. G., Kubesh, J. T., Naegeli, D. W. and Campbell, P. "Modeling NO_X Emissions from Lean-Burn Natural Gas Engines," SAE Paper No. 981389, Warrendale, PA, 1998.

[101]. Chase, M. W. and Lide, D. R. "JANAF Thermochemical Tables," Journal of Physical and Chemical Reference Data, V 14 1985 Supplement Number 01 Parts 1 and 2, American Chemical Society, 1986.

[102]. Swartz, M. M., Tissera, C. A., Tatli, E., Vellaisamy, R., Clark, N. N., Thompson, G. J. and Atkinson, R. J. "Nitric Oxide Conversion in a Spark Ignited Natural Gas Engine," SAE Paper No. 2005-01-0234, Warrendale, PA, 2005.

[103]. Vellaisamy, R., Clark, N. N., Thompson, G. J., Atkinson, R. J., Tissera, C. A. and Swartz, M. M. "Assessment of NOx Destruction in Diesel Engines by Injecting NOx in the Intake Manifold," SAE Paper No. 2005-01-0370, Warrendale, PA, 2005.

[104]. Product Bulletin, Centaur ® 4x6 granular activated carbon, Calgon Carbon Corporation, P.O. Box 717, Pittsburgh PA 15230, PB-107 1-08/98

[105]. Zimmerman, A. J., Tissera, C. A., Tatli, E., Clark, N. N., Atkinson, R. J., Thompson, G. J. and Turton, R. "System Model for Selective NOx Recirculation (SNR) to be used in Stationary Lean-Burn Natural Gas Engines," ASME Paper No. ICEF2006-1542, Sacramento, CA, 2006.

[106]. O. Levenspiel, *Engineering Flow and Heat Exchange*, Plenum Press, NY (1995)

[107]. R. Turton, R.C. Bailie, W. B. Whiting, and J.A. Shaeiwitz, *Analysis, Synthesis, and Design of Chemical Processes*, Prentice-Hall, 2nd edition, Upper Sadle, NJ (2003)

[108]. K.M. Guthrie. Capital Cost Estimating, Chem Eng 76, 114 (1969)

[109]. K.M. Guthrie. *Process Plant Estimating, Evaluation, and Control of Chemical Construction Projects*, Solana Beach CA, Solana (1974)

[110]. Kong, Y., and Cha, C.Y. "NOx Adsorption on Char in Presence of Oxygen and Moisture," Carbon, Vol. 34, No 8, pp. 1027-1033, 1996.